The LeiCNS-PK3.0 model development and applications: healthy-to-diseased CNS pharmacokinetic translation

Saleh, M.A.A.E.W.

Chapter 6

Drug distribution in brain and cerebrospinal fluids in relation to IC_{50} values in aging and Alzheimer's disease, using the physiologically based LeiCNS-PK3.0 model

Mohammed A.A. Saleh, Julia S Bloemberg, Jeroen Elassaiss-Schaap, Elizabeth C.M. de Lange

Pharmaceutical Research, 2022; 39 (7): 1303-1319

Abstract

Background. Very little knowledge exists on the impact of Alzheimer's disease on the CNS target site pharmacokinetics (PK).

Aim. To predict the CNS PK of cognitively healthy young and elderly and of Alzheimer's patients using the physiologically based LeiCNS-PK3.0 model.

Methods. LeiCNS-PK3.0 was used to predict the PK profiles in brain extracellular ($brain_{ECF}$) and intracellular ($brain_{ICF}$) fluids and cerebrospinal fluid of the subarachnoid space (CSF_{SAS}) of donepezil, galantamine, memantine, rivastigmine, and semagacestat in young, elderly, and Alzheimer's patients. The physiological parameters of LeiCNS-PK3.0 were adapted for aging and Alzheimer's based on an extensive literature search. The CNS PK profiles at plateau for clinical dose regimens were related to *in vitro* IC_{50} values of acetylcholinesterase, butyrylcholinesterase, N-methyl-D-aspartate, or gamma-secretase.

Results. The PK profiles of all drugs differed between the CNS compartments regarding plateau levels and fluctuation. $Brain_{ECF}$, $brain_{ICF}$ and CSF_{SAS} PK profile relationships were different between the drugs. Aging and Alzheimer's had little to no impact on CNS PK. Rivastigmine acetylcholinesterase IC_{50} values were not reached. Semagacestat brain PK plateau levels were below the IC_{50} of gamma-secretase for half of the interdose interval, unlike CSF_{SAS} PK profiles that were consistently above $IC_{50.}$

Conclusion. This study provides insights into the relations between CNS compartments PK profiles, including target sites. CSF_{SAS} PK appears to be an unreliable predictor of brain PK. Also, despite extensive changes in blood-brain barrier and brain properties in Alzheimer's, this study shows that the impact of aging and Alzheimer's pathology on CNS distribution of the five drugs is insignificant.

Keywords: LeiCNS-PK3.0; PBPK; Alzheimer's disease; Target site; PK prediction

Introduction

For Alzheimer's disease (AD) treatment, currently only four small molecule drugs are available that can help reduce the symptoms (1). These include the selective acetylcholinesterase inhibitors donepezil and galantamine, the acetylcholinesterase and butyrylcholinesterase dual inhibitor rivastigmine (for early- to mid-stage AD) (2, 3), and the N-methyl-D-aspartate (NMDA) receptor antagonist memantine (for moderate or severe AD) (4). Cholinesterase inhibitors inhibit the enzyme acetylcholinesterase from breaking down the neurotransmitter acetylcholine into choline and acetate (2, 3). Cholinesterases exist in different forms that can be found in cells, or can be attached to the outer cell membrane (2, 3). Memantine blocks extracellularly the cell membrane bound NMDA receptors (4). Despite their anticipated sites of actions in brain intracellular ($brain_{ICF}$) and/or extracellular ($brain_{ECF}$) fluids, accessible information on AD drug distribution in the human brain is lacking, let aside how this PK profile may be affected by changes in the CNS physiology associated with aging and/or AD. At best, limited data exist on concentrations in subarachnoid cerebrospinal fluid (CSF_{SAS}) at the lumbar region, which is often believed to reflect $brain_{ECF}$ concentrations (5,6,7,8,9). Also for AD drug discovery and development, it is important to understand the unbound (brain) target site(s) concentrations, that drive their effects (10). However, assessment of the right information on human brain PK is challenging. First, the best possible direct measurement of unbound drug PK profiles in human brain by microdialysis is limited by ethical restrictions based on the method's invasiveness. Second, while noninvasive CNS imaging techniques provide crucial information on CNS drug distribution they do not distinguish between the bound and the unbound drug or the parent drug and its metabolites (11). Third, while (invasive) sampling of the lumbar cerebrospinal fluid (CSF) is ethically possible and provides unbound drug concentrations, its use remains limited (5,6,7,8,9), while also it has been shown to be an inaccurate surrogate of brain PK, particularly in the context of CNS diseases (12, 13).

We have previously developed the comprehensive physiologically-based LeiCNS-PK3.0 model (Fig. 1), that has been demonstrated to adequately predict the unbound PK of multiple small molecule drugs in healthy human $brain_{ECF}$ and lumbar CSF_{SAS} (13, 14). The LeiCNS-PK3.0 model accounts for the drug physicochemical properties such as lipophilicity, charge, and molecular weight and for the physiological properties of the human CNS, including the $brain_{ECF}$ and $brain_{ICF}$, and the different CSF compartments, on the basis of the compartments

size and surface area. The model accounts for other physiological processes including drug transport across the blood-brain (BBB) and blood-CSF (BCSFB) barrier, physiological fluid flow, intra-extracellular drug distribution, brain tissue non-specific binding, and compartment-specific pH values. The LeiCNS-PK3.0 model can be used to predict the unbound PK profiles at CNS target sites for small molecule CNS drugs and off-target sites for non-CNS drugs and thus predicting potential CNS related toxicities or side effects. In addition, the mechanistic structure of the model allows translation of PK predictions across species but also between the different CNS physiological states, i.e. healthy, diseased, maturing, etc.

Previous studies with the LeiCNS-PK3.0 model have predicted that CNS pathophysiological changes can alter the rate and/or extent of drug transport into the CNS (13,14,15). These studies addressed the impact of individual CNS pathophysiological changes for multiple small molecule drugs. AD is associated with a complex, multifactorial pathophysiology, which includes but is not limited to brain shrinkage, CSF spatial expansion, brain tissue and cellular composition alteration, and BBB breakdown. Any of these factors has the potential to impact the unbound CNS PK profiles. For a disease (like AD), the impact of disease induced changes on CNS PK should be addressed in combination and not in isolation. Also, AD processes should be distinguished from processes that occur during "normal" aging. Aging represents the best-known risk factor of AD and is associated with similar, but otherwise mild pathophysiological changes (16). Thus, accounting for the pathophysiological changes observed in aging and AD should be performed in a holistic manner to improve the accuracy of CNS PK predictions in these populations (17).

In this paper, we translate the LeiCNS-PK3.0 model to predict the impact of healthy aging and AD-specific pathophysiological changes on brain and CSF PK profiles. The pathophysiological changes associated with each condition were identified from an extensive literature search. The aging and AD versions of the LeiCNS-PK3.0 model will then be used to predict the $brain_{ECF}$ and $brain_{ICF}$ PK profiles of donepezil, galantamine, memantine, and rivastigmine. In addition, two case studies of potential model applications will be performed. In case study 1, the predicted PK profiles of virtual AD patients under chronic treatment with either of the four AD drugs are compared to the relevant unbound IC_{50} at $brain_{ECF}$, $brain_{ICF}$ and CSF_{SAS}. CSF_{SAS} includes the lumbar CSF region and, in this sense, represents the most feasible sampling site of the human CNS.

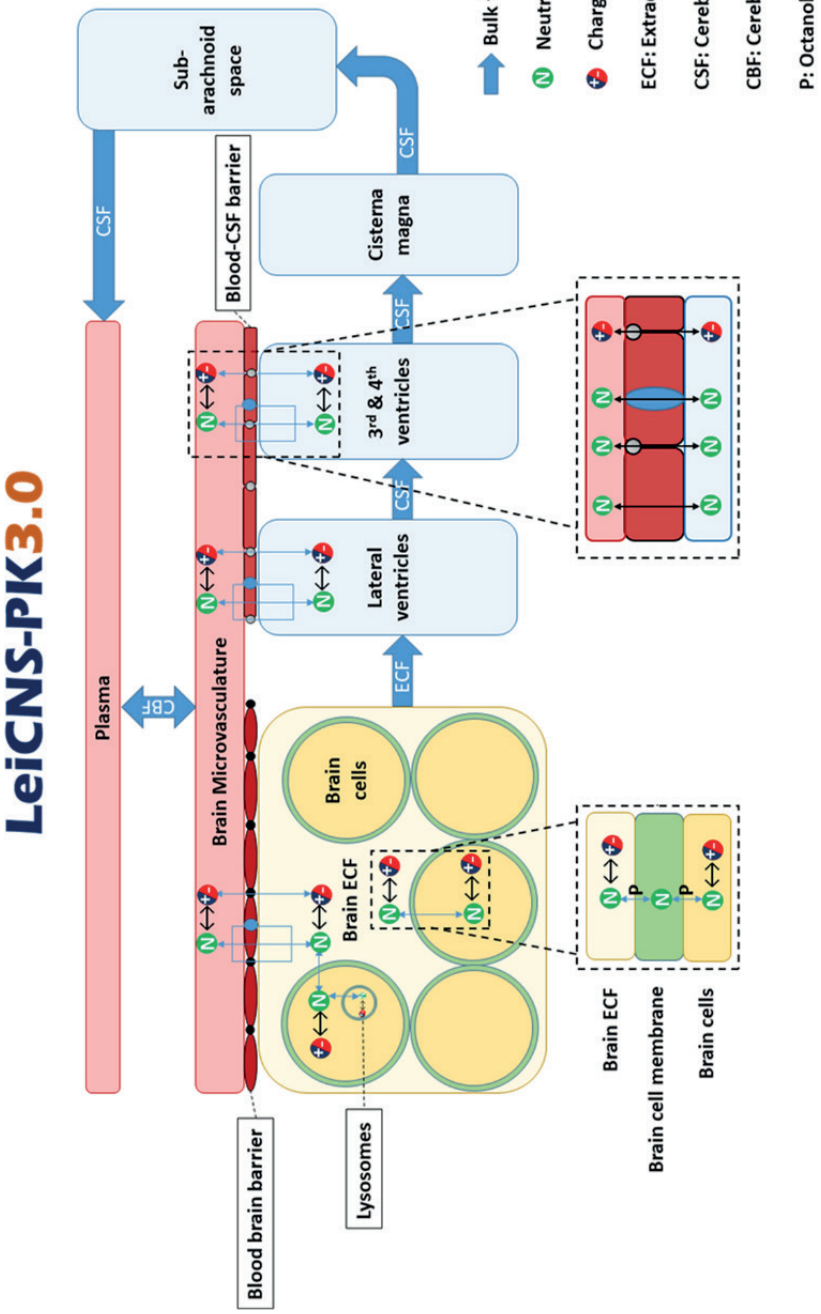

***Figure 1*. The physiologically based LeiCNS-PK3.0 model structure.** *This model uses drug physicochemical and biological properties and CNS physiology that together govern the CNS PK of a small molecule drug. This allows the translation of PK predictions in multiple CNS compartments between species and between physiological conditions (health, disease, etc.).*

In case study 2, the fluctuation of semagacestat PK profiles at $brain_{ECF}$ and $brain_{ICF}$ *versus* CSF_{SAS}, and the relation to its IC_{50} is explored. Semagacestat is a gamma secretase inhibitor that failed in clinical trials due to the lack of efficacy and safety concerns (18).

Furthermore, the LeiCNS-PK3.0 model is published as a web-based application at https://cns-pbpk.shinyapps.io/AD-SHINYAPP/ and can be used to predict the PK profiles of healthy and AD subjects. In addition, the impact of the pathophysiological changes of $brain_{ECF}$ pH and of paracellular transport on CNS PK can be assessed. These parameters were selected based on the sensitivity analysis results and represent an example of parameters with a drug-dependent impact on CNS PK, while the numerical values are the average change of these parameters in CNS diseases (15).

Methods

Translation Strategy

A knowledge-based approach was implemented to translate the predicted PK profiles of cognitively healthy young adult population (CHY) to that of cognitively healthy elderly (CHE) and of AD patients. An extensive literature study of the physiological changes of CNS parameters and processes associated with AD and aging was performed (see Literature Search for details). Results of this literature study were used to inform LeiCNS-PK3.0 parameters.

Literature Search

An extensive literature search on aging and AD-associated changes in CNS physiology was performed in the PUBMED database (19), with a focus on the parameters that are relevant to parameterization of the LeiCNS-PK3.0 model. Search queries included the terms “Alzheimer’s” or “Aging”, the terms “brain”, “CNS”, etc. and terms related to the CNS physiological parameter in question, for example “cerebrospinal fluid flow”, “blood-brain barrier”. A representation of the search terms used in this literature study is presented in the Supplementary Table 3. In addition, manual forward and backward searches using a seed article were carried out, particularly for CNS parameters with little literature information. Studies including human subjects were selected for further analysis and when humans studies were unavailable, parameter values from animal studies were used. The scaling method of a given parameter, where required, is described in the results section. Where multiple

values of the same parameter are found in literature, the mean was calculated weighed by the number of subjects included in the study.

Aging Versus AD

In this study, aging in CHE is defined as the physiological changes that occur in the CNS, from 60 years old onwards, for subjects without cognitive impairment as defined by mini-mental score examination (MMSE) scores. Subjects younger than 60 years old were therefore not considered CHE. Parameter rate of change over age was calculated as the percentage change per year from 60 years old onwards. Where literature information was not suitable for calculating %change per year, the population was divided into 3 categories: young (<60 years old), old (60–75 years old), and older old (>75 years old) and the parameter %change per year was calculated for the parameters of the older categories relative to the young category.

Age as such is not a good marker of AD progression (20), and therefore cognitive scales such as MMSE and clinical dementia rating (CDR) were used to categorize AD patients into mild, moderate, and severe patients (Table I). Information on changes in CNS physiological parameters in moderate-to-severe stages of AD are very rare and therefore we focused on predicting the PK profiles of mild AD patients, which is in line with clinical studies that target the mild AD population. Rate of change of parameters was calculated as the percentage rate of change relative to that in the age matched CHE.

Table 1. Alzheimer's Disease (AD) Severity according to CDR, MMSE, and Braak Severity Scores (21,22,23,24,25)

CDR	MMSE	Braak	AD Severity
0	30	0-II	Normal cognition
0.5	26–29	II-III	Questionable
1	21–25	III-IV	Mild
2	11–20	IV-V	Moderate
3	0–10	V-VI	Severe

CDR: Clinical Dementia Rating; MMSE: Mini-Mental State Examination

LeiCNS-PK3.0

The previously published physiologically based LeiCNS-PK3.0 model (13) was used as the base model that was translated to predict CNS PK profiles in CHE and AD patients. The model structure (Fig. 1) is composed of 9 compartments representing different physiological compartments of the CNS including brain

cells and the surrounding extracellular fluid, lysosomes, brain ventricles, cisterna magna, and CSF_{SAS}, including lumbar CSF. Plasma PK is used as input into the LeiCNS-PK3.0 model and is typically described by empirical 1-, 2-, or 3-compartment models. Other physiological processes are accounted for in the model such as brain tissue non-specific binding, the actual physiological pH in each compartment to calculate drug ionization as input for ionized and neutral drug transport across cell membranes and across the BBB and BCSFB via paracellular and transcellular routes, and drug transport by bulk fluid flow. Active transport across BBB and BCSFB is accounted for by using the asymmetry factors that are calculated and are translated as described previously (13, 14, 26). Asymmetry factors can be regarded as pure Kp_{uu} values, without influences of other steady state brain processes, for example the constant $brain_{ECF}$ bulk flow. Further details on model equations have been reported previously (13).

The LeiCNS-PK3.0 model input includes drug physicochemical, CNS physiological, and plasma PK parameters, in addition to the unbound tissue-to-plasma partition coefficient across the BBB ($Kp_{uu,BBB}$) and across BCSFB ($Kp_{uu,LV}$ and $Kp_{uu,lumbar}$) (see Table II), which can be obtained from *in vivo* or *in vitro* data. No clinically measured CNS PK data are, thus, required to run the model.

Physiological Parameters

Physiological parameters represent the CNS physiology in values such as volumes of different compartments, tissue composition, pH of fluids, flows, and transport rates across the membranes (i.e. brain barriers). Physiological parameters of the CHY were as previously described in our work (13). Physiological parameters of CHE and AD patients were calculated using the physiological values of CHY in combination with rates of change as identified from the literature search.

Plasma PK Parameters

Parameters of the empirical plasma models of the drugs are available from literature (Table III). Plasma PK parameters that were estimated based on PK data of AD patients were selected when available.

Kp_{uu} Values

$Kp_{uu,BBB}$, $Kp_{uu,LV}$, and $Kp_{uu,lumbar}$ values are used to calculate the asymmetry factor to account for the active transport of drugs across the BBB and BCSFB. $Kp_{uu,LV}$ and $Kp_{uu,lumbar}$ are calculated based on limited clinical CSF data. $Kp_{uu,BBB}$ is

rarely available in humans because of the ethical constraints of the human brain sampling with microdialysis. Therefore, $Kp_{uu,BBB}$ measured with microdialysis in rats, where available, were used to calculate $AF_{BBB,rat}$ that was translated to $AF_{BBB,human}$ based on the decision tree described previously (14). When *in vivo* $Kp_{uu,BBB}$ could not be found, Kp brain measured by brain homogenate was used and converted to $Kp_{uu,BBB,}$ by correcting for plasma protein and brain tissue binding and also for the unequal distribution of charged drug between $brain_{ECF}$ and $brain_{ICF}$ as a result of the pH difference. Equations used to convert Kp to $Kp_{uu,BBB}$ are described in the supplementary materials.

Table 2. Drug-Specific Parameters

Drug	Donepezil	Galantamine	Memantine	Rivastigmine	Semagacestat
Drug physicochemical parameters (27)					
Molecular mass (g/mol)	379.49	287.35	179.3	250.3	361.4
logP	4.14	1.16	3.31	2.45	0.44
pKa	17.02	14.81	NA	NA	11.91
pKb	8.62	8.58	10.7	8.89	–3.7
Kp_{uu} and calculated asymmetry factors (AF)[1]					
$Kp_{uu,BBB}$[2]	0.482 (28, 29)	0.826 (30)	2 (31, 32)	0.733 (29)	0.55[3]
$AF_{in,ECF}$	2.1	1	191.3	1	1
$AF_{ef,ECF}$	1	18.4	1	8.6	20.4
$Kp_{uu,LV}$[4]	1.8 (9)	1.2 (33)	0.89 (5)	0.663 (7)	0.55 (34)
$AF_{in,LV}$	1.2	19.5	1	1	1
$AF_{ef,LV}$	1	1	27	10.2	18
$Kp_{uu,lumbar}$[4]	1.8 (9)	1.2 (33)	0.89 (5)	0.663 (7)	0.55 (34)
$AF_{in,TFV}$	1.2	16.4	1	1	1
$AF_{ef,TFV}$	1	1	24.5	10.6	18.6

[1]AF factors are calculated for AD populations; [2]Rat values; [3]Assumed the same as $Kp_{uu,lumbar}$; [4]Human values

Table 3. Plasma PK Model Parameters and Dosing Regimens of Different Drugs

Drug	Donepezil	Galantamine	Memantine	Rivastigmine	Semagacestat
Plasma PK model parameters					
Population	Elderly (35)	Alzheimer's (36)	Alzheimer's (37)	Alzheimer's (7)	Volunteers (38)
Number of subjects	129	1089	108	18	14
CL_{cen} (mL min^{-1})[1]	2048	192	228	3333 [5]	846
$Q_{cen\text{-}per1}$ (mL min^{-1})[1]	0	51	0	0	0
V_{cen} (mL)	391,000	157,000	194,000	236,000	71,700
V_{per1} (mL)	0	59,000	0	0	0
K_a (min^{-1})	0.022	0.051	0.005	0.052	0.012 (39)
Biological drug properties					
$f_{u,p}$[7]	0.07 (40) [6,8]	0.83 (40) [6,9]	0.55 (40) [6]	0.6 (40) [6]	0.382 (41) [2]
$f_{u,b}$[7]	0.107 (42) [10]	0.333 (42) [2]	0.071 (43) [3, 10]	0.376 (42) [10]	0.413 (42) [2]
IC_{50} (ng mL^{-1})	0.57 (44) [4]	55 (44) [4]	109 (5)	857.2 (44) [4]	5.4 (18)
Dosing parameters					
Dose (mg)	10	10	20	6	140
Dosing	Once daily	Twice daily	Once daily	Twice daily	Once daily

[1]Apparent values and are corrected for plasma protein binding, i.e. represent unbound drug; [2]Predicted values; [3]Rat values; [4]Corrected for fraction unbound in brain ($f_{u,b}$); [5]F = 1.4 for 6 mg dose, representing relative bioavailability to 1–5 mg dose; [6]Human values; [7]$f_{u,p}$: fraction of unbound drug in plasma; $f_{u,b}$: fraction of unbound drug in brain; [8]$f_{u,p}$ was determined by ultrafiltration; [9]$f_{u,p}$ was determined by equilibrium dialysis; [10]fu,b was determined by equilibrium dialysis of brain homogenates (45)

6

Drug Properties

Drug physicochemical properties: molecular weight, lipophilicity (logP), and acid/base ionization constants were available from DrugBank release version 5.1.8 (27) and are presented in Table II. ALOGPS (46) and CHEMAXON (47) were the methods of choice to predict logP and acid/base ionization constants, respectively. Galantamine lipophilicity from the CHEMAXON method was used, as its ALOGPS value was unavailable.

Sensitivity Analysis

A sensitivity analysis was performed to assess the impact of altered CNS physiology on CNS PK and to support parameter translation where literature information gaps exist. Parameters of the AD model were increased and decreased one-at-time by two and ten folds, except for pH values that were altered by ±1 and ± 2 pH units. The C_{max}, T_{max}, half-life, and AUC of the altered PK profiles at steady state at the $brain_{ECF/ICF}$ and at the CSF_{SAS} were compared to those of the original profiles.

LeiCNS-PK3.0 Simulation and Case Studies

The AD and aging versions of LeiCNS-PK3.0 were simulated to assess the impact of aging and AD on steady state PK profiles, i.e. during chronic treatment, at $brain_{ECF}$, $brain_{ICF}$, and CSF_{SAS} as compared to those of CHY. Simulations were performed for drugs that are marketed for AD: donepezil, galantamine, memantine, and rivastigmine. The same plasma PK profile of every drug was used as input for the three populations, in order to isolate the impact of differences in CNS parameters from those of plasma. The AD PK predictions at the $brain_{ECF}$ and $brain_{ICF}$ (the CNS target sites) and the CSF_{SAS} (the CNS sampling site) were, also, compared to the respective unbound IC_{50}. *In vitro* IC_{50} values of the four drugs were available from literature. IC_{50} of donepezil, galantamine, and rivastigmine were measured *in vitro* using human brain homogenate (44) and were corrected for brain non-specific binding. IC_{50} of NMDA receptor inhibition by memantine was also quantified *in vitro* using HEK293T cells (48). In addition, a previous analysis performed by de Strooper (18) was revisited to study the fluctuation of semagacestat PK profile at $brain_{ECF}$ and $brain_{ICF}$ *versus* CSF_{SAS} while accounting for the impact of chronic dosing and AD on the PK profiles.

Software

LeiCNS-PK3.0 simulations were performed in R (version 4.0.3) using the package RxODE (version 0.9.2–0) and the LSODA (Livermore Solver for Ordinary Differential Equations) Fortran package. Literature data were digitized with WebPlotDigitizer version 4.2 (https://apps.automeris.io/wpd/).

Results

Literature Findings on CNS Pathophysiology in CHE and AD Patients

An extensive literature search was used to adapt all 35 LeiCNS-PK3.0 parameters to AD- and aging-specific pathophysiology. Results of longitudinal studies on aging-related CNS pathophysiology, where available, were preferable to cross-sectional studies, particularly when studying changes of small magnitude, e.g. brain volume shrinkage (49, 50). Data from cross-sectional designs were extracted from studies with the appropriate control, i.e. CHE *versus* CHY and AD patients *versus* CHE, such that each study would serve as its own control. Mild AD patients represent the major target population of CNS drug development and were therefore the focus of the literature study. Age is a poor marker of AD progression (20), AD severity scores (Table I) were hence used to classify AD patients. Studies comparing AD patients to age-matched CHE were selected

to distinguish between aging and AD pathophysiology, unless such studies were unavailable. A summary table of the literature study results is reported in Supplementary Table 4, including relevant references. CNS physiological parameters of CHY, CHE, and AD patients that were used as input to LeiCNS-PK3.0 are reported in Supplementary Table 1.

Total Brain Volume

Brain shrinkage begins around 50 years of healthy aging (51, 52). Longitudinal studies reported brain shrinkage as % volume shrinkage /year or as ml volume shrinkage/year, which was converted to % shrinkage/year by normalizing to baseline brain volume. Brain shrinkage rates (in %/year) were not significantly different across the different age groups (results not shown), and hence the mean of brain shrinkage (%/year) across the age groups, weighed by the study size, was calculated as 0.401%/year. The brain of an AD patient shrinks at a faster rate than that of a CHE. Data from cross-sectional studies estimated an average of 5% lower brain volume in AD patients, compared to CHE.

$Brain_{ECF}$ and $Brain_{ICF}$ Volume Fraction

$Brain_{ECF}$ and $brain_{ICF}$ volume fractions represent the volume ratio of the $brain_{ECF}$ and $brain_{ICF}$ to total brain, which in healthy conditions are 0.2 and 0.8, respectively (13). $Brain_{ECF}$ volume fraction decreased by 16% in senescent rats (26–32 months) compared to adult rats (2–3 months) and by 26% in senescent mice (17–25 months) compared to 6–8 months mice. $Brain_{ICF}$ volume fraction of the aging, shrinking brain does not change (53). $Brain_{ECF}$ volume fraction increased in mouse AD models compared to age-matched senescent mice by about 40%. No information on $brain_{ICF}$ volume fraction was retrieved and was calculated as the difference of unity and $brain_{ECF}$ volume fraction.

Volume of Brain Microvasculature

The volume of brain microvasculature declines significantly with age (54), more in the grey matter than the white matter (55, 56). The ratio of the volume of brain microvasculature to total cerebral blood flow (CBF), however, stays the same with age (54, 57) and the two parameters show a significant, linear correlation (57). In addition, brain microvascular volume to total brain tissue volume stays the same (58). Therefore, brain microvascular volume was calculated to maintain the ratio of brain microvascular volume-to-cerebral blood flow of young age. Similarly, the volume of brain microvasculature does not change in AD patients *versus* CHE and was therefore translated by correcting for the atrophied brain volume.

Brain Phospholipid Volume Fraction

Brain tissue non-specific binding of drugs is assumed to occur in LeiCNS-PK3.0 to brain phospholipids. The volume of brain phospholipids is calculated as 5% of the total brain volume and that decreases with age. The decline of the brain phospholipid volume fraction is reported to be biphasic, declining by about 10% in the CHE population between 60 and 80 years old, and further declining by another 8% in the 80–100 years CHE population. The decline rates were calculated as the mean of the values from two studies, weighted by study sample size. The relative volume of different brain structures, e.g. white *versus* grey matter volume, was also accounted for. The fraction of the unbound drug in the AD brain is higher compared to age-matched CHE (43), which is in line with a decrease of the volume fraction of brain phospholipids of 10% on average. The decrease in phospholipids was reported as region-specific (59,60,61), where it decreases in the cerebellum, frontal cortex and hippocampus, but not in prefrontal cortex and anterior temporal cortex (62, 63). Patients with early onset AD showed a 20% decrease, while late onset AD patients showed no change compared to age-matched CHE (64). The weighted average was calculated considering the differences of the volume of different brain regions, the proportions of the different phospholipids, and the study size.

CSF Volume

CSF volume expansion was calculated in a similar fashion as was brain shrinkage. The lateral and 3rd and 4th ventricles were assumed to expand at the same rate, 3.45%/year. The Cisterna magna volume expansion (1.09%/year) was calculated as the extraventricular expansion rate, using the cranial CSF and ventricular expansion rates, considering their relative volumes. The CSF_{SAS} expands at a rate of 0.78%/year. This was calculated as the extraventricular CSF expansion rate as described before and accounting for the contraction of the spinal CSF_{SAS} (65).

Similarly, in AD patients, CSF volume of the ventricles, i.e. lateral, 3rd and 4th ventricles, was assumed to be larger by 39% in AD patients that CHE. Extraventricular CSF, including cisterna magna and cranial CSF_{SAS}, expands at a different rate than ventricular CSF and is 21% larger in AD patients compared to CHE. No quantitative information were available on spinal CSF_{SAS} expansion, it can, however, be deduced that it might increase in AD as a consequence of the decrease of spinal cord volume (66), and it was, therefore, assumed to increase at the same rate as cranial CSF_{SAS}.

Cerebral Blood Flow (CBF)

CBF is reported in literature either as the total CBF (mL/min), representing blood flow to the whole brain, or as normalized CBF, where total CBF is corrected by brain mass (mL/min/100 g brain). Total CBF declines with age (67,68,69,70,71), which is attributed to brain atrophy and not to aging per se (71, 72). Normalized CBF showed no change with age, particularly above 60 years of age (73). Normalized CBF was calculated based on the CHY total CBF and brain volume and was used to calculate the total CBF at different ages, thus correcting for the impact of CHE brain shrinkage on total CBF. In AD patients, normalized CBF decreases compared to CHE in a brain region-dependent manner (74, 75). Normalized CBF is 15% lower in mild AD patients compared to CHE. Total CBF in AD patients was calculated by accounting for the AD- and brain atrophy-related reductions.

Brain$_{ECF}$ Bulk Flow

Total brain$_{ECF}$ bulk flow is known to decrease during aging and AD as a result of brain atrophy and other physiological changes including glymphatic system dysfunction, altered aquaporin-4 channel polarization and expression, and amyloid β deposition (76,77,78,79). 14C-inulin clearance in mice was reduced in senescent mice (18 months) compared to adult mice (2–3 months) by about 33% (76). Therefore, brain$_{ECF}$ bulk flow, after correction for brain atrophy, was assumed to decrease by about 33% in CHE compared to CHY. Brain$_{ECF}$ bulk flow was shown to decrease by 15% in an AD mouse model compared to wild type mouse and thus brain$_{ECF}$ bulk flow in AD patients was reduced by 15% and was corrected for brain atrophy. Results of the model's sensitivity analysis suggest that changes in brain$_{ECF}$ bulk flow has no impact on brain$_{ECF/ICF}$ PK profiles.

CSF Flow

CSF flow (mL/min) in LeiCNS-PK3.0 model is assumed to have a constant rate across the CSF spaces and is calculated using CSF turnover (day^{-1}) and the total CSF volume. CSF production did not differ significantly between CHY and CHE, neither did its flow patterns or velocity at different CSF compartments. There was, however, a small significant increase to CSF outflow with aging. CSF flow is measured at the aqueduct and at the craniocervical junction using MRI. At the aqueduct, CSF flow did not differ significantly with age, except in one study where CHE males showed a 70% higher CSF flow than younger males. At the craniocervical junction, results were contradictory. Two studies showed a decrease of CSF flow with age of about 12.5–25%, while a third study showed about 50% increase in CHE *versus* CHY. CSF production might decrease in AD (80),

although this reduction might be an artifact of the measurement technique and not AD per se (81). CSF flow is not altered in AD patients, at both the aqueduct and craniocervical junction. Given the available results, we assumed that CSF flow does not change with increasing age or with AD.

Surface Areas of the BBB and BCSFB

Surface area of the BBB represents the surface area of brain microvessels including capillaries and arterioles. BBB SA decreases with aging (82), possibly a result of the observed decrease in capillary density (58, 83, 84), the loss of brain capillaries, and the increase of brain arterioles. The decline of the BBB surface area with aging is reflected by the 10% decrease of the ratio of the brain capillary surface area to brain capillary volume and to brain tissue volume (58). Therefore, total surface area of the BBB was calculated by correcting the CHY BBB surface area for brain atrophy and for the aging-related decrease of 10%.

Direct information on the differences of surface area of the BBB in AD patients compared to CHE was not available. BBB SA can be calculated as the product of the blood vessel's perimeter, its length, and the capillary number or density. Results of the literature study implied a non-significant change of brain capillary length in AD *versus* CHE (85); a no change to a 5%-increase of capillary diameter; and a no change to 24%-increase of capillary density. Surface area of BBB in AD patients is hence the same or up to 29.3% higher than that in CHE. BBB SA was, hence, corrected for brain atrophy, in addition to an increase of 11.23% compared to CHE.

No information related to the change of BCSFB SA in aging and AD could be found and it was therefore assumed the same in CHY, CHE, and AD patients.

Paracellular Transport

BBB paracellular transport represents the drug transport across the torturous paths between the endothelial cells of the BBB. Tight junction proteins between the BBB endothelial cells limit the free passive drug diffusion and reduce the rate of paracellular transport across the BBB. During aging, tight junction protein expression is reduced (86, 87), implying the opening of the BBB and an increase in passive paracellular transport. This effect is counteracted by thickening of the basement membrane, which might reduce passive paracellular transport (86, 87). BBB passive transport is evaluated in the clinic using imaging of gadolinium-based contrast agents. In one study, an increase of BBB passive permeability of about 40% was observed at the hippocampus and caudate

nucleus, but not at the superior frontal and inferior temporal gyrus cortex, thalamus, striatum, white matter (WM), corpus collosum, or internal capsule; all these showed no significant difference (88). In another study, an increase of BBB passive permeability of 0.0001%/year or $1.48*10^{-12}$ min^{-1}/year was estimated in grey and white matter (89). Given these data, aging is not expected to impact BBB passive permeability.

Similar to aging, in AD the decrease of tight junction proteins expression and the thickening of the basement membrane impact passive paracellular transport in opposite directions (90). BBB passive paracellular transport, as measured with MRI and contrast agents, demonstrated up to 1.25-, 5-, and 10-fold increase at the hippocampus, grey matter, and cortex, respectively (91). Other regions such as white matter and basal ganglia showed no change of paracellular transport. A mean value of 4.4-fold increase of paracellular transport was used.

Studies comparing the paracellular transport at BCSFB between CHY and CHE and between AD and age-matched CHE were not available in literature. CSF-to-plasma ratio of creatinine and urea showed an increase of 23% and 7%, respectively in AD patients compared to young volunteers (92). Given the small magnitude and the lack of age matching controls in the available study we assumed that paracellular transport at BCSFB is the same in all three populations.

BBB Active Transport

The expression and function of Pgp at the BBB in CHE *versus* CHY have been evaluated. Pgp protein and mRNA expression measured with immunohistochemistry showed no significant difference between CHY and CHE populations. Pgp function in CHY *versus* CHE was examined using MR imaging of 11C-verapamil BBB transport and calculating the ratio of the efflux to influx transfer rate constants. Such approach demonstrated that the change of BBB Pgp transport of verapamil ranges from no significant change to about 40% decrease in the Pgp function at the BBB. Interestingly, CHE population demonstrated a higher susceptibility to Pgp inhibition (93). The coadministration of 11C-verapamil and tariquidar resulted in a 30% decrease of Pgp function compared to the administration of solely 11C-verapamil, while Pgp function was not impacted in the young population (93). Collectively, these findings imply that with aging Pgp expression and function do not change, except when a drug is co-administrated with another Pgp substrate or inhibitor. No information could be retrieved on BCRP expression or function at the BBB and its activity was assumed the same in CHE as in CHY.

Information on expression and function of the active transporters, Pgp and BCRP, indicate that BBB active transport might decrease in AD patients. Expression studies of Pgp and BCRP proteins with immunohistochemistry showed a no change to a decrease of expression of 15% and 20%, respectively. Pgp and BCRP protein expression measured with other quantitative techniques such as western blot and LC-MS demonstrated no significant change of the protein expression of both transporters. Studies of BBB Pgp function indicated a no change to a 15–30% decrease of BBB Pgp activity in AD patients. No quantitative information could be retrieved on the changes of active transporters activity and expression at the BCSFB.

The impact of the potential difference of BBB active transporters expression and function on brain PK should be assessed on a drug-by-drug basis, considering the affinity of a single or multiple active transporter to the drug. Donepezil is a substrate of choline transporters (CHT) (94), Pgp, and BCRP (95). No studies could be identified that report on rat-to-human differences in CHT's expression. Pgp and BCRP protein expression is 0.22- and 1.1-fold different, respectively, in human's brain microvessels *versus* that of rat (15). The asymmetry factors of donepezil were calculated based on rat $Kp_{uu,BBB}$ and were converted to those of humans by multiplying by 0.22 and 1.1. Galantamine is not a substrate of the major BBB transporters: Pgp, BCRP, MRP4, or of cationic transporters: CHT and OCT; no conversion of asymmetry factors was required. Memantine is a substrate of OCTN1 transporter (96, 97), the expression of which does not change in the brains of AD patients *versus* CHE (98). No information on the rat-to-human differences of OCTN1 expression could be found. Brain-to-plasma drug concentration ratio measured in human was similar to that of rats (99) and therefore asymmetry factors based on rat $Kp_{uu,BBB}$ were calculated. Rivastigmine is a substrate of the CHT (94); the asymmetry factors based on preclinical data were used.

$Brain_{ECF}$, $Brain_{ICF}$ and CSF pH

Multiple studies reported a 0.001 unit decrease of brain pH per year of aging (100,101,102,103); these studies did not distinguish intracellular and extracellular brain pH. Other studies reported no change of brain extracellular pH (104, 105), which is supported with data from preclinical species, where only brain intracellular pH decreased but not brain extracellular pH (106). Brain intracellular pH was, hence, assumed to decrease by 0.001 pH unit/year, while $brain_{ECF}$ pH stays the same. The pH of CSF of CHE was similar to that of CHY (107).

Studies reported changes in brain pH from pre- and postmortem CHE and AD patients, without discerning intra- or extracellular brain pH. Studies with postmortem data were excluded, as the potential of postmortem brain acidosis increases, particularly with long postmortem-to-tissue collection intervals and in individual with high premortem agony. Changes of brain pH ranged from 0 to an increase of 0.009 pH units, as measured in the brain cortex and hippocampus. The white matter on the other hand decreased by 0.007 pH units in AD patients. No information was available from premortem subjects on cranial CSF pH, which was found to decrease by an average of 0.11 pH units in postmortem samples. Lumbar CSF pH, on the contrary, might increase by 0.018 pH units in AD patients, as compared to healthy young subjects.

Model Simulations and Case Studies

The LeiCNS-PK3.0 model was used to explore the impact of the pathophysiological changes of aging and AD on the steady state PK profiles of AD drugs at the $brain_{ECF}$, $brain_{ICF}$, and the CSF_{SAS}. The parameters of the plasma PK model were based on datasets that included AD patients, except for donepezil, which was based on a CHE population.

Aging and AD Have a Minor Impact on $Brain_{ECF}$, $Brain_{ICF}$, and CSF_{SAS} PK Profiles

Model simulations of CHY, CHE, and AD populations of the four drugs are depicted in Fig. 2. $Brain_{ECF}$, $brain_{ICF}$ and CSF_{SAS} PK profiles were minimally altered with aging- and AD-related pathophysiological alterations. The change of rivastigmine steady state C_{max}, while the most prominent, was less than two-fold.

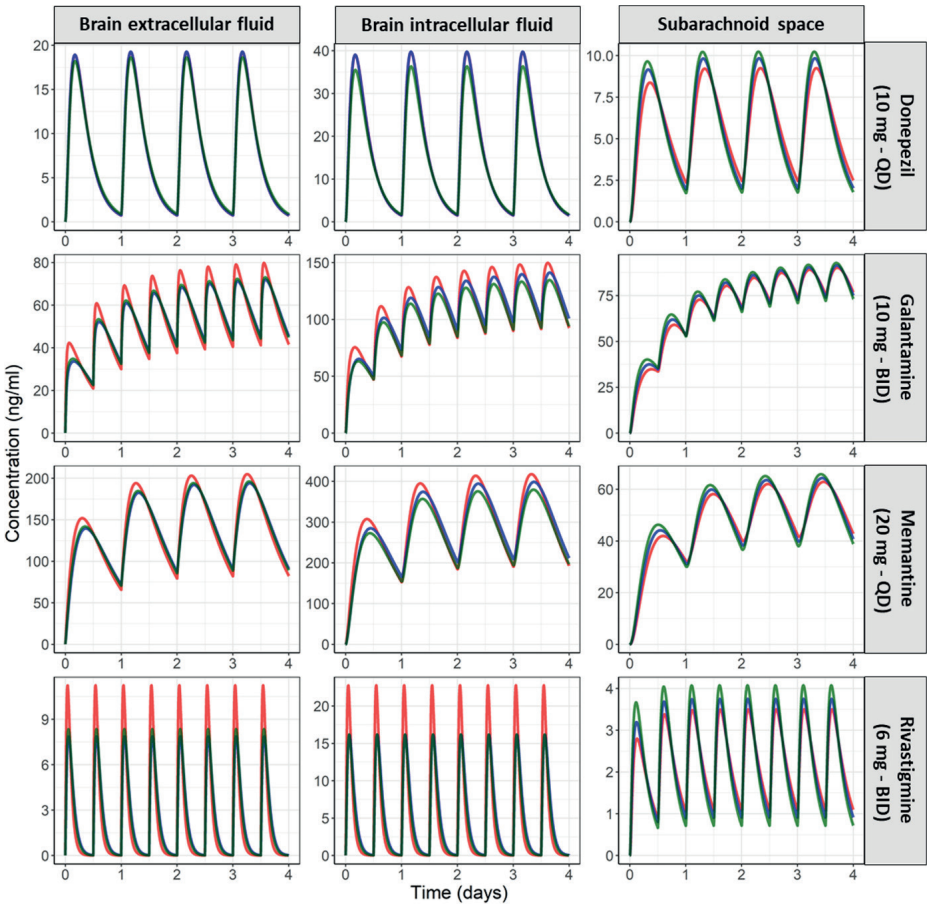

Figure 2. Simulated unbound PK profiles of the four marketed AD drugs at brain$_{ECF}$, brain$_{ICF}$, and subarachnoid space (CSF$_{SAS}$) of CHY (green), CHE (blue), and AD (red) populations. *Aging and AD pathophysiological changes have a minor impact on brain$_{ECF}$, brain$_{ICF}$, and CSF$_{SAS}$ PK profiles. Model simulations were performed using the clinical dosing regimens. For each drug, the plasma PK input in the model was based on plasma PK data of CHE or AD patients. Thus, any change of PK profile is attributed to changes of CNS physiology. Please note the different y-axis scale of every panel. Brain$_{ECF}$: brain extracellular fluid, brain$_{ICF}$: brain intracellular fluid, CSF$_{SAS}$: cerebrospinal fluid of the subarachnoid space, CHY: cognitively healthy young adults, CHE: cognitively healthy elderly.*

Case Study 1: Brain and CSF_{SAS} PK Profiles Compared to IC_{50} of the Respective Target

A comparison between predicted AD PK profile at the $brain_{ECF}$, $brain_{ICF}$, and CSF_{SAS} *versus* the IC_{50} of the respective drug target is depicted in Fig. 3. The $brain_{ECF}$ and $brain_{ICF}$ represent the target site of the cholinesterase inhibitors: donepezil, galantamine, and rivastigmine (108), while $brain_{ECF}$ is the target site of the N-methyl-D-aspartate receptor antagonist, memantine (4). The predicted rivastigmine PK profiles at different CNS locations were consistently below IC_{50}, while the $brain_{ECF}$ and $brain_{ICF}$ PK profiles of memantine and galantamine were below the IC_{50} briefly between the doses. The predicted PK profile of memantine at the CSF_{SAS} was below the IC_{50}, but not at the $brain_{ECF/ICF}$.

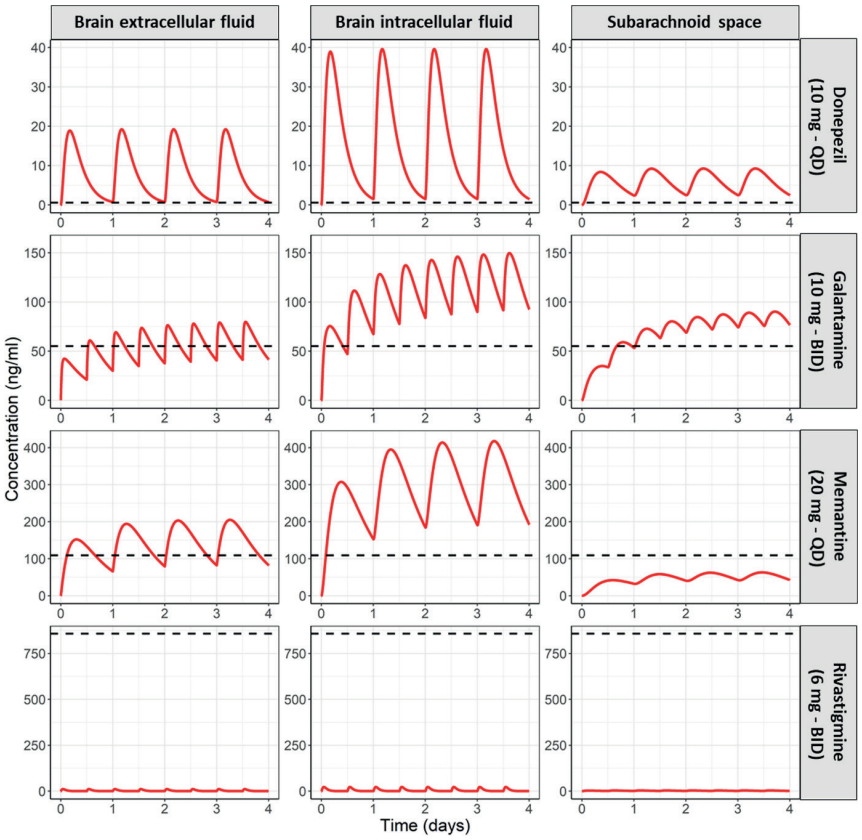

Figure 3. AD predicted PK profiles of the 4 marketed AD drugs at the $brain_{ECF}$, $brain_{ICF}$, and CSF_{SAS} versus the IC_{50} of the respective drug target. Target site concentrations are the driver of drug effect and should therefore be evaluated during early stages of drug development. *The predicted PK profiles of rivastigmine are below the IC_{50} of acetylcholinesterase. Memantine PK profile at the CSF_{SAS} and not at the $brain_{ECF}$ were lower than the IC_{50} of NMDA receptor, which might imply that lumbar CSF_{SAS} drug concentration is an inaccurate surrogate of that of $brain_{ECF}$.*

Case Study 2: The Importance of Addressing Target Site Concentrations

The PK profiles of semagacestat in $brain_{ECF}$, $brain_{ICF}$, and CSF_{SAS} of CHY and AD patients are depicted in Fig. 4. Model simulations indicate a higher fluctuation of the PK profile at the $brain_{ECF}$ and $brain_{ICF}$ (C_{max}:C_{min} ≈ 9*10^4) than at the CSF_{SAS} (C_{max}:C_{min} ≈ 13). In addition, they show that the brain enters a drug-free period as of 12 hours post dose, unlike CSF_{SAS} PK profiles that are consistently above the IC_{50}.

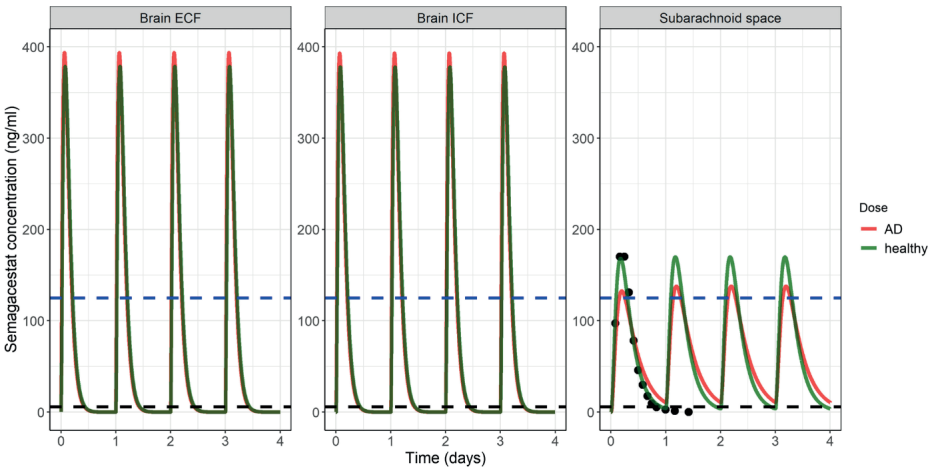

Figure 4. Semagacestat PK profiles of cognitively healthy (CHY) young volunteers (green) and AD patients (red) at the $brain_{ECF}$, $brain_{ICF}$ and at the CSF_{SAS}. *The black dots in the CSF_{SAS} are semagacestat concentrations at a single dose of 140 mg, measured in CSF samples from CHY volunteers (34). The blue horizontal dashed line represents the paradoxical value used by de Strooper (18) of notch inhibition, while black dashed line represents the IC_{50} of gamma-secretase inhibition by semagacestat. These simulations support the take home messages of the de Strooper (18) analysis on the importance of addressing the fluctuation of the drug concentrations and, in addition, indicate the importance of considering the steady state, potentially disease-altered, PK profiles at the target sites in the $brain_{ECF}$ and $brain_{ICF}$.*

Discussion

In this study, the CNS PBPK LeiCNS-PK3.0 model was translated to predict the CNS drug distribution of the elderly and AD populations. Model predictions under chronic dosing of the four marketed AD small molecule drugs showed a different pattern of PK profiles fluctuation (C_{max}:C_{min}) between different compartments. In addition, comparing the predicted PK profiles at the CNS target sites in

$brain_{ECF}$ and $brain_{ICF}$ and at the CSF_{SAS} to the IC_{50} value of the respective drug target demonstrated the importance of target site drug concentrations, rather than surrogate compartments, as drivers of drug effect. Interestingly, model simulations showed a little to no impact of AD and healthy aging on the CNS PK profiles, including the target sites.

AD pathophysiology has been studied intensively in humans and in preclinical species, particularly the changes related to BBB integrity but also those related to CBF, $brain_{ECF}$ bulk flow, CSF flow, etc. (109), suggesting the possible alteration of CNS PK. Little, however, is available on the overall impact of the AD pathophysiological changes on CNS PK per se (110). This study is the first, to the best of the authors' knowledge, to investigate the potential changes of CNS PK associated with healthy aging or AD, showing that both are of little effect. $Brain_{ECF}$ and $brain_{ICF}$ PK profiles of rivastigmine showed the largest difference between CHY/CHE and AD patients, the predicted increase of C_{max} was, however, less than two-fold. We identified the four-fold increase of paracellular transport as the major contribution to the predicted change of rivastigmine brain PK. This was assessed by testing the AD altered parameter values in the model one parameter at a time and observing the parameter's impact on brain PK (results not shown). These results are in line with a clinical study that demonstrated a minor increase in the exposure of LY2886721 lumbar CSF exposure in AD patients compared to healthy volunteers (111) and with a preclinical study that showed no change of the extent of drug transport across the BBB in a transgenic AD mouse model (112). Taken together, it can be implied that CNS drug concentration measured in young adults might represent that of AD patients. Accounting for the interpopulation differences in physiological characteristics improves brain exposure predictions (113), towards personalized medicine in aging and AD populations (17).

$Brain_{ECF,}$ $brain_{ICF}$, and CSF_{SAS} PK profiles of the four marketed AD drugs were compared to the *in vitro* IC_{50} values of the brain cholinesterases and of the NMDA receptor. The dosing regimens of these drugs were the same as the ones used in the clinic. $Brain_{ECF}$ PK profiles, the target site of the four drugs (4, 108), were above the IC_{50} value, except for rivastigmine. Apart from rivastigmine, these results are expected for successful drugs on the market. Rivastigmine is a dual inhibitor of acetylcholinesterase (IC_{50} = 857.2 ng/ml (44)) and butyrylcholinesterase (IC_{50} = 9.3 ng/ml (114)) and acts at both the $brain_{ECF}$ and $brain_{ICF}$. At 6 mg twice daily dosing, the $brain_{ECF}$ unbound concentrations of rivastigmine were below the IC_{50} of both enzymes. The $brain_{ICF}$ PK profiles were,

however, above the IC_{50} of butyrylcholinesterase (Supplementary Fig. 1), the activity of which has been demonstrated to increase with AD progression, in contrast to the activity of acetylcholinesterase, which might decrease (2, 3, 115). Thus, the known therapeutic benefit of rivastigmine can be attributed to dual inhibition of the two cholinesterase enzymes.

The pattern of drug exposure compared to IC_{50} was the same in the CSF_{SAS} and $brain_{ECF/ICF}$ for all drugs, except memantine. Memantine exposure was lower than the IC_{50} at the CSF_{SAS}, but not at the $brain_{ECF/ICF}$. This is in line with a previous clinical study, where memantine CSF concentration of the majority of the study subjects was lower than IC_{50}, despite an observed clinical effect. This mismatch between the PK profiles at $brain_{ECF}$ and $brain_{ICF}$ and CSF_{SAS} further corroborate previous findings (12, 13) that lumbar CSF is an inaccurate surrogate of brain drug concentrations.

Unestablished target site PK has resulted in as high as one-third of the failures observed in drug development in general (116). Our model predicts the unbound PK of the $brain_{ECF/ICF}$ in CHE and AD patients, by holistically accounting for the associated multifactorial pathophysiology and thus addresses the previously identified PK information gaps and focuses on the AD population that is a prime target population of CNS drug development (90, 110). De strooper (18) identified the learned lessons of a failed clinical trial, studying semagacestat and highlighted the consequences of a fluctuating PK profile on the observed (un)desired drug effect (18). The analysis was, however, performed based on a single dose PK profile from healthy, young volunteers and did not consider the potential impact of AD on CNS PK, the target site PK profile, and steady state PK condition. Our model simulations (Fig. 5) indicate a drastically higher fluctuation of the PK profile at the $brain_{ECF}$ and $brain_{ICF}$ than at the CSF_{SAS}, resulting in the different pattern of drug availability of the two compartments. This further highlights the importance of studying target site concentrations as surrogates of drug effect.

Literature information was used to adapt the physiological parameters of LeiCNS-PK3.0 to AD and aging conditions. Comparison of parameter values from different populations across the different studies was avoided where possible, primarily because of different measurement and analysis techniques used in by each study. A clear example was the four orders of magnitude difference of the paracellular permeability calculated as K_{trans} in two different studies (88, 89), which could be attributed to the difference of the imaging protocols, contrast

agents, and MR devices. Careful interpretation of heterogeneous literature data on a parameter-by-parameter basis is a crucial requirement to ensure an "as accurate as" possible CNS PK prediction. Meta-analysis studies, performed for each parameter, could provide an unbiased estimate of the parameter mean and the associated variability, further improving the accuracy of model predictions.

A major limitation of this work is that the AD/aging models were not validated against clinical PK data. To the best of the authors' knowledge, no PK measurements in AD and elderly brain are available. We identified several clinical studies where lumbar CSF PK profiles were measured in AD patients on chronic treatment with either donepezil, memantine, or rivastigmine (5,6,7,8,9). The data were, however, inadequate for model validation either because of the missing sampling time after the donepezil dose (9), the unrealistically higher plasma and CSF donepezil and memantine concentrations at the end of the dosing interval (5, 6), or the unavailability of population plasma PK profile of rivastigmine (7, 8). Another limitation related to the knowledge-based translation approach is that the accuracy of the PK predictions is reliant on the extent and quality of available literature. Literature studies on few parameters were either missing, inaccurate, or contradictory and might reduce the reliability and accuracy of the model. For example, no literature reports could be identified on AD- or aging-related changes of lysosomal volume, lysosomal de-acidification, surface area and the paracellular transport of the blood-CSF barrier. To address this drawback, a sensitivity analysis of the AD model was performed (Supplementary Fig. 2) and indicated that these parameters do not have a major impact on the major target site, i.e. $brain_{ECF}$ PK profile and were therefore assumed the same as the healthy condition (13). In addition, contradictory results were found regarding changes of CSF flow in AD, ranging from no change to an increase in AD patients compared to CHE. CSF flow does not impact the $brain_{ECF}$ PK profiles, but does impact the sampling site, i.e. lumbar CSF, and might result in inaccurate implication regarding the rate of drug removal from the CNS. Addressing the knowledge gaps and inaccuracies of AD-related pathophysiology would further improve the model's reliability. The model as currently presented, thus, cannot yet replace preclinical and clinical studies. LeiCNS-PK3.0 nevertheless is suited to support early stages of drug development, mainly in initial drug screening and design and analysis of first-in-human trials.

The LeiCNS-PK3.0 model provides insights of small molecule drug PK of $brain_{ECF}$ and $brain_{ICF}$ in AD patients, and can therefore help in optimizing and

accelerating the development of small molecule drugs for AD. To date, the marketed small molecule drugs have been approved for merely the symptomatic management of AD. Emerging multitarget treatment approach have shown potential as disease modifying agent and potential treatment of AD. This can be either by polypharmacy (i.e. combining multiple drugs) (117) or by multi-target-directed ligand (i.e. single drug acting on multiple targets) (118). To this end, in silico methods are useful to explore the therapeutic advantages of this multitarget approach. For example, combining our model (i.e. PK component) with a quantitative systems pharmacology model (i.e. pharmacodynamic component) of AD disease pathways will allow the exploration of possible interaction of drug target site exposure (in case of polypharmacy) or effect (117).

Conclusion

In this study, a literature-based approach was used to translate the CNS PBPK LeiCNS-PK3.0 model to predict the CNS PK profile of elderly and AD populations. Steady state $brain_{ECF}$ PK predictions of donepezil, galantamine, and memantine were above the respective IC_{50}. Fluctuations of the PK profile of semagacestat showed distinct patterns in brain compared to CSF_{SAS}. CNS PK profiles were comparable among CHY, CHE, and AD patients implying a minor impact of healthy aging and AD on CNS PK, including the target sites.

LeiCNS-PK3.0 is available as a web-based application (https://cns-pbpk.shinyapps.io/AD-SHINYAPP/) that can be used to predict CNS PK profiles of CHY and AD populations, in addition to the impact of selected pathophysiological changes on CNS PK.

Acknowledgements
The authors would like to acknowledge Dr. Makoto Hirasawa for his help on reviewing the model's code and the manuscript. We would like also to thank Ms. Luhe Xia, Ms. Banu Özbakir, and Mr. Bart Faas for their contribution to the literature study.

References

1. Raina P, Santaguida P, Ismaila A, Patterson C, Cowan D, Levine M, et al. Effectiveness of cholinesterase inhibitors and memantine for treating dementia: evidence review for a clinical practice guideline. Ann Intern Med. 2008;148(5):379–97.
2. Greig NH, Lahiri DK, Sambamurti K. Butyrylcholinesterase: an important new target in Alzheimer's disease therapy. Int Psychogeriatrics. 2002;14(SUPPL. 1):77–91.
3. Lane RM, Potkin SG, Enz A. Targeting acetylcholinesterase and butyrylcholinesterase in dementia. Int J Neuropsychopharmacol. 2006;9(1):101–24.
4. Parsons CG, Gilling KE, Jatzke C. Memantine does not show intracellular block of the NMDA receptor channel. Eur J Pharmacol 2008;587(1–3):99–103.
5. Valis M, Herman D, Vanova N, Masopust J, Vysata O, Hort J, et al. The concentration of memantine in the cerebrospinal fluid of Alzheimer's disease patients and its consequence to oxidative stress biomarkers. Front Pharmacol. 2019;10:943.
6. Valis M, Masopust J, Vysata O, Hort J, Dolezal R, Tomek J, et al. Concentration of donepezil in the cerebrospinal fluid of AD patients: evaluation of dosage sufficiency in standard treatment strategy. Neurotox Res. 2017;31(1):162–8.
7. Gobburu JVS, Tammara V, Lesko L, Jhee SS, Sramek JJ, Cutler NR, et al. Pharmacokinetic-pharmacodynamic modeling of rivastigmine, a cholinesterase inhibitor, in patients with Alzheimer's disease. J Clin Pharmacol. 2001;41(10):1082–90.
8. Cutler NR, Polinsky RJ, Sramek JJ, Enz A, Jhee SS, Mancione L, et al. Dose-dependent CSF acetylcholinesterase inhibition by SDZ ENA 713 in Alzheimer's disease. Acta Neurol Scand. 1998;97:244–50.
9. Darreh-Shori T, Meurling L, Pettersson T, Hugosson K, Hellström-Lindahl E, Andreasen N, et al. Changes in the activity and protein levels of CSF acetylcholinesterases in relation to cognitive function of patients with mild Alzheimer's disease following chronic donepezil treatment. J Neural Transm. 2006;113(11):1791–801.
10. De Lange ECM, van den Brink W, Yamamoto Y, de Witte WEA, Wong YC. Novel CNS Drug discovery and development approach: model-based integration to predict neuro-pharmacokinetics and pharmacodynamics. Expert Opin drug Discov. 2017;12(12):1207–18.
11. Guo Y, Chu X, Parrott NJ, Brouwer KLR, Hsu V, Nagar S, et al. Advancing predictions of tissue and intracellular drug concentrations using in vitro, imaging and physiologically based pharmacokinetic modeling approaches. Clin Pharmacol Ther. 2018;104(5):865–89.
12. Gaohua L, Neuhoff S, Johnson TN, Rostami-hodjegan A. Development of a permeability-limited model of the human brain and cerebrospinal fl uid (CSF) to integrate known physiological and biological knowledge : estimating time varying CSF drug concentrations and their vari. Drug Metab Pharmacokinet. 2016;31(3):224–33.
13. Saleh MAA, Loo CF, Elassaiss-Schaap J, De Lange ECM. Lumbar cerebrospinal fluid-to-brain extracellular fluid surrogacy is context-specific: insights from LeiCNS-PK3.0 simulations. J Pharmacokinet Pharmacodyn. 2021;48(5):725–41.
14. Yamamoto Y, Välitalo PA, Wong YC, Huntjens DR, Proost JH, Vermeulen A, et al. Prediction of human CNS pharmacokinetics using a physiologically-based pharmacokinetic modeling approach. Eur J Pharm Sci. 2018;112(September 2017):168–79.
15. Saleh MAA, de Lange ECM. Impact of CNS diseases on drug delivery to brain extracellular and intracellular target sites in human: a "WHAT-IF" simulation study. Pharmaceutics. 2021;13(1):1–17.

16. Xia X, Jiang Q, McDermott J, Han JDJ. Aging and Alzheimer's disease: comparison and associations from molecular to system level. Aging Cell. 2018;17(5):1–14.
17. Schlender JF, Meyer M, Thelen K, Krauss M, Willmann S, Eissing T, et al. Development of a whole-body physiologically based pharmacokinetic approach to assess the pharmacokinetics of drugs in elderly individuals. Clin Pharmacokinet. 2016;55(12):1573–89.
18. De Strooper B. Lessons from a failed γ-secretase Alzheimer trial. Cell. 2014;159(4):721–6.
19. Coordinators NR. Database resources of the National Center for biotechnology information. Nucleic Acids Res. 2018;46(D1):D8–13.
20. Jack CR, Bennett DA, Blennow K, Carrillo MC, Dunn B, Haeberlein SB, et al. NIA-AA research framework: toward a biological definition of Alzheimer's disease. Alzheimers Dement. 2018;14(4):535–62.
21. McKhann G, Drachman D, Folstein M, Katzman R, Price D, Stadlan EM. Clinical diagnosis of Alzheimer's disease: report of the NINCDS-ADRDA work group under the auspices of Department of health and human servicestask force on Alzheimer's disease. Neurology. 1984;34(7):939–44.
22. Braak H, Alafuzoff I, Arzberger T, Kretzschmar H, Tredici K. Staging of Alzheimer disease-associated neurofibrillary pathology using paraffin sections and immunocytochemistry. Acta Neuropathol. 2006;112(4):389–404.
23. Perneczky R, Wagenpfeil S, Komossa K, Grimmer T, Diehl J, Kurz A. Mapping scores onto stages: mini-mental state examination and clinical dementia rating. Am J Geriatr Psychiatry. 2006;14(2):139–44.
24. Pangman VC, Sloan J, Guse L. An examination of psychometric properties of the mini-mental state examination and the standardized mini-mental state examination: implications for clinical practice. Appl Nurs Res. 2000;13(4):209–13.
25. Wischik CM, Harrington CR, Storey JMD. Tau-aggregation inhibitor therapy for Alzheimer's disease. Biochem Pharmacol. 2014;88(4):529–39.
26. Yamamoto Y, Välitalo P, Huntjens D, Proost J, Vermeulen A, Krauwinkel W, et al. Predicting drug concentration-time profiles in multiple relevant CNS compartments using a comprehensive physiologically-based pharmacokinetic model. CPT Pharmacometrics Syst Pharmacol. 2017;6(11):765–77.
27. Wishart DS, Feunang YD, Guo AC, Lo EJ, Marcu A, Grant JR, et al. DrugBank 5.0: a major update to the DrugBank database for 2018. Nucleic Acids Res. 2017;46(D1):D1074–82.
28. Summerfield SG, Zhang Y, Liu H. Examining the uptake of central nervous system drugs and candidates across the blood-brain barrier. J Pharmacol Exp Ther. 2016;358(2):294–305.
29. Karasova JZ, Hrabinova M, Krejciova M, Jun D, Kuca K. Donepezil and rivastigmine: pharmacokinetic profile and brain-targeting after intramuscular administration in rats. Iran J Pharm Res. 2020;19(3):95–102.
30. Bickel U, Thomsen T, Fischer JP, Weber W, Kewitz H. Galanthamine: pharmacokinetics, tissue distribution and cholinesterase inhibition in brain of mice. Neuropharmacology. 1991;30(5):447–54.
31. Kitamura A, Okura T, Higuchi K, Deguchi Y. Cocktail-dosing microdialysis study to simultaneously assess delivery of multiple organic-cationic drugs to the brain. J Pharm Sci. 2016;105(2):935–40.

32. Hesselink MB, De Boer BG, Breimer DD, Danysz W. Brain penetration and in vivo recovery of NMDA receptor antagonists amantadine and memantine: a quantitative microdialysis study. Pharm Res. 1999;16(5):637–42.

33. Bakker C, van der Aart J, Hart EP, Klaassen ES, Bergmann KR, van Esdonk MJ, et al. Safety, pharmacokinetics, and pharmacodynamics of Gln-1062, a prodrug of galantamine. Alzheimer's Dement Transl Res Clin Interv. 2020;6(1):1–10.

34. Bateman RJ, Siemers ER, Mawuenyega KG, Wen G, Browning KR, Sigurdson WC, et al. A γ-secretase inhibitor decreases amyloid-γproduction in the central nervous system. Ann Neurol. 2009;66(1):48–54.

35. Noetzli M, Guidi M, Ebbing K, Eyer S, Wilhelm L, Michon A, et al. Population pharmacokinetic approach to evaluate the effect of CYP2D6, CYP3A, ABCB1, POR and NR1I2 genotypes on donepezil clearance. Br J Clin Pharmacol. 2014;78(1):135–44.

36. Piotrovsky V, Van Peer A, Van Osselaer N, Armstrong M, Aerssens J. Galantamine population pharmacokinetics in patients with Alzheimer's disease: modeling and simulations. J Clin Pharmacol. 2003;43(5):514–23.

37. Noetzli M, Guidi M, Ebbing K, Eyer S, Wilhelm L, Michon A, et al. Population pharmacokinetic study of memantine: effects of clinical and genetic factors. Clin Pharmacokinet. 2013;52(3):211–23.

38. Willis BA, Zhang W, Ayan-Oshodi M, Lowe SL, Annes WF, Sirois PJ, et al. Semagacestat pharmacokinetics are not significantly affected by formulation, food, or time of dosing in healthy participants. J Clin Pharmacol. 2012;52(6):904–13.

39. Madrasi K, Das R, Mohmmadabdul H, Lin L, Hyman BT, Lauffenburger DA, et al. Systematic in silico analysis of clinically tested drugs for reducing amyloid-beta plaque accumulation in Alzheimer's disease. Alzheimer's Dement. 2021;17(9):1487–98.

40. Noetzli M, Eap CB. Pharmacodynamic, pharmacokinetic and pharmacogenetic aspects of drugs used in the treatment of alzheimer's disease. Clin Pharmacokinet. 2013;52(4):225–41.

41. Watanabe R, Esaki T, Kawashima H, Natsume-Kitatani Y, Nagao C, Ohashi R, et al. Predicting fraction unbound in human plasma from chemical structure: improved accuracy in the low value ranges. Mol Pharm. 2018;15(11):5302–11.

42. Esaki T, Ohashi R, Watanabe R, Natsume-Kitatani Y, Kawashima H, Nagao C, et al. Computational model to predict the fraction of unbound drug in the brain. J Chem Inf Model. 2019;59(7):3251–61.

43. Gustafsson S, Sehlin D, Lampa E, Hammarlund-Udenaes M, Loryan I. Heterogeneous drug tissue binding in brain regions of rats, Alzheimer's patients and controls: impact on translational drug development. Sci Rep. 2019;9(1):5308.

44. Jackisch R, Förster S, Kammerer M, Rothmaier AK, Ehret A, Zentner J, et al. Inhibitory potency of choline esterase inhibitors on acetylcholine release and choline esterase activity in fresh specimens of human and rat neocortex. J Alzheimers Dis. 2009;16(3):635–47.

45. Di L, Umland JP, Chang G, Huang Y, Lin Z, Scott DO, et al. Species independence in brain tissue binding using brain homogenates. Drug Metab Dispos. 2011;39(7):1270–7.

46. Mannhold R, Poda GI, Ostermann C, Tetko IV. Calculation of molecular lipophilicity: state-of-the-art and comparison of LogP methods on more than 96,000 compounds. J Pharm Sci. 2009;98(3):861–93.

47. Manchester J, Walkup G, Rivin O, You Z. Evaluation of pka estimation methods on 211 Druglike compounds. J Chem Inf Model. 2010;50(4):565–71.

48. Kotermanski SE, Johnson JW. Mg 2+ imparts NMDA receptor subtype selectivity to the Alzheimer's drug memantine. J Neurosci. 2009;29(9):2774–9.

49. Sigurdsson S, Aspelund T, Forsberg L, Fredriksson J, Kjartansson O, Oskarsdottir B, et al. Brain tissue volumes in the general population of the elderly. The AGES-Reykjavik Study. Neuroimage. 2012;59(4):3862–70.
50. Resnick SM, Pham DL, Kraut MA, Zonderman AB, Davatzikos C. Longitudinal magnetic resonance imaging studies of older adults: a shrinking brain. J Neurosci. 2003;23(8):3295–301.
51. Liu RSN, Lemieux L, Bell GS, Sisodiya SM, Shorvon SD, Sander JWAS, et al. A longitudinal study of brain morphometrics using quantitative magnetic resonance imaging and difference image analysis. Neuroimage. 2003;20(1):22–33.
52. Matsumae M, Kikinis R, Mórocz IA, Lorenzo AV, Sándor T, Albert MS, et al. Age-related changes in intracranial compartment volumes in normal adults assessed by magnetic resonance imaging. J Neurosurg. 1996;84(6):982–91.
53. Thulborn K, Lui E, Guntin J, Jamil S, Sun Z, Claiborne TC, et al. Quantitative sodium MRI of the human brain at 9.4T provides assessment of tissue sodium concentration and cell volume fraction during normal aging. NMR Biomed. 2016;29(2):137–43.
54. Leenders KL, Perani D, Lammertsma AA, Heather JD, Buckingham P, Jones T, et al. Cerebral blood flow, blood volume and oxygen utilization: Normal values and effect of age. Brain. 1990;113(1):27–47.
55. Wenz F, Rempp K, Brix G, Knopp MV, Gückel F, Hess T, et al. Age dependency of the regional cerebral blood volume (rCBV) measured with dynamic susceptibility contrast MR imaging (DSC). Magn Reson Imaging. 1996;14(2):157–62.
56. Rempp KA, Brix G, Wenz F, Becker CR, Gückel F, Lorenz WJ. Quantification of regional cerebral blood flow and volume with dynamic susceptibility contrast-enhanced MR imaging. Radiology. 1994;193(3):637–41.
57. Marchal G, Rioux P, Petit Taboué MC, Sette G, Travère JM, Le Poec C, et al. Regional cerebral oxygen consumption, blood flow, and blood volume in healthy human aging. Arch Neurol. 1992;49(10):1013–20.
58. Bell MA, Ball MJ. Morphometric comparison of hippocampal microvasculature in ageing and demented people: diameters and densities. Acta Neuropathol. 1981;53(4):299–318.
59. Guan Z, Wang Y, Cairns NJ, Lantos PL, Dallner G, Sindelar PJ. Decrease and structural modifications of phosphatidylethanolamine plasmalogen in the brain with Alzheimer disease. Neurol J Neuropathol Exp. 1999;58(7):740–7.
60. Pettegrew JW, Panchalingam K, Hamilton RL, Mcclure RJ. Brain membrane phospholipid alterations in Alzheimer's disease. Neurochem Res. 2001;26(7):771–82.
61. Söderberg M, Edlund C, Alafuzoff I, Kristensson K, Dallner G. Lipid composition in different regions of the brain in Alzheimer's disease/senile dementia of Alzheimer's type. J Neurochem. 1992;59(5):1646–53.
62. Stokes CE, Hawthorne JN. Reduced phosphoinositide concentrations in anterior temporal cortex of Alzheimer-diseased brains. J Neurochem. 1987;48(4):1018–21.
63. Igarashi M, Ma K, Gao F, Kim HW, Rapoport SI, Rao JS. Disturbed choline plasmalogen and phospholipid fatty acid concentrations in Alzheimer's disease prefrontal cortex. J Alzheimers Dis. 2011;24(3):507–17.
64. Svennerholm L, Gottfries C-G. Membrane lipids, selectively diminished in Alzheimer brains, suggest synapse loss as a primary event in early-onset form (type I) and demyelination in late-onset form (type II). J Neurochem. 1994;62(3):1039–47.
65. Sass LR, Khani M, Natividad GC, Tubbs RS, Baledent O, Martin BA. A 3D subject-specific model of the spinal subarachnoid space with anatomically realistic ventral and dorsal spinal cord nerve rootlets. Fluids Barriers CNS. 2017;14(1):1–16.

66. Lorenzi RM, Palesi F, tellazzi G, Vitali P, Anzalone N, Bernini S, et al. Unsuspected involvement of spinal cord in Alzheimer disease. Front Cell Neurosci. 2020;14(January):1–10.

67. Melamed E, Lavy S, Bentin S, Cooper G, Rinot Y. Reduction in regional cerebral blood flow during normal aging in man. Stroke. 1980;11(1):31–5.

68. Buijs PC, Krabbe-Hartkamp MJ, Bakker CJG, de Lange EE, Ramos LMP, Breteler MMB, et al. Effect of age on cerebral blood flow : measurement with ungated two-dimensional phase-contrast MR angiography in 250 adults. Radiology. 1998;209(3):667–74.

69. Stoquart-ElSankari S, Balédent O, Gondry-Jouet C, Makki M, Godefroy O, Meyer ME. Aging effects on cerebral blood and cerebrospinal fluid flows. J Cereb Blood Flow Metab. 2007;27(9):1563–72.

70. Parkes LM, Rashid W, Chard DT, Tofts PS. Normal cerebral perfusion measurements using arterial spin labeling: reproducibility, stability, and age and gender effects. Magn Reson Med. 2004;51(4):736–43.

71. van Es ACGM, van der Grond J, ten Dam VH, de Craen AJM, Blauw GJ, Westendorp RGJ, et al. Associations between total cerebral blood flow and age related changes of the brain. PLoS One. 2010;5(3):1–6.

72. Catchlove SJ, Macpherson H, Hughes ME, Chen Y, Parrish TB, Pipingas A. An investigation of cerebral oxygen utilization, blood flow and cognition in healthy aging. PLoS One. 2018;13(5):1–21.

73. Hu Y, Liu R, Gao F. Arterial spin labeling magnetic resonance imaging in healthy adults: mathematical model fitting to assess age-related perfusion pattern. Korean J Radiol. 2021;22:1–9.

74. Soininen H, Helkala E, Kuikka J, Hartikainen P, Lehtovirta M, Sr PJR. Regional cerebral blood flow measured by 99mTc-HMPAO SPECT differs in subgroups of Alzheimer's disease. J Neural Transm 1995;9:95–109.

75. Van Dyck CH, Lin CH, Robinson R, Cellar J, Smith EO, Nelson JC, et al. The acetylcholine releaser linopirdine increases parietal regional cerebral blood flow in Alzheimer's disease. Psychopharmacology. 1997;132(3):217–26.

76. Kress BT, Iliff JJ, Xia M, Wang M, Wei Bs HS, Zeppenfeld D, et al. Impairment of paravascular clearance pathways in the aging brain. Ann Neurol. 2014;76(6):845–61.

77. Arbel-Ornath M, Hudry E, Eikermann-Haerter K, Hou S, Gregory JL, Zhao L, et al. Interstitial fluid drainage is impaired in ischemic stroke and Alzheimer's disease mouse models. Acta Neuropathol. 2013;126(3):353–64.

78. Rasmussen MK, Mestre H, Nedergaard M. The glymphatic pathway in neurological disorders. Lancet Neurol. 2018;17(11):1016–24.

79. Zeppenfeld DM, Simon M, Haswell JD, D'Abreo D, Murchison C, Quinn JF, et al. Association of perivascular localization of aquaporin-4 with cognition and Alzheimer disease in aging brains. JAMA Neurol. 2017;74(1):91–9.

80. Silverberg GD, Heit G, Huhn S, Jaffe RA, Chang SD, Bronte-Stewart H, et al. The cerebrospinal fluid production rate is reduced in dementia of the Alzheimer's type. Neurology. 2001;57(10):1763–6.

81. Fishman RA. The cerebrospinal fluid production rate is reduced in dementia of the Alzheimer's type. Neurology. 2002;58(12):1866.

82. Buée L, Hof PR, Bouras C, Delacourte A, Perl DP, Morrison JH, et al. Pathological alterations of the cerebral microvasculature in Alzheimer's disease and related dementing disorders. Acta Neuropathol. 1994;87(5):469–80.

83. Bell MA, Ball MJ. Neuritic plaques and vessels of visual cortex in aging and Alzheimer's dementia. Neurobiol Aging. 1990;11(4):359–70.
84. Riddle DR, Sonntag WE, Lichtenwalner RJ. Microvascular plasticity in aging. Ageing Res Rev. 2003;2(2):149–68.
85. Bouras C, Kövari E, Herrmann FR, Rivara CB, Bailey TL, Von Gunten A, et al. Stereologic analysis of microvascular morphology in the elderly: Alzheimer disease pathology and cognitive status. J Neuropathol Exp Neurol. 2006;65(3):235–44.
86. Liu C-B, Wang R, Dong M-W, Gao X-R, Yu F. Amyloid-beta transporter expression at the choroid plexus in normal aging: the possibility of reduced resistance to oxidative stress insults. Acta Physiol Sin. 2014;66(2):158–68.
87. Bors L, Tóth K, Tóth EZ, Bajza Á, Csorba A, Szigeti K, et al. Age-dependent changes at the blood-brain barrier. A comparative structural and functional study in young adult and middle aged rats. Brain Res Bull. 2018;139(January):269–77.
88. Montagne A, Barnes SR, Sweeney MD, Halliday MR, Sagare AP, Zhao Z, et al. Blood-brain barrier breakdown in the aging human hippocampus. Neuron. 2015;85(2):296–302.
89. Verheggen ICM, de Jong JJA, van Boxtel MPJ, Gronenschild EHBM, Palm WM, Postma AA, et al. Increase in blood–brain barrier leakage in healthy, older adults. GeroScience. 2020;42(4):1183–93.
90. Pan Y, Nicolazzo JA. Impact of aging, Alzheimer's disease and Parkinson's disease on the blood-brain barrier transport of therapeutics. Adv Drug Deliv Rev. 2018;135:62–74.
91. Van De Haar HJ, Burgmans S, Jansen JFA, Van Osch MJP, Van Buchem MA, Muller M, et al. Blood-brain barrier leakage in patients with early Alzheimer disease. Radiology. 2016;281(2):527–35.
92. Ott BR, Jones RN, Daiello LA, de la Monte SM, Stopa EG, Johanson CE, et al. Blood-cerebrospinal fluid barrier gradients in mild cognitive impairment and Alzheimer's disease: Relationship to inflammatory cytokines and chemokines. Front Aging Neurosci. 2018;10(AUG):1–12.
93. Bauer M, Wulkersdorfer B, Karch R, Philippe C, Jäger W, Stanek J, et al. Effect of P-glycoprotein inhibition at the blood–brain barrier on brain distribution of (R)-[11C] verapamil in elderly vs. young subjects. Br J Clin Pharmacol 2017;83(9):1991–9.
94. Lee NY, Kang YS. The inhibitory effect of rivastigmine and galantamine on choline transport in brain capillary endothelial cells. Biomol Ther. 2010;18(1):65–70.
95. Takeuchi R, Shinozaki K, Nakanishi T, Tamai I. Local drug-drug interaction of donepezil with cilostazol at breast cancer resistance protein (ABCG2) increases drug accumulation in heart. Drug Metab Dispos. 2016;44(1):68–74.
96. Mehta DC, Short JL, Nicolazzo JA. Memantine transport across the mouse blood-brain barrier is mediated by a cationic influx H+ antiporter. Mol Pharm. 2013;10(12):4491–8.
97. Higuchi K, Kitamura A, Okura T, Deguchi Y. Memantine transport by a proton-coupled organic cation antiporter in hCMEC/D3 cells, an in vitro human blood-brain barrier model. Drug Metab Pharmacokinet. 2015;30(2):182–7.
98. Sekhar GN, Fleckney AL, Boyanova ST, Rupawala H, Lo R, Wang H, et al. Region-specific blood-brain barrier transporter changes leads to increased sensitivity to amisulpride in Alzheimer's disease. Fluids Barriers CNS. 2019;16(1):1–19.
99. Rohrig TP, Hicks CA. Brain tissue: a viable postmortem toxicological specimen. J Anal Toxicol. 2015;39(2):137–9.
100. Cichocka M, Kozub J, Urbanik A. Brain aging: evaluation of pH using phosphorus magnetic resonance spectroscopy. Geriatr Gerontol Int. 2018;18(6):881–5.

101. Lyros E, Ragoschke-Schumm A, Kostopoulos P, Sehr A, Backens M, Kalampokini S, et al. Normal brain aging and Alzheimer's disease are associated with lower cerebral pH: an in vivo histidine 1H-MR spectroscopy study. Neurobiol Aging. 2020;87:60–9.

102. Forester BP, Berlow YA, Harper DG, Jensen JE, Lange N, Froimowitz MP, et al. Age-related changes in brain energetics and phospholipid metabolism. NMR Biomed. 2010;23(3):242–50.

103. Decker Y, Németh E, Schomburg R, Chemla A, Fülöp L, Menger MD, et al. Decreased pH in the aging brain and Alzheimer's disease. Neurobiol Aging. 2021;101:40–9.

104. Monoranu CM, Apfelbacher M, Grünblatt E, Puppe B, Alafuzoff I, Ferrer I, et al. PH measurement as quality control on human post mortem brain tissue: a study of the BrainNet Europe consortium. Neuropathol Appl Neurobiol. 2009;35(3):329–37.

105. Preece P, Cairns NJ. Quantifying mRNA in postmortem human brain: influence of gender, age at death, postmortem interval, brain pH, agonal state and inter-lobe mRNA variance. Mol Brain Res. 2003;118(1–2):60–71.

106. Roberts EL, Sick TJ. Aging impairs regulation of intracellular pH in rat hippocampal slices. Brain Res. 1996;735(2):339–42.

107. Spector R, Johanson CE. Sustained choroid plexus function in human elderly and Alzheimer's disease patients. Fluids Barriers CNS. 2013 Sep;10(1):28.

108. Li SM, Mo MS, Xu PY. Progress in mechanisms of acetylcholinesterase inhibitors and memantine for the treatment of Alzheimer's disease. Neuroimmunol Neuroinflammation. 2015;2(4):274–80.

109. Sweeney MD, Sagare AP, Zlokovic BV. Blood-brain barrier breakdown in Alzheimer disease and other neurodegenerative disorders. Nat Rev Neurol. 2018;14(3):133–50.

110. Reeve E, Trenaman SC, Rockwood K, Hilmer SN. Pharmacokinetic and pharmacodynamic alterations in older people with dementia. Expert Opin Drug Metab Toxicol. 2017;13(6):651–68.

111. A Study of LY2886721 in Healthy Participants and Participants Diagnosed With Alzheimer's Disease [Internet]. [cited 2022 Jan 10]. Available from: https://clinicaltrials.gov/ct2/show/NCT01807026.

112. Gustafsson S, Lindström V, Ingelsson M, Hammarlund-Udenaes M, Syvänen S. Intact blood-brain barrier transport of small molecular drugs in animal models of amyloid beta and alpha-synuclein pathology. Neuropharmacology. 2018;128:482–91.

113. Fendt R, Hofmann U, Schneider ARP, Schaeffeler E, Burghaus R, Yilmaz A, et al. Data-driven personalization of a physiologically based pharmacokinetic model for caffeine: a systematic assessment. CPT Pharmacometrics Syst Pharmacol. 2021;10(7):782–93.

114. Rivastigmine product sheet [Internet]. [cited 2021 Oct 27]. Available from: https://www.selleckchem.com/products/rivastigmine.html.

115. Giacobini E. Cholinesterase inhibitors: new roles and therapeutic alternatives. Pharmacol Res. 2004;50(4):433–40.

116. Cook D, Brown D, Alexander R, March R, Morgan P, Satterthwaite G, et al. Lessons learned from the fate of AstraZeneca's drug pipeline: a five-dimensional framework. Nat Rev Drug Discov. 2014;13(6):419–31.

117. Geerts H, van der Graaf P. Computational approaches for supporting combination therapy in the post-Aducanumab era in Alzheimer's disease. J Alzheimer's Dis Reports. 2021;5(1):815–26.

118. Li Q, He S, Chen Y, Feng F, Qu W, Sun H. Donepezil-based multi-functional cholinesterase inhibitors for treatment of Alzheimer's disease. Eur J Med Chem. 2018;158:463–77.

Supplementary material

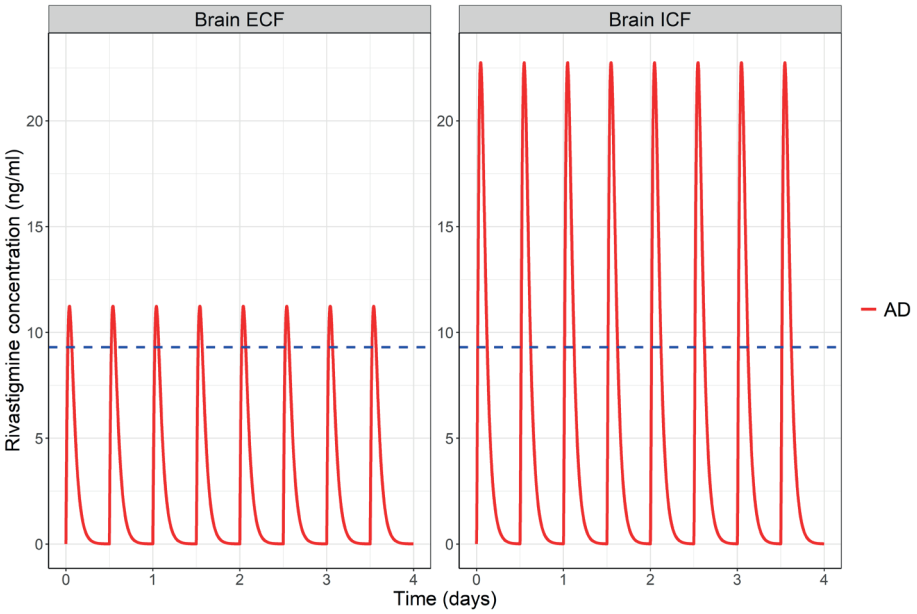

Supplementary figure 1. AD predicted PK profiles of rivastigmine (6 mg, twice daily) at brain$_{ECF}$ and brain$_{ICF}$ versus the IC$_{50}$ of butyrylcholinesterase. *The blue dashed line represents the IC$_{50}$ value of butyrylcholinesterase. The predicted PK profiles of rivastigmine are below the IC$_{50}$ of acetylcholinesterase but exceed that of butyrylcholinesterase at the brain$_{ECF/ICF}$.*

Sensitivity analysis of the AD version of LeiCNS-PK3.0

A sensitivity analysis was performed on the AD version of LeiCNS-PK3.0 for donepezil, galantamine, memantine, and rivastigmine. Model parameters were altered by two and ten folds, while pH values were changed by one and two pH units. The pharmacokinetic parameters: C_{max}, T_{max}, AUC, and half-life were used to assess the impact of parameters alterations on PK profiles at the compartments of interest: brain$_{ECF}$, brain$_{ICF}$, and CSF_{SAS}. Sensitivity analysis results are depicted in supplementary figure 2. The PK profiles of the compartments of interest were not impacted by changes of ventricular volume, brain microvasculature volume, brain$_{ECF}$ bulk flow, CSF pH, and the surface area of blood-CSF barrier. Changes of related to CSF parameters: CSF flow and volumes of the SAS and of the cisterna magna affected the CSF but not brain$_{ECF}$ and brain$_{ICF}$ PK profiles, which is in line with our previous results [1]. The other parameters affected the PK profiles depending on the drug's physicochemical properties. PK changes due pH depended on the acidic and basic ionization constants of the drug. Those due to cerebral blood flow and volume fraction of

phospholipids relied on the drug's lipophilicity, evident by the notable change observed for lipophilic drug, donepezil (logP = 4.14). PK parameters of the more hydrophilic drugs, rivastigmine and galantamine, were impacted by changes of the brain cell and lysosomal surface area. Changes of surface area of the BBB and that of BBB paracellular transport affect the PK profiles depending on the paracellular-to-transcellular drug transport ratio, which is determined according to the drug's molecular weight and lipophilicity and if the drug is actively transported at the BBB.

See supplementary figure 2 on next page

Supplementary figure 2. Sensitivity analysis of the AD LeiCNS-PK3.0. Parameters (top) were varied (bottom) by two and ten folds, while pH values were changed by one and two pH units. *The final profiles at the brain$_{ECF/ICF}$ and CSF$_{SAS}$ (right) were evaluated according to the changes in the PK parameters (left): C_{max}, T_{max}, AUC, and half-life. The magnitude of change in percentage of pharmacokinetic parameters is given by the color scale (right), where blue, red, and white represent increase, decrease, and no change, respectively. pHCSF: pH of cerebrospinal fluid, pHECF: pH of brain extracellular fluid, pHICF: pH of brain cells, pHLYS: pH of brain lysosomes, pHMV: pH of brain microvasculature, PPA-BBB: effective surface area of paracellular transport at the blood-brain barrier, PPA-CSF: effective surface area of paracellular transport at the blood-CSF barrier, QCBF: cerebral blood flow, QCSF: cerebrospinal fluid flow, QECF: brain$_{ECF}$ bulk flow, SABBB: blood brain barrier surface area, SABC: surface area of brain cell membrane, SACSFB: surface area of blood-CSF barrier, SALYSO: lysosomal surface area, VCM: volume of cisterna magna, VECF: volume of brain extracellular fluid, VICF: volume of brain cells, VLV: volume of lateral ventricles, VLYS: volume of lysosomes, VMV: volume of brain microvasculature, Vphb: volume fraction of brain phospholipid, VSAS: subarachnoid space volume, VTFV: volume of third and fourth ventricles.*

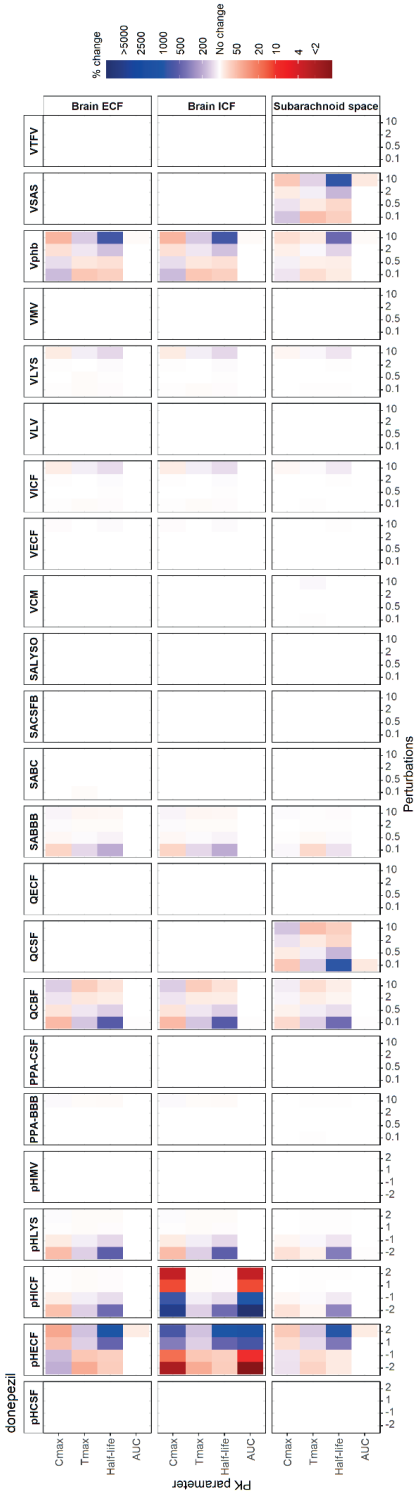
% change
>5000
2500
1000
500
200
No change
50
20
10
4
<2
Brain ECF
Brain ICF
Subarachnoid space
VTFV
VSAS
Vphb
VMV
VLYS
VLV
VICF
VECF
VCM
SALYSO
SACSFB
SABC
SABBB
QECF
QCSF
QCBF
PPA-CSF
PPA-BBB
pHMV
pHLYS
pHICF
pHECF
pHCSF
10
2
0.5
0.1
2
1
-1
-2
Perturbations
Cmax
Tmax
Half-life
AUC
PK parameter
donepezil


% change
>5000
2500
1000
500
200
No change
50
20
10
4
<2
Brain ECF
Brain ICF
Subarachnoid space
VTFV
VSAS
Vphb
VMV
VLYS
VLV
VICF
VECF
VCM
SALYSO
SACSFB
SABC
SABBB
QECF
QCSF
QCBF
PPA-CSF
PPA-BBB
pHMV
pHLYS
pHICF
pHECF
pHCSF
10
2
0.5
0.1
2
1
-1
-2
Perturbations
Cmax
Tmax
Half-life
AUC
PK parameter
galantamine

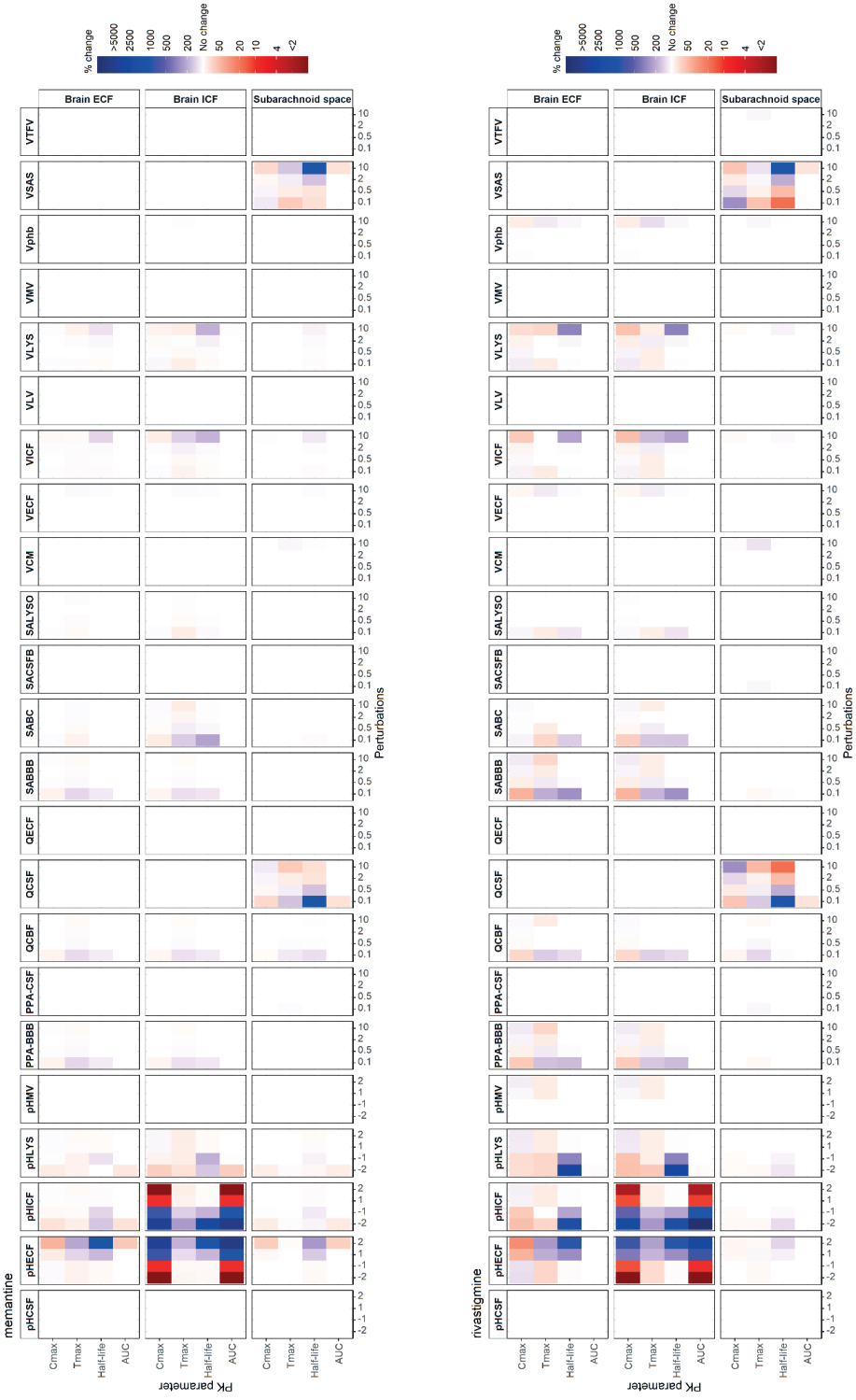
% change
>5000
2500
1000
500
200
No change
50
20
10
4
<2
Brain ECF
Brain ICF
Subarachnoid space
VTFV
VSAS
Vphb
VMV
VLYS
VLV
VICF
VECF
VCM
SALYSO
SACSFB
SABC
SABBB
QECF
QCSF
QCBF
PPA-CSF
PPA-BBB
pHMV
pHLYS
pHICF
pHECF
pHCSF
Perturbations
memantine
rivastigmine
Cmax
Tmax
Half-life
AUC
PK parameter

Supplementary equations to convert Kp_{brain} into $Kp_{uu,BBB}$

These equations are used to convert Kp_{brain} to $Kp_{uu,BBB,}$ by correcting for plasma protein and brain tissue binding and also for the unequal distribution of charged drug between $brain_{ECF}$ and $brain_{ICF}$ as a result of the pH difference. The following assumptions were made. Active transport is not present at brain cells level or at lysosomes. Unbound drug exists in the brain extracellular and intracellular fluids and in lysosomes, and drug can bind to the phospholipids of the brain cell membrane.

Definitions

C_{brain}: brain concentration as measured by homogenate methods; A: amounts; ECF: brain ECF; ICF: brain ICF; LYS: lysosomes; BCM: brain cell membrane; V_{br}: brain volume; Cp: total plasma concentration; $C_{P,u}$: unbound plasma concentration; $f_{u,p}$: unbound fraction of plasma; $V_{u,Br}$: unbound volume of distribution in brain as measured by brain slice method; WT_{Br}: brain weight; PHF: neutral drug fraction

Equations

- In the presence of experimentally measured Vu,br

$$Kp_{uu,BBB} = Kp*(1/fu,p)*(V_{br} / (WT_{Br}*V_{u,Br}))$$

If experimentally measured $V_{u,Br}$ is not available,

$$C_{brain} = \frac{A_{ECF} + A_{ICF} + A_{LYS} + A_{BCM}}{V_{br}}$$

$$C_{brain} = \frac{C_{ECF} * V_{ECF} + C_{ICF} * V_{ICF} + C_{LYS} * V_{LYS} + C_{BCM} * V_{BCM}}{V_{br}}$$

At Steady State,

$$C_{ECF}*PHF_{ECF} = C_{ICF}*PHF_{ICF} = C_{LYS}*PHF_{LYS}$$

$$P_{oct/water} = \frac{C_{BCM}}{C_{ECF} * PHF_{ECF}}$$

Every C_x in terms of C_{ECF},

$$C_{brain} = \frac{C_{ECF} * V_{ECF} + C_{ECF} * \frac{PHF_{ECF}}{PHF_{ICF}} * V_{ICF} + C_{ECF} * \frac{PHF_{ECF}}{PHF_{LYS}} * V_{LYS} + C_{ECF} * PHF_{ECF} * P_{Octanol/Water} * V_{BCM}}{V_{br}}$$

Every V_X in terms of V_{Br},

$$V_{ECF} = 0.2*V_{Br};\ V_{ICF} = 0.74*V_{Br};\ V_{LYS} = 0.01*V_{Br};\ V_{BCM} = 0.05*V_{Br}$$

$$C_{brain} = \frac{C_{ECF} * 0.2 * V_{Br} + C_{ECF} * \frac{PHF_{ECF}}{PHF_{ICF}} * 0.74 * V_{Br} + C_{ECF} * \frac{PHF_{ECF}}{PHF_{LYS}} * 0.01 *}{V_{br}}$$

Taking C_{ECF} as common factor, V_{Br} cancels each other out,

$$C_{brain} = C_{ECF} * (0.2 + \frac{PHF_{ECF}}{PHF_{ICF}} * 0.74 + \frac{PHF_{ECF}}{PHF_{LYS}} * 0.01 + PHF_{ECF} * P_{\frac{O}{W}} * 0.05)$$

Dividing both sides by C_P,

$$\frac{C_{brain}}{C_P} = \frac{C_{ECF}}{C_P} * (0.2 + \frac{PHF_{ECF}}{PHF_{ICF}} * 0.74 + \frac{PHF_{ECF}}{PHF_{LYS}} * 0.01 + PHF_{ECF} * P_{\frac{O}{W}} * 0.05)$$

$$Cp = \frac{C_{p,u}}{f_{u,p}} \,||\, Kp = \frac{C_{brain}}{C_P}$$

$$Kp = \frac{f_{u,p} * C_{ECF}}{C_{P,u}} * (0.2 + \frac{PHF_{ECF}}{PHF_{ICF}} * 0.74 + \frac{PHF_{ECF}}{PHF_{LYS}} * 0.01 + PHF_{ECF} * P_{\frac{O}{W}} * 0.05)$$

$$Kp, uu, BBB = \frac{C_{ECF}}{C_{p,u}}$$

$$Kp = Kp_{uu,BBB} * f_{u,p} * (0.2 + \frac{PHF_{ECF}}{PHF_{ICF}} * 0.74 + \frac{PHF_{ECF}}{PHF_{LYS}} * 0.01 + PHF_{ECF} * P_{\frac{O}{W}} * 0.05)$$

Supplementary table 1. CNS physiological parameters of cognitively healthy young, cognitively healthy elderly, and Alzheimer's disease patients

Parameter		Adults	75-elder		AD	
		value [1]	value	%[1]	value	%[1]
Volume (mL)	Total brain	1251	1131	90.4	1081	86.5
	Brain extracellular fluid ($brain_{ECF}$)	254	181	71.3	247	97.3
	Brain intracellular fluid ($brain_{ICF}$)	1001	905	90.4	834	83.4
	Brain cell lysosomes (VLYS)	13	11	90.4	10	83.4
	Lateral ventricles	20	47	233.3	65	324.3
	3rd and 4th ventricles	3.0	7.0	233.3	9.8	324.3
	Cisterna magna	1.0	1.3	131.2	1.6	158.8
	Subarachnoid space	116	141	121.4	170	146.9
	Brain microvasculature	46	41	90.4	34	74.1
Flow (mL/min)	Brain bulk flow	0.20	0.15	72.4	0.20	98.7
	CSF flow	0.42	0.42	100	0.42	100
	Cerebral blood flow (CBF)	689	623	90.4	510	74.1
Surface area (cm^2)	Blood–brain barrier (SABBB)	150000	121962	81.3	129695	86.5
	Blood CSF barrier (SABCSFB)	15000	15000	100	15000	100
	Brain cell membrane (SABCM)	2666517	2511324	94.2	2379051	89.2
	Lysosomes membrane	1980260	1809922	91.4	1668827	84.3
width (µm)	Blood brain barrier Blood	0.5	0.5	100	0.5	100
	Blood CSF barrier	0.5	0.5	100	0.5	100
pH	Plasma and brain MV	7.4	7.4	100	7.4	100
	Brain extracellular fluid (pHECF)	7.3	7.3	100	7.309	100.1
	Brain cells (pHICF)	7.0	6.975	99.6	6.984	99.8
	Brain cell lysosomes	5.0	5.0	100	5.0	100
	Cerebrospinal fluid	7.3	7.3	100	7.19	98.5
Effective surface area (%)	BBB Transcellular transport	0.998	0.998	100	0.998	100
	BCSFB Transcellular transport	0.998	0.998	100	0.998	100
	BBB paracellular transport	0.00004	0.00004	100	0.00018	444.8
	BCSFB paracellular transport	0.00016	0.00016	100	0.00016	100

Supplementary table 1. Continued

Parameter		Adults	75-elder		AD	
		value [1]	value	%[1]	value	%[1]
Volume fraction	Brain phospholipids	0.0565	0.0513	90.8	0.0469	82.9
	$Brain_{ECF}$	0.2	0.16	80.0	0.2284	114.2
	$Brain_{ICF}$	0.8	0.8	100	0.7716	96.4
	Lysosomes	0.0125	0.0125	100	0.0125	100
Count	Total brain cells (Nbr.cells)	1,71E+11	1,71E+11	100	1,71E+11	100

[1]Compared to adults

Supplementary table 2. Age versus aging stage of different species

Species	Stage	Age	Age units	
Mouse	young	3-6	month	
Mouse	middle aged	10-15	month	[2]
Mouse	old	18-26	month	
rat	young	6-12	month	
rat	middle aged	18-24	month	[3, 4]
rat	old	30-36	month	
human	young	20-30	year	
human	middle aged	38-47	year	[2]
human	old	59-69	year	

Supplementary table 3. Examples of the different search queries used in the literature study

CNS parameter	Search queries
Aging	
Brain volume	"brain" AND ("volume" OR "structure" OR "shrinkage") AND ("elderly"OR "aging" OR "age" "old");
Brain microvascular volume	("cerebral" OR "brain") AND ("blood volume" OR "vascular volume" OR "microvasculature" OR "microvascular") AND ("volume") AND ("aging")
Cerebral blood flow	("cerebral blood flow" [tiab]) AND ("aging" [tiab] OR "ageing"[ti] OR "age"[ti])
Cerebrospinal fluid flow	("CSF flow"[tiab] OR "cerebrospinal fluid flow"[tiab] OR "CSF flows"[tiab] OR "cerebrospinal fluid flows"[tiab]) AND ("aging"[tiab] OR "elderly"[tiab] OR "age"[title] OR "ageing"[tiab])
CSF pH	("Aging" OR "AGE" OR "ELDERLY" OR "AGEING") AND ("CSF" OR "cerebrospinal fluid") AND "pH"
Ventricular volume	("ventricles volume" OR "ventricular volume"[tiab] OR "cerebrospinal fluid volume"[tiab] OR "CSF volume"[tiab]) AND ("aging"[tiab] OR "ageing"[tiab] OR "elderly"[tiab])
BBB Pgp	("central nervous system" OR "CNS" OR "brain" OR "blood-brain barrier" OR "BBB" OR "blood brain barrier") AND ("aging" OR "ageing" OR "Elderly") AND ("p-gp" OR "p-glycoprotein" OR "pgp" OR "permeability glycoprotein")
BBB BCRP	("CNS" OR "central nervous system" OR "brain" OR "blood-brain barrier" OR "BBB" OR "blood brain barrier") AND ("aging" OR "ageing" OR "Elderly") AND ("BCRP" OR "breast cancer Resistance protein" OR "ABCG2")
BBB MRP4	("CNS" OR "central nervous system" OR "brain" OR "blood-brain barrier" OR "BBB" OR "blood brain barrier") AND ("aging" OR "ageing" OR "Elderly") AND ("multidrug resistance protein" OR "ABCC4" OR "MRP4")
BBB OAT/OCT	("CNS"[tiab] OR "central nervous system"[tiab] OR "brain"[tiab] OR "blood-brain barrier"[tiab] OR "BBB"[tiab] OR "blood brain barrier"[tiab]) AND ("aging"[tiab] OR "ageing"[tiab] OR "Elderly"[tiab]) AND ("OAT"[tiab] OR "OCT"[tiab] OR "organic anionic transporter"[tiab] OR "organic cationic transporter"[tiab]) NOT ("retina" OR "retinal")
Blood-CSF barrier active transport	("CP" OR "choroid plexus" OR "cerebrospinal fluid" OR "CSF" OR "blood-cerebrospinal" OR "BCSFB") AND ("aging" OR "ageing" OR "Elderly") AND ("p-gp" OR "p-glycoprotein" OR "pgp" OR "permeability glycoprotein" OR "BCRP" OR "breast cancer Resistance protein" OR "ABCG2" OR "multidrug resistance protein" OR "ABCC4" OR "MRP4")
BBB paracellular transport	("paracellular") AND ("BBB" OR "blood-brain barrier" OR "blood brain barrier") AND ("aging" OR "ageing" OR "elderly" OR "senescence")
	("blood-brain barrier"[tiab] OR "blood brain barrier"[tiab] OR "BBB"[tiab]) AND ("permeability"[tiab]) AND ("aging"[tiab] OR "ageing"[tiab] OR "elderly"[tiab])
Non-specific binding	phospholipids[tiab] AND "brain"[tiab] AND "aging"[tiab]
$Brain_{ECF}$ fraction	(brain) AND ("interstitial" OR "extracellular") AND ("aging" OR "ageing") AND ("fraction")

Supplementary table 3. Continued

CNS parameter	Search queries
$Brain_{ICF}$ fraction	(brain OR CNS OR "central nervous system") AND ("aging" OR "ageing" OR "elderly" OR "elder" OR "senescence" OR "senescent") AND ("volume fraction" OR "volume ratio") AND ("intracellular" OR "cellular")
BBB surface area	("brain"[tiab] OR "cerebral"[tiab]) AND ("aging"[tiab] OR "ageing"[tiab] OR "elderly"[tiab] OR "elder"[tiab] OR "senescence"[tiab] OR "senescent"[tiab]) AND ("vascular volume" OR "microvascular volume" OR "vascular area" OR "microvascular area" OR "vascular density" OR "microvascular density")
Blood-CSF barrier surface area	("choroid plexus"[tiab] OR "blood cerebrospinal fluid barrier"[tiab] OR "cerebrospinal fluid barrier"[tiab] OR "blood CSF barrier"[tiab] OR "BCSFB"[tiab]) AND ("aging"[tiab] OR "ageing"[tiab] OR "age"[tiab] OR "senescence"[tiab] OR "elderly"[tiab]) AND ("surface area" OR morphology[tiab])
Alzheimer's disease	
Brain microvascular volume	(alzheimer's[tiab] OR alzheimer[tiab]) AND (brain[tiab] OR cerebral[tiab]) AND ("vascular volume"[tiab] OR "vasculature volume"[tiab] OR "microvascular volume"[tiab] OR "blood volume"[tiab])
$Brain_{ICF}$ fraction	(intracellular OR cell) AND ("volume ratio" OR "volume fraction") AND (alzheimer's OR alzheimer)
Blood-CSF barrier surface area	("choroid plexus"[tiab] OR "blood cerebrospinal fluid barrier"[tiab] OR "cerebrospinal fluid barrier"[tiab] OR "blood CSF barrier"[tiab] OR "BCSFB"[tiab] OR "blood-cerebrospinal fluid barrier"[tiab] OR "blood-CSF barrier"[tiab]) AND ("alzheimer"[tiab] OR "alzheimer's"[tiab]) AND ("surface area" OR morphology[tiab] OR structure[tiab] OR length[tiab] OR villi[tiab] OR pathophysiology[tiab])
Blood-CSF barrier paracellular transport	("choroid plexus"[tiab] OR "cerebrospinal fluid barrier"[tiab] OR "blood CSF barrier"[tiab] OR "BCSFB"[tiab] OR "blood-cerebrospinal fluid barrier"[tiab] OR "blood-CSF barrier"[tiab]) AND ("alzheimer"[tiab] OR "alzheimer's"[tiab]) AND (permeability OR paracellular OR gadolinium)
$Brain_{ECF}$ fraction	("extracellular"[tiab] OR "interstitial"[tiab]) AND ("brain"[tiab]) AND ("volume"[tiab]) AND ("alzheimer"[tiab] OR "alzheimer's"[tiab])
BBB surface area	("alzheimer's"[tiab] OR "alzheimer"[tiab]) AND ("brain microvessels"[tiab] OR "brain microvascular"[tiab] OR "cerebrovascular"[tiab] OR "blood-brain barrier"[tiab] OR "blood brain barrier"[tiab]) AND ("surface area"[tiab] OR "density"[tiab] OR "diameter"[tiab])
Cerebral blood flow	("cerebral blood flow"[tiab] OR "brain blood flow"[tiab]) AND ("Alzheimer's" [tiab] OR "Alzheimer" [tiab] OR "AD" [tiab])
Paracellular transport	("paracellular") AND ("BBB" OR "blood-brain barrier" OR "blood brain barrier" OR "Blood CSF Barrier" OR "BCSFB") AND ("Alzheimer's" OR "Alzheimer" OR "AD")
CSF volume	("ventricles volume"[tiab] OR "ventricular volume"[tiab] OR "cerebrospinal fluid volume"[tiab] OR "CSF volume"[tiab]) AND ("alzheimer's"[tiab] OR "alzheimer"[tiab]) NOT ("heart" OR "cardiac") AND ("MRI" OR "magnetic resonance ")

Supplementary table 4. Changes of CNS physiology during healthy aging in humans

Parameter	Study design (follow up years)	Value	unit	%	Population (Database)
Brain volume					
Vbrain	longitudinal (2.5)	-0.62	%/year	NA	(AGES-Reykjavik)
Vbrain	cross-sectional	-0.41	%/year	NA	(AGES-Reykjavik)
Vbrain	longitudinal (1)	-0.38	%/year	NA	(ADNI)
Vbrain	longitudinal (4.1)	1158.8	ml	NA	(Volunteers - South Korea)
Vbrain	longitudinal (4.1)	-2.65	ml/year	NA	(Volunteers - South Korea)
Vbrain	longitudinal (4.1)	-0.23	%/year	NA	(Volunteers - South Korea)
Vbrain	longitudinal	1000	ml	NA	(BLSA)
Vbrain	longitudinal (9)	-7.35	ml/year	NA	(BLSA)
Vbrain	longitudinal (9)	-0.735	%/year	NA	(BLSA)
Vbrain	longitudinal (1.9)	-0.23	%/year	NA	(Volunteers - Japan)
Vbrain	longitudinal (1.5)	-0.32	%/year	NA	(Volunteers - England)
Vbrain	longitudinal (1.4)	-0.5	%/year	NA	(Mayo AD Res Center/ AD Patient Registry)
Vbrain	longitudinal (4.3)	-0.4	%/year	NA	(Mayo AD Res Center/ AD Patient Registry)
Vbrain	longitudinal (1)	-0.44	%/year	NA	(ADNI)
Vbrain	longitudinal (4)	-2.14	%/year	NA	(OASIS repository)
Vbrain	cross-sectional	999.7	ml	NA	(BLSA)
Vbrain	cross-sectional	946.8	ml	NA	(BLSA)
Vbrain	longitudinal (1)	0	ml/year	NA	(BLSA)
Vbrain	longitudinal (1)	0	%/year	NA	(BLSA)
Vbrain	longitudinal (3.5)	1217	ml	NA	(Volunteers - UK)
Vbrain	longitudinal (3.5)	1171	ml	NA	(Volunteers - UK)
Vbrain	longitudinal (3.5)	-0.64	%scan-to-scan	NA	(Volunteers - UK)
Vbrain	longitudinal (3.5)	-1.35	%scan-to-scan	NA	(Volunteers - UK)
Vbrain	longitudinal (3.5)	-0.18	%/year	NA	(Volunteers - UK)
Vbrain	longitudinal (3.5)	-0.39	%/year	NA	(Volunteers - UK)
Vbrain	longitudinal (1.8)	-0.45	%/year	NA	(Volunteers - USA)

Age (years)	Age range (SD)	Number patients	Technique	Notes	Ref.
75	5	367	MRI	NA	[5]
76.1	66-96 (5.4)	4303	MRI	NA	[5]
75.6	59.8-90.2	142	MRI	Median value of 48 ROI	[6]
59.5	(6.66)	984	MRI	Estimated from a linear regression model	[7]
59.5	(6.66)	984	MRI	Estimated from a linear regression model	[7]
59.5	(6.66)	984	MRI	Normalized by baseline brain volume (1158.8 ml)	[7]
64	NA	120	MRI	NA	[8]
70.58	64-86 (6.11)	120	MRI	Estimated from a linear regression model	[8]
70.58	64-86 (6.11)	120	MRI	Normalized by brain volume at 64 yr (1000 ml)	[8]
56.4	38.1-82.9 (9.9)	199	MRI	NA	[9]
NA	31-84	39	MRI	NA	[10]
81.9**	(7.5)	91	MRI	NA	[11]
79*	56-93	40	MRI	NA	[12]
75.4*	60-90 (5.1)	132	MRI	NA	[13]
77.1	60-97	72	MRI	NA	[14]
NA	59-69	63	MRI	NA	[15]
NA	70-85	53	MRI	NA	[15]
NA	59-85	116	MRI	NA	[15]
NA	59-85	116	MRI	NA	[15]
44.5	35-53 (5.7)	37	MRI	NA	[16]
67.9	57-77 (6.4)	9	MRI	NA	[16]
44.5	35-53 (5.7)	37	MRI	NA	[16]
67.9	57-77 (6.4)	9	MRI	NA	[16]
44.5	35-53 (5.7)	37	MRI	caclulated as (%scan-to-scan)**(1/yrs scan-to-scan)	[16]
67.9	57-77 (6.4)	9	MRI	caclulated as (%scan-to-scan)**(1/yrs scan-to-scan)	[16]
78	65-95 (8)	38	MRI	NA	[17]

Supplementary table 4. Continued

Parameter	Study design (follow up years)	Value	unit	%	Population (Database)
Cerebrospinal fluid volume					
CSF,cran	longitudinal (2.5)	1.61	%/year	NA	(AGES-Reykjavik)
CSF,cran	cross-sectional	1.07	%/year	NA	(AGES-Reykjavik)
V,LV	longitudinal (1)	4.4	%/year	NA	21
V,inf LV	longitudinal (1)	5.47	%/year	NA	(ADNI)
V,3rd V	longitudinal (1)	3.07	%/year	NA	(ADNI)
V,4thV	longitudinal (1)	0.71	%/year	NA	(ADNI)
Vtot,CSF	longitudinal (4.1)	209.7	ml	NA	(Volunteers - South Korea)
Vtot,CSF	longitudinal (4.1)	2.84	ml/year	NA	(Volunteers - South Korea)
CSF,cran	longitudinal (4.1)	1.35	%/year	NA	(Volunteers - South Korea)
Vtot,CSF	longitudinal (9)	1.31	ml/year	NA	(BLSA)
Ventricles	longitudinal (1.5)	0.65	ml/year	NA	(Volunteers - England)
Ventricles	longitudinal (1.4)	2.4	%/year	NA	(Mayo AD Res Center/ AD Patient Registry)
Ventricles	longitudinal (4.3)	1.7	%/year	NA	(Mayo AD Res Center/ AD Patient Registry)
Ventricles	longitudinal (1)	4.57	%/year	NA	(ADNI)
V,LV	longitudinal (1)	4.61	%/year	NA	(ADNI)
V,inf LV	longitudinal (1)	4.63	%/year	NA	(ADNI)
V,3rd V	longitudinal (1)	3.13	%/year	NA	(ADNI)
V,4thV	longitudinal (1)	0.99	%/year	NA	(ADNI)
V,LV	longitudinal (1)	3.31	%/year	NA	(OASIS repository)
Ventricles	cross-sectional	25.2	ml	NA	(BLSA)
Ventricles	cross-sectional	41.1	ml	NA	(BLSA)
Ventricles	longitudinal (1)	1.53	ml/year	NA	(BLSA)
Ventricles	longitudinal (1)	6.07	%/year	NA	(BLSA)
Ventricles	longitudinal (1)	39	ml	NA	(ADNI)
Ventricles	longitudinal (1)	1.4	ml/year	NA	(ADNI)
Ventricles	longitudinal (1)	3.59	%/year	NA	(ADNI)
Ventricles	longitudinal (4.1)	0.62	ml/year	NA	<60 years (SMART-MR)

Age (years)	Age range (SD)	Number patients	Technique	Notes	Ref.
75	(5)	367	MRI	NA	[5]
76.1	66-96 (5.4)	4303	MRI	NA	[5]
75.6*	59.8-90.2	142	MRI	NA	[6]
75.6*	59.8-90.2	142	MRI	NA	[6]
75.6*	59.8-90.2	142	MRI	NA	[6]
75.6*	59.8-90.2	142	MRI	NA	[6]
59.5*	(6.66)	984	MRI	Estimated from a linear regression model	[7]
59.5*	(6.66)	984	MRI	Estimated from a linear regression model	[7]
59.5*	(6.66)	984	MRI	rate: calculated as %/ year by rate (ml/yr)/ CSF volume (209.7 ml)	[7]
70.58	64-86 (6.11)	120	MRI	Estimated from a linear regression model	[8]
NA	31-84	39	MRI	NA	[10]
81.9**	-7.5	91	MRI	NA	[11]
79*	56-93	40	MRI	NA	[12]
75.4*	60-90 (5.1)	79	MRI	NA	[13]
75.4*	60-90 (5.1)	79	MRI	NA	[13]
75.4*	60-90 (5.1)	79	MRI	NA	[13]
75.4*	60-90 (5.1)	79	MRI	NA	[13]
75.4*	60-90 (5.1)	79	MRI	NA	[13]
77.1	60-97	72	MRI	NA	[14]
NA	59-69	63	MRI	NA	[15]
NA	70-85	53	MRI	NA	[15]
NA	59-85	53	MRI	NA	[15]
NA	59-85	53	MRI	normalized to baseline volume (25.2 ml)	[15]
75	72-78	92	MRI	NA	[18]
75	72-78	92	MRI	NA	[18]
75	72-78	92	MRI	normalized to baseline volume (39 ml)	[18]
58	(9)	331	MRI	NA	[19]

Supplementary table 4. Continued

Parameter	Study design (follow up years)	Value	unit	%	Population (Database)
Ventricles	longitudinal (4.1)	2.52	%/year	NA	<60 years (SMART-MR)
Ventricles	longitudinal (4.1)	1.42	ml/year	NA	>60 years (SMART-MR)
Ventricles	longitudinal (4.1)	4.22	%/year	NA	>60 years (SMART-MR)
Ventricles	longitudinal (6.4)	3.54	%/year	NA	(Oregon brain aging)
Ventricles	longitudinal (6.4)	37.1	ml	NA	(Oregon brain aging)
Ventricles	longitudinal (1)	31.7	ml	NA	Volunteers
Ventricles	longitudinal (1)	0.9	ml/year	NA	Volunteers
Ventricles	longitudinal (1)	2.83	%/year	NA	Volunteers
Ventricles	longitudinal (1)	1.9	%/year	NA	Volunteers
Ventricles	longitudinal (2.4)	3.5	%/year	NA	(Oregon brain aging)
Ventricles	longitudinal (2.4)	40.6	ml	NA	(Oregon brain aging)
CSF,cran	cross-sectional	3.6	ml/year	NA	(Epid. Vascular aging)
CSF,cran	cross-sectional	357	ml	NA	(Epid. Vascular aging)
CSF,cran	cross-sectional	1.01	%/year	NA	(Epid. Vascular aging)
extraventricular	cross-sectional	2.75	%/year	NA	Volunteers
CSF,SASspinal	cross-sectional	-0.27	ml/year	NA	NA
Vphb					
Vphb	cross-sectional	73.5	mmol/kg	100	Postmortum (Sweden)
Vphb	cross-sectional	70	mmol/kg	N.S.	Postmortum (Sweden)
Vphb	cross-sectional	66.5	mmol/kg	90,4	Postmortum (Sweden)
Vphb	cross-sectional	60	mmol/kg	81,6	Postmortum (Sweden)
Vphb	cross-sectional	NA	mg/gm wet wt	100	Postmortum

Age (years)	Age range (SD)	Number patients	Technique	Notes	Ref.
58	(9)	331	MRI	NA	[19]
58	(9)	331	MRI	NA	[19]
58	(9)	331	MRI	NA	[19]
82.3	64.7 - 100.5 (7.8)	42	MRI	NA	[20]
82.3	64.7 - 100.5 (7.8)	42	MRI	NA	[20]
69.3	(7)	19	MRI	NA	[21]
69.3	(7)	19	MRI	NA	[21]
69.3	(7)	19	MRI	normalized to baseline volume (31.7 ml)	[21]
71.5	(3.4)	14	MRI	NA	[22]
83	(7)	88	MRI	NA	[23]
83	(7)	88	MRI	NA	[23]
69.5	63.69-75.6	662	MRI	NA	[24]
69.5	63.69-75.6	662	MRI	NA	[24]
69.5	63.69-75.6	662	MRI	normalized to baseline volume (357 ml)	[24]
NA	24-80	49	MRI	normalized to baseline volume (85 ml)	[25]
NA	29-70	87	MRI	Estimated from a linear regression model	[26]
NA	20-39	44	dry weight	average of male and female data	[27]
NA	40-59	46	dry weight	average of male and female data	[27]
NA	60-79	47	dry weight	average of male and female data	[27]
NA	80-100	47	dry weight	average of male and female data	[27]
NA	33-36	7	chemical extraction	GM, WM, Nucleus caudatus, hippocampus, pons, cerebellum, medulla oblongata	[28]

Supplementary table 4. Continued

Parameter	Study design (follow up years)	Value	unit	%	Population (Database)
Vphb	cross-sectional	NA	mg/gm wet wt	NS	Postmortum
Vphb	cross-sectional	NA	mg/gm wet wt	p<0,05	Postmortum
Vphb	cross-sectional	NA	mg/gm wet wt	NS	Postmortum
Vphb	cross-sectional	NA	mg/gm wet wt	p<0,05	Postmortum
Vphb	cross-sectional	NA	mg/gm wet wt	p<0,05	Postmortum
Vphb	cross-sectional	NA	mg/gm wet wt	N.S.	Postmortum
Vphb	cross-sectional	18.2	mg/gm wet wt	100	Postmortum
Vphb	cross-sectional	17.4	mg/gm wet wt	N.S.	Postmortum
Vphb	cross-sectional	35.1	mg/gm wet wt	100	Postmortum
Vphb	cross-sectional	29.9	mg/gm wet wt	85,2	Postmortum
Vphb	cross-sectional	NA	NA	100	Postmortum
Vphb	cross-sectional	NA	NA	93,34	Postmortum
Vphb	cross-sectional	18.2	mg/gm wet wt	100	Postmortum
Vphb	cross-sectional	16.4	mg/gm wet wt	90,1	Postmortum
Vphb	cross-sectional	35.1	mg/gm wet wt	100	Postmortum
Vphb	cross-sectional	28.2	mg/gm wet wt	80,3	Postmortum
Vphb	cross-sectional	NA	NA	100	Postmortum
Vphb	cross-sectional	NA	NA	85,7	Postmortum

Age (years)	Age range (SD)	Number patients	Technique	Notes	Ref.
NA	54-57	8	chemical extraction	GM, WM, Nucleus caudatus, pons, cerebellum, medulla oblongata.	[28]
NA	54-57	8	chemical extraction	Hippocampus (vs youngest group)	[28]
NA	69-72	8	chemical extraction	GM, WM, Nucleus caudatus, hippocampus, pons, cerebellum, medulla oblongata	[28]
NA	69-72	8	chemical extraction	WM, pons, Hippocampus ($p<0.05$, youngest group)	[28]
NA	89-92	7	chemical extraction	GM, WM, Nucleus caudatus, hippocampus, pons, cerebellum, medulla oblongata	[28]
NA	89-92	7	chemical extraction	cerebellum (vs youngest group)	[28]
NA	33-36	7	chemical extraction	GM	[28]
NA	69-72	8	chemical extraction	GM	[28]
NA	33-36	7	chemical extraction	WM	[28]
NA	69-72	8	chemical extraction	WM	[28]
NA	33-36	7	chemical extraction	average over grey and white matters, accounting for volume differences	[28]
NA	69-72	8	chemical extraction	average over grey and white matters, accounting for volume differences	[28]
NA	33-36	7	chemical extraction	GM	[28]
NA	89-92	7	chemical extraction	GM	[28]
NA	33-36	7	chemical extraction	WM	[28]
NA	89-92	7	chemical extraction	WM	[28]
NA	33-36	7	chemical extraction	average over grey and white matters, accounting for volume differences	[28]
NA	89-92	7	chemical extraction	average over grey and white matters, accounting for volume differences	[28]

Supplementary table 4. Continued

Parameter	Study design (follow up years)	Value	unit	%	Population (Database)
GM:WM ratio					
GM:WM ratio	NA	1.243	unitless	NA	NA
QCSF					
QCSF	cross-sectional	1.02	ml/min	100	(Volunteers)
QCSF	cross-sectional	1.14	ml/min	N.S.	(Volunteers)
QCSF	cross-sectional	1.5	ml/min	N.S.	(Volunteers)
QCSF	cross-sectional	40.825	ml/min	NA	Young (Volunteers)
QCSF	cross-sectional	35.646	ml/min	NA	Elderly (Volunteers)
QCSF	cross-sectional	3.408	ml/min	NA	Young (Volunteers)
QCSF	cross-sectional	2.652	ml/min	NA	Elderly (Volunteers)
QCSF	cross-sectional	NA	NA	NA	Young (Volunteers)
QCSF	cross-sectional	NA	NA	NA	Elderly (Volunteers)
QCSF	Longitudinal (5.5)	N.S.	ml/min	NA	(Volunteers)
QCSF	cross-sectional	2.76	ml/min	100	Young (Volunteers)
QCSF	cross-sectional	3.5	ml/min	N.S.	Elderly (Volunteers)
QCSF	cross-sectional	23.46	ml/min	100	Young (Volunteers)
QCSF	cross-sectional	35.7	ml/min	152,1	Elderly (Volunteers)
QCSF	cross-sectional	0.96	ml/min	100	Young (Male volunteers)
QCSF	cross-sectional	1.62	ml/min	168,8	Elderly (Male volunteers)
QCSF	cross-sectional	0.72	ml/min	100	Young (Female volunteers)

	Age (years)	Age range (SD)	Number patients	Technique	Notes	Ref.
	NA	NA	NA	NA	NA	[29]
	NA	20-34	24	PC-MRI	Aqueduct	[30]
	NA	35-49	24	PC-MRI	Aqueduct	[30]
	NA	50-64	24	PC-MRI	Aqueduct	[30]
	27.5	(4.4)	19	PC-MRI	Craniocervical junction, calc. as stroke volume (ml/cycle)*heart rate (71 cycle/min)	[31]
	71	(9)	12	PC-MRI	Craniocervical junction, calc. as stroke volume (ml/cycle)*heart rate (78 cycle/min)	[31]
	27.5	(4.4)	19	PC-MRI	Aqueduct, calc. as stroke volume (ml/cycle)*heart rate (71 cycle/min)	[31]
	71	(9)	12	PC-MRI	Aqueduct, calc. as stroke volume (ml/cycle)*heart rate (78 cycle/min)	[31]
	29.6	25-36	11	Cine PC-MRI	Non-significant increase of CSF flow at aqueduct	[32]
	68.6	57-76	9	Cine PC-MRI	Non-significant increase of CSF flow at aqueduct	[32]
	47.4	(12.9)	20	Cine PC-MRI	Aqueduct	[33]
	31	26-44 (7)	16	PC-MRI	Aqueduct, calc. as flow rate (ml/cycle)*heart rate (69 cycle/min)	[34]
	73	63-82 (6)	19	PC-MRI	Aqueduct, calc. as flow rate (ml/cycle)*heart rate (70 cycle/min)	[34]
	31	26-44 (7)	16	PC-MRI	Craniocervical junction, calc. as flow rate (ml/cycle)*heart rate (69 cycle/min)	[34]
	73	63-82 (6)	19	PC-MRI	Craniocervical junction, calc. as flow rate (ml/cycle)*heart rate (70 cycle/min)	[34]
	NA	17-50	31	PC-MRI	Aqueduct	[35]
	NA	51-88	31	PC-MRI	Aqueduct	[35]
	NA	17-50	32	PC-MRI	Aqueduct	[35]

Supplementary table 4. Continued

Parameter	Study design (follow up years)	Value	unit	%	Population (Database)
QCSF	cross-sectional	0.9	ml/min	N.S.	Elderly (Female volunteers)
QCSF	cross-sectional	6.7	ml/min	100	Young (Volunteers)
QCSF	cross-sectional	7.5	ml/min	N.S.	Elderly (Volunteers - Switzerland)
QCSF	cross-sectional	121	ml/min	100	Young (Volunteers)
QCSF	cross-sectional	93	ml/min	76,86	Elderly (Volunteers - Switzerland)
QCSF	cross-sectional	NA	NA	N.S.	(Volunteers)
QCSF	cross-sectional	2.6	ml/min	100	Young (Volunteers)
QCSF	cross-sectional	2.3	ml/min	N.S.	Elderly (Volunteers)
CSF production	cross-sectional	0.69	ml/min	100	Young (Volunteers)
CSF production	cross-sectional	0.68	ml/min	N.S.	Elderly (Volunteers)
CSF production	cross-sectional	NA	NA	NA	(Volunteers)
CSF outflow	cross-sectional	NA	NA	NA	(Volunteers)
QCBF					
CBF	cross sectional	0	ml/year		(Volunteers)
CBF	cross sectional	-6.2	ml/year		(PROSPER)
CBF	longituinal (4)	54.1	ml/100g/min		(DLBS)
CBF	longituinal (4)	51.8	ml/100g/min		(DLBS)
CBF	longituinal (4)	48.4	ml/100g/min		(DLBS)
CBF	longituinal (4)	44.5	ml/100g/min		(DLBS)
CBF	longituinal (4)	43.4	ml/100g/min		(DLBS)
CBF	longituinal (4)	41.4	ml/100g/min		(DLBS)
CBF	longituinal (4)	39.8	ml/100g/min		(DLBS)
CBF	cross sectional	-0.37	% / year		(Volunteers)
CBF	cross sectional	-0.33	ml/100g/ min/year		(Volunteers)
CBF	cross sectional	N.S.	ml/100g/ min/year		(Volunteers)

Age (years)	Age range (SD)	Number patients	Technique	Notes	Ref.
NA	51-88	34	PC-MRI	Aqueduct	[35]
24	(3)	11	MRI	Aqueduct	[36]
70	(5)	11	MRI	Aqueduct	[36]
24	(3)	11	MRI	Craniocervical junction	[36]
70	(5)	11	MRI	Craniocervical junction	[36]
31.2	6-70	60	MRI	non-significant increase of average flow & decrease of flow velocity	[37]
29.8	22-40 (7.6)	8	MRI	Aqueduct (craniocaudal - caudocranial)	[38]
69	58-76 (8)	5	MRI	Aqueduct (craniocaudal - caudocranial)	[38]
29.8	22-40 (7.6)	8	MRI	Aqueduct	[38]
69	58-76 (8)	5	MRI	Aqueduct	[38]
47.9	22-79 (15.8)	40	MRI	No age effect on CSF flow patterns or velocity at LV, TFV, aqueduct, monro	[39]
60	20-88	52	Lumbar computerized infusion	A small, significant increase of resistance to CSF outflow with age	[40]
35	20-63 (12)	48	Transcranial color duplex	No correction for brain atrophy	[41]
75	(3)	NA	MRI	Accounted for brain atrophy	[42]
NA	20-30	NA	MRI	Accounted for brain atrophy	[43]
NA	30-40	NA	MRI	Accounted for brain atrophy	[43]
NA	40-50	NA	MRI	Accounted for brain atrophy	[43]
NA	50-60	NA	MRI	Accounted for brain atrophy	[43]
NA	60-70	NA	MRI	Accounted for brain atrophy	[43]
NA	70-80	NA	MRI	Accounted for brain atrophy	[43]
NA	80-90	NA	MRI	Accounted for brain atrophy	[43]
41	20-67 (14)	34	MRI	Accounted for brain atrophy	[44]
47.7	20-80	17	MRI	No correction for brain atrophy	[45]
39	20-72 (19)	26	PET	No correction for brain atrophy	[46]

Supplementary table 4. Continued

Parameter	Study design (follow up years)	Value	unit	%	Population (Database)
CBF	cross sectional	N.S.	ml/100ml/min		(Volunteers)
CBF	cross sectional	-9.38	ml/year		(Volunteers)
CBF	cross sectional	no change	ml/100g/min		(Volunteers)
CBF	cross sectional	-4.8	ml/year		(Volunteers)
$Kp_{uu,BBB}$ P-gp					
BBB pgp mRNA expression	cross-sectional	NA	%area stained	NS	Harvard Brain Tissue Resource Center at
BBB pgp mRNA expression	cross-sectional	NA	%area stained	NS	Harvard Brain Tissue Resource Center at
BBB pgp protein expression	cross-sectional	NA	%area stained	NS	Harvard Brain Tissue Resource Center at
BBB pgp protein expression	cross-sectional	NA	%area stained	NS	Harvard Brain Tissue Resource Center at
(R)-[11C] verapamil distribution volume	cross-sectional	0.62	NA	100	Young (Volunteers)
(R)-[11C] verapamil distribution volume	cross-sectional	0.73	NA	118	Elderly (Volunteers)
(R)-[11C] verapamil distribution volume	cross-sectional	0.38	NA	100	Young (Volunteers)
(R)-[11C] verapamil distribution volume	cross-sectional	0.61	NA	160	Elderly (Volunteers)
(R)-[11C] verapamil distribution volume	cross-sectional	0.79	NA	100	Young (Volunteers)
(R)-[11C] verapamil distribution volume	cross-sectional	0.78	NA	NS	Elderly (Volunteers)
(R)-[11C] verapamil distribution volume	cross-sectional	0.79	NA	100	Young (Volunteers)

	Age (years)	Age range (SD)	Number patients	Technique	Notes	Ref.
	46.2	20-80 (20)	27	MRI	Accounted for brain atrophy	[47]
	71	(9)	12	MRI	No correction for brain atrophy	[31]
	50	50-85	28	PET	No correction for brain atrophy	[48]
	NA	19-88	250	2D phase-contrast MRI	No correction for brain atrophy	[49]
	45.7	20-60	6	IHC	NA	[50]
	76	61-100	8	IHC	NA	[50]
	45.7	20-60	6	IHC	NA	[50]
	76	61-100	8	IHC	NA	[50]
	25	21-27 (2.3)	5	MRI	NA	[51]
	61	59-68 (3.6)	5	MRI	NA	[51]
	24	(2)	7	MRI	NA	[52]
	60	(11)	10	MRI	NA	[52]
	26	(1)	5	MRI	NA	[53]
	68	(6)	5	MRI	NA	[53]
	26	(1)	5	MRI	NA	[53]

Supplementary table 4. Continued

Parameter	Study design (follow up years)	Value	unit	%	Population (Database)
(R)-[11C] verapamil distribution volume	cross-sectional	0.8	NA	NS	Young (Volunteers)
(R)-[11C] verapamil distribution volume	cross-sectional	0.78	NA	100	Elderly (Volunteers)
(R)-[11C] verapamil distribution volume	cross-sectional	1.08	NA	138,4	Elderly (Volunteers)
(R)-[11C] verapamil distribution volume	cross-sectional	0.71	NA	100	Young (Volunteers)
(R)-[11C] verapamil distribution volume	cross-sectional	0.75	NA	NS	Middle-aged (Volunteers)
(R)-[11C] verapamil distribution volume	cross-sectional	0.84	NA	NS	Elderly (Volunteers)
(R)-[11C] verapamil efflux rate constant	cross-sectional	NA	NA	100	Young (Volunteers)
(R)-[11C] verapamil efflux rate constant	cross-sectional	NA	NA	NS	Elderly (Volunteers)
(R)-[11C] verapamil distribution volume	cross-sectional	0.65	NA	100	Young (Volunteers)
(R)-[11C] verapamil distribution volume	cross-sectional	0.75	NA	NS	Elderly (Volunteers)
PPA-BBB					
BBB permeability (Ktrans)	cross-secional	NA		100	Young (Volunteers)

	Age (years)	Age range (SD)	Number patients	Technique	Notes	Ref.
	26	(1)	5	MRI	partial inhibition of pgp with tariquidar	[53]
	68	(6)	5	MRI	NA	[53]
	68	(6)	5	MRI	partial inhibition of pgp with tariquidar	[53]
	24	21-27 (2)	9	MRI	Regional significant changes (18-38%) of Vd, but not global	[54]
	46	42-50 (3)	10	MRI	Regional significant changes (18-38%) of Vd, but not global	[54]
	63	57-69 (4)	16	MRI	Regional significant changes (18-38%) of Vd, but not global	[54]
	27	(4)	7	MRI	NA	[55]
	69	(9)	6	MRI	NA	[55]
	27	(4)	7	MRI	NA	[55]
	69	(9)	6	MRI	NA	[55]
	NA	23-47	6	CE-MRI	superior frontal & inferior temporal gyrus cortex, thalamys, striatum, WM, corpus collosum, internal capsule	[56]

Supplementary table 4. Continued

Parameter	Study design (follow up years)	Value	unit	%	Population (Database)
BBB permeability (Ktrans)	cross-secional	NA	min-1/year	N.S.	Elderly (Volunteers)
passive permeability	cross-secional	1.22	min-1	100	Young (Volunteers)
passive permeability	cross-secional	1.59	min-1	130	Elderly (Volunteers)
passive permeability	cross-secional	0.00093	min-1	100	Young (Volunteers)
passive permeability	cross-secional	0.0013	min-1	139,8	Elderly (Volunteers)
WM passive permeability increase/year	cross-secional	0.121	min-1.yr-1	NA	Volunteers
GM passive permeability increase/year	cross-secional	0.109	min-1.yr-1	NA	Volunteers
passive permeability increase/year	cross-secional	0.114	min-1.yr-1	NA	Volunteers
SABBB					
capillary SA/unit tissue volume	cross-sectional	1.98	mm2/mm3	100	postmortum
capillary SA/unit tissue volume	cross-sectional	1.78	mm2/mm3	89,9	postmortum
capillary volume/unit tissue volume	cross-sectional	0.0025	mm3/mm3	100	postmortum
capillary volume/unit tissue volume	cross-sectional	0.0025	mm3/mm3	N.S.	postmortum
capillary SA/unit capillary volume	cross-sectional	792	mm2/mm3	100	postmortum
capillary SA/unit capillary volume	cross-sectional	712	mm2/mm3	89,9	postmortum
cappilaries	cross-sectional	NA	NA	NA	postmortum

Age (years)	Age range (SD)	Number patients	Technique	Notes	Ref.
NA	55-90	18	CE-MRI	superior frontal & inferior temporal gyrus cortex, thalamys, striatum, WM, corpus collosum, internal capsule	[56]
NA	23-47	6	CE-MRI	caudate nucleus	[56]
NA	55-91	18	CE-MRI	caudate nucleus	[56]
	23-47	6	CE-MRI	Hippocampus	[56]
	55-91	18	CE-MRI	Hippocampus	[56]
65.8	47-91 (10.2)	57	CE-MRI	calculated from Bstd, by multiplying Bstd with sd of Ki (cubic root (Ki*1000) & 1/sd of AGE)	[57]
65.8	47-91 (10.2)	57	CE-MRI	calculated from Bstd, by multiplying Bstd with sd of Ki (cubic root (Ki*1000) & 1/sd of AGE)	[57]
65.8	47-91 (10.2)	57	CE-MRI	average over grey and white matters, accounting for volume differences	[57]
38	21-51	5	microscopy	NA	[58]
74	60-88	5	microscopy	NA	[58]
38	21-51	5	microscopy	NA	[58]
74	60-88	5	microscopy	NA	[58]
38	21-51	5	microscopy	NA	[58]
74	60-88	5	microscopy	NA	[58]
69	26-96 (15.2)	24	stereology	Capillary surface area:tissue vol and capillary length: tissue volume signnificantly correlated with age in frontal cortex	[59]

Supplementary table 4. Continued

Parameter	Study design (follow up years)	Value	unit	%	Population (Database)
cappilaries	cross-sectional	NA	NA	NA	postmortum
cappilaries	cross-sectional	NA	NA	NA	postmortum
SABCSFB					
Choroid plexus cells height	cross-sectional	14.3	um	N.S.	Post-mortum
Choroid plexus cells height	cross-sectional	13.7	um	100	Post-mortum

Supplementary table 5. CNS pathophysiology in mild Alzheimer's patients

Value	unit	%	Database	cohort	Severity score (method)
Brain volume					
1453	mL	94.7	NA	Mild AD	22 (MMSE)
1534	mL	100	NA	healthy elderly	28 (MMSE)
952.3	mL	95.4	ADNI	Mild AD	23.7 (MMSE)
997.9	mL	100	ADNI	healthy elderly	29.1 (MMSE)
1007	mL	96	ADNI	Mild AD	23.5 (MMSE)
1049	mL	100	ADNI	healthy elderly	29.2 (MMSE)
1106	mL	96	NA	not reported	(National Institute on Aging–Alzheimer's criteria)
1152	mL	100	NA	not reported	(National Institute on Aging–Alzheimer's criteria)
CSF flow					
2.65	mL/min	NS	NA	Mild AD	≥20 (MMSE)
2.81	mL/min	100	NA	Age-matched control	29 (MMSE)

Age (years)	Age range (SD)	Number patients	Technique	Notes	Ref.
69	26-96 (15.2)	24	stereology	Capillary volume:tissue volume, capillary surface area: volume, capillary diameter did not significantly correlate with age in frontal cortex	[59]
68	26-96 (15.6)	25	stereology	capillary volume:tissue volume, capillary surface area:tissue vol, capillary length:tissue volume, capillary surface area:capillary volume, capillary diameter did not signficantly correlate with age in temporal cortex	[59]
46	NA	1	microscopy	NA	[60]
89.1	82-96 (5.4)	8	microscopy	NA	[60]

Age	Age range	Number pts	Technique	Notes	Ref.
67	(9)	64	MRI	NA	[61]
67	(9)	34	MRI	NA	[61]
74.9	(7.6)	65	MRI	NA	[62]
75.8	(5.5)	87	MRI	NA	[62]
75.3	(6.9)	99	MRI	NA	[63]
76	(5.1)	131	MRI	NA	[63]
79.1	(5)	18	MRI	NA	[64]
77	(6.6)	26	MRI	NA	[64]
79	(5)	9	MRI	Aqueduct, calc. as stroke volume (ul/cycle)*heart rate	[65]
71	(9)	12	MRI	Aqueduct, calc. as stroke volume (ul/cycle)*heart rate	[65]

Supplementary table 5. Continued

Value	unit	%	Database	cohort	Severity score (method)
35.64	mL/min	NS	NA	Mild AD	21 (MMSE)
32.4	mL/min	100	NA	Age-matched control	29 (MMSE)
8.81	mL/min	NS	NA	AD patients	NA
8.42	mL/min	100	NA	Volunteers	NA
CSF volume					
1241	ml	108.2	LAARC	Mild-Moderate AD	19.4 (MMSE)
1147	ml	100	LAARC	Healthy	28.2 (MMSE)
19.70	%/ICV	111.3	LAARC	Mild-Moderate AD	19.4 (MMSE)
17.70	%/ICV	100	LAARC	Healthy	28.2 (MMSE)
5.60	%/ICV	155.6	LAARC	Mild-Moderate AD	19.4 (MMSE)
3.60	%/ICV	100	LAARC	Healthy	28.2 (MMSE)
128.3	ml	131.5	NA	AD	NA
97.60	ml	100	NA	Control, Normal volunteers	NA
44.46	ml	145.5	ADNI	Mild AD	23.14 (MMSE)
30.56	ml	100	ADNI	Healthy	28.67 (MMSE)
22.20	ml	133.7	ADNI-1	Mild AD	20-26 (MMSE)
16.60	ml	100	ADNI-1	Healthy	24-30 (MMSE)
1.50	%/ICV	136.4	ADNI-1	Mild AD	20-26 (MMSE)
1.10	%/ICV	100	ADNI-1	Healthy	24-30 (MMSE)
1493	ml	102.3	NA	AD	NA
1459	ml	100	Volunteers	Control	>27 (MMSE)
247	ml	130.7	NA	AD	NA

Age	Age range	Number pts	Technique	Notes	Ref.
79	(5)	9	MRI	Craniocervical junction, calc. as stroke volume (ul/cycle)*heart rate	[65]
71	(9)	12	MRI	Craniocervical junction, calc. as stroke volume (ul/cycle)*heart rate	[65]
71.2	50-87	46	MRI	Aqueduct	[66]
80.3	62-91	47	MRI	Aqueduct	[66]
71.9	(8)	39	MRI	Intracranial volume; All AD; sign differed compared to control	[67]
83.9	(7.2)	166	MRI	Intracranial volume; No dementia/Normal	[67]
71.9	(8)	39	MRI	SAS:ICV; All AD; sign diff compared to control and questionable	[67]
83.9	(7.2)	166	MRI	SAS/ICV; no dementia/ Normal	[67]
71.9	(8)	39	MRI	Total ventricles colume/ICV; all AD; sign diff compared to control and questionable	[67]
83.9	(7.2)	166	MRI	Total ventricles colume/ ICV;no dementia/Normal	[67]
54	NA	1	MRI	Extraventricular intracranial CSF	[68]
37	18-74	10	MRI	Extraventricular intracranial CSF	[68]
74.58	55-90 (1.06)	46	MRI	Total ventricular volume	[69]
72.98	55-91 (0.84)	73	MRI	Total ventricular volume	[69]
74	(7.7)	108	MRI	Total ventricular volume at baseline	[70]
75	(4.8)	156	MRI	Total ventricular volume at baseline	[70]
74	(7.7)	108	MRI	Total ventricular volume/ ICV at baseline	[70]
75	(4.8)	155	MRI	Total ventricular volume/ ICV at baseline	[70]
72.6	(4.7)	10	MRI	ICV	[71]
71.1	(3.9)	8	MRI	ICV	[71]
72.6	(4.7)	10	MRI	Intracranial CSF volume/ICV	[71]

Supplementary table 5. Continued

Value	unit	%	Database	cohort	Severity score (method)
189	ml	100	Volunteers	Control	>27 (MMSE)
18.20	%/ICV	144.6	NA	AD	NA
12.59	%/ICV	100	Volunteers	Control	>27 (MMSE)
6.06	%/ICV	162.0	NA	Mild-Moderate AD	19 (MMSE)
4.78	%/ICV	127.8	NA	Mild-Moderate AD	19 (MMSE)
3.74	%/ICV	100	NA	Healthy	29 (MMSE)
49.90	ml	130.3	ADNI	Mild AD	23.3 (MMSE)
38.30	ml	100	ADNI	Healthy	29.1 (MMSE)
48.70	ml	131.6	ADNI	Questionable-Mild AD	23.7 (CDR)
37.00	ml	100	ADNI	Healthy	29.1 (CDR)
1254.1	ml	105.1	Univeristy of Heidelberg dep Psychiatry	Mild-Moderate AD	17.2 (MMSE)
1193.5	ml	100	Community	Healthy	29.3 (MMSE)
1215.5	ml	101.9	Section of Geriatric psych of Uni of Heidelberg	Mild-Moderate AD	16.92 (MMSE)
1193.4	ml	100	Volunteers	Healthy	29.33 (MMSE)
1209.6	ml	102.3	Section of Geriatric psych of Uni of Heidelberg	Mild-Moderate AD	16.92 (MMSE)
1182	ml	100	Volunteers	Healthy	29.33 (MMSE)
428.9	ml	138	Univeristy of Heidelberg dep Psychiatry	Mild-Moderate AD	17.2 (MMSE)
310.8	ml	100	Community	Healthy	29.33 (MMSE)
1657	ml	100	Aging and Dementia Center	Control	29.5 (MMSE)
1336	ml	80.6	Aging and Dementia Center	Mild-Advaced AD	19.2 (MMSE)
589	ml	100	Aging and Dementia Center	Healthy	29.5 (MMSE)

Age	Age range	Number pts	Technique	Notes	Ref.
71.1	(3.9)	8	MRI	Intracranial CSF volume/ICV	[71]
72.6	(4.7)	10	MRI	Intracranial CSF volume/ICV	[71]
71.1	(3.9)	8	MRI	Intracranial CSF volume/ICV	[71]
78.9	(4.4)	38	MRI	Total ventricular volume/ ICV (with lacune)	[72]
78.9	(4.4)	38	MRI	Total ventricular volume/ ICV (without lacune)	[72]
78.1	(5.6)	40	MRI	Total ventricular volume/ICV	[72]
74.9	(15)	104	MRI	Total ventricular volume at baseline	[73]
76.4	(5.2)	152	MRI	Total ventricular volume at baseline	[73]
74.9	(7.6)	65	MRI	Total ventricular volume	[62]
75.8	(5.5)	87	MRI	Total ventricular volume	[62]
71.9	57-85 (8)	27	MRI	ICV (duncan's test: NS)	[74]
68.2	59-87 (5.3)	13	MRI	ICV (duncan's test: NS)	[74]
68.23	(0.78)	22	MRI	Intracranial CSF volume not adjusted for age	[74]
71.04	(8.56)	13	MRI	Intracranial CSF volume not adjusted for age	[74]
68.23	(0.78)	22	MRI	Intracranial CSF volume adjusted for age	[74]
71.04	(8.56)	13	MRI	Intracranial CSF volume adjusted for age	[74]
71.9	57-85 (8)	27	MRI	Intracranial CSF volume (Duncan's test: NS)	[74]
68.2	59-87 (5.3)	13	MRI	Intracranial CSF volume (duncan's test: NS)	[74]
69.7	59-84 (7)	18	MRI	ICV	[75]
72.1	53-87 (11)	17	MRI	ICV	[75]
69.7	59-84 (7)	18	MRI	ICV CSF volume, no sign difference across groups	[75]

Supplementary table 5. Continued

Value	unit	%	Database	cohort	Severity score (method)
565	ml	95.9	Aging and Dementia Center	Mild-Advaced AD	19.2 (MMSE)
91	ml	133.8	Aging and Dementia Center	Mild-Advaced AD	19.2 (MMSE)
68	ml	100	Aging and Dementia Center	Healthy	29.5 (MMSE)
4.8	%/ICV	137.1	ADNI	Mild-Moderate AD	22.9 (MMSE)
3.5	%/ICV	100	ADNI	Healthy	28.8 (MMSE)
54	ml	138.5	ADNI	Mild AD	24 (MMSE)
39	ml	100	ADNI	Healthy	29 (MMSE)
4.4	ml/year	NA	ADNI	Mild	24 (MMSE)
1.4	ml/year	NA	ADNI	Healthy	29 (MMSE)
Cerebral blood flow					
36.8	ml·100 g− 1·min− 1	88.5		Mild - Moderate AD	20.8 (MMSE)
41.6	ml·100 g− 1·min− 1	100.0		Age matched	28.9 (MMSE)
38.2	ml·100 g− 1·min− 1	76.6		Mild - Moderate AD	19.9 (MMSE)
49.9	ml·100 g− 1·min− 1	100.0		Age matched	29.5 (MMSE)
27.8	ml·100 g− 1·min− 1	75.7		Mild - Moderate AD	20.1 (MMSE)
36.7	ml·100 g− 1·min− 1	100.0		Age matched	29.4 (MMSE)
27.3	ml·100 g− 1·min− 1	86.7		Mild - Moderate AD	21 (MMSE)
31.5	ml·100 g− 1·min− 1	100.0		Age matched	28 (MMSE)

Age	Age range	Number pts	Technique	Notes	Ref.
72.1	53-87 (11)	17	MRI	ICV CSF volume, no sign difference across groups, p = 0.88	[75]
72.1	53-87 (11)	17	MRI	Total ventricular volume, p = 0.11	[75]
69.7	59-84 (7)	18	MRI	Total ventricular volume, p = 0.11	[75]
76.4	62.3-86.6	30	MRI & ASL	Total ventricular volume/ ICV at baseline	[76]
73.5	63.2-84.7	41	MRI & ASL	Total ventricular volume/ ICV at baseline	[76]
77	71-81	71	MRI	Total ventricular volume; MRI and cogn assessment at 0, 6 and 12 months; but only 0 and 12 months incl because CSF measurements also at 0 and 12 months	[18]
75	72-78	92	MRI	Total ventricular volume; MRI and cogn assessment at 0, 6 and 12 months; but only 0 and 12 months incl because CSF measurements also at 0 and 12 months	[18]
77	71-81	71	MRI	Total ventricular volume; Longitudinal study (1 year)	[18]
75	72-78	92	MRI	Total ventricular volume; Longitudinal study (1 year)	[18]
70.6	56-78 (6.2)	30	SPECT	Global	[77]
68.3	55-78 (6.1)	62	SPECT	Global	[77]
72	(6.3)	15	3D ASL	Whole brain GM, corrected for atrophy and enlarged ventricles	[78]
69.2	(7.6)	19	3D ASL	Whole brain GM, corrected for atrophy and enlarged ventricles	[78]
74.5	55-89 (8.6)	19	3D ASL	Global	[79]
72.8	50-81 (6.8)	22	3D ASL	Global	[79]
66	(7)	129	3D ASL	Whole brain CBF	[80]
64	(5)	61	3D ASL	Whole brain CBF	[80]

Supplementary table 5. Continued

Value	unit	%	Database	cohort	Severity score (method)
41.8	ml·100 g− 1·min− 1	88.9		Mild - Moderate AD	21 (MMSE)
47	ml·100 g− 1·min− 1	100.0		Age matched	28 (MMSE)
44.28	ml·100 g− 1·min− 1	91.0		Mild Cognitive Impairment	26.57 (MMSE)
41.47	ml·100 g− 1·min− 1	85.2		Mild - Moderate AD	20.6 (MMSE)
49	ml·100 g− 1·min− 1	100.0		Age matched	28 (MMSE)
42	ml·100 g− 1·min− 1	85.7		Mild - Moderate AD	21 (MMSE)
BBB active transporters: pgp protein expression					
6.6	pmol/gm GM	100		Age Matched	-
6.8	pmol/gm GM	N.S.		Severe AD	IV-VI (Braak)
4.6	pmol/gm GM	100		Age Matched	-
4.4	pmol/gm GM	N.S.		Severe AD	IV-VI (Braak)
196.3	a.u.	100		Age Matched	NA
146.4	a.u.	74.6		AD patients	NA
NA	NA	100		Age Matched	NA
NA	NA	N.S.		AD patients	NA
6	not reported	100		Age Matched	NA
4	not reported	N.S.		AD patients	NA
43.6	not reported	100		Age Matched	I-II (Braak)
44.5	not reported	N.S.		Severe AD	V-VI (Braak)
2.58	pmol/gm total protein	100		Age Matched	NA
2.25	pmol/gm total protein	N.S.		AD patients	NA
BBB active transporters: BCRP protein expression					
16.3	pmol/gm GM	100		Age Matched	-
16.08	pmol/gm GM	N.S.		Severe AD	IV-VI (Braak)
8.7	pmol/gm GM	100		Age Matched	-
8.5	pmol/gm GM	N.S.		Severe AD	IV-VI (Braak)
190	a.u.	100		Age Matched	NA
200	a.u.	N.S.		AD patients	NA
2.2	not reported	100		Age Matched	NA
1.8	not reported	N.S.		AD patients	NA
7	not reported	100		Age Matched	NA
5	not reported	N.S.		AD patients	NA

	Age	Age range	Number pts	Technique	Notes	Ref.
	66	(7)	129	3D ASL	PVC cortical CBF, corrected for PVE	[80]
	64	(5)	61	3D ASL	PVC cortical CBF, corrected for PVE	[80]
	65.24	(7.2)	95	3D ASL	PVC cortical CBF, corrected for brain atrophy	[81]
	65.93	(7)	161	3D ASL	PVC cortical CBF, corrected for brain atrophy	[81]
	62	(6)	50	3D ASL	Corrected for brain atrophy	[82]
	65	(7)	48	3D ASL	Corrected for brain atrophy	[82]
	81	70-98 (7)	38	LC-MS/MS	Cerebellum	[83]
	84	75-100 (7)	41	LC-MS/MS	Cerebellum	[83]
	81	70-98 (7)	38	LC-MS/MS	Hippocampus	[83]
	84	75-100 (7)	41	LC-MS/MS	Hippocampus	[83]
	NA	48-89	8	IHC	NA	[84]
	NA	51-84	8	IHC	NA	[84]
	NA	48-89	8	Western Blot	NA	[84]
	NA	51-84	8	Western Blot	NA	[84]
	NA	48-89	8	RT-PCR	NA	[84]
	NA	51-84	8	RT-PCR	NA	[84]
	NA	64-91	5	IHC	Global brain	[85]
	NA	66-89	5	IHC	Global brain	[85]
	78.75	53-90 (14.3)	12	LC-MS/MS	NA	[86]
	78.75	53-90 (14.3)	5	LC-MS/MS	NA	[86]
	81	70-98 (7)	38	LC-MS/MS	Cerebellum	[83]
	84	75-100 (7)	41	LC-MS/MS	Cerebellum	[83]
	81	70-98 (7)	38	LC-MS/MS	Hippocampus	[83]
	84	75-100 (7)	41	LC-MS/MS	Hippocampus	[83]
	NA	48-89	8	IHC	NA	[84]
	NA	51-84	8	IHC	NA	[84]
	NA	48-89	8	Western Blot	NA	[84]
	NA	51-84	8	Western Blot	NA	[84]
	NA	48-89	8	RT-PCR	NA	[84]
	NA	51-84	8	RT-PCR	NA	[84]

Supplementary table 5. Continued

Value	unit	%	Database	cohort	Severity score (method)
65.5	not reported	100		Age Matched	I-II (Braak)
69.5	not reported	N.S.		Severe AD	V-VI (Braak)
2.22	pmol/gm total protein	100		Age Matched	NA
1.91	pmol/gm total protein	N.S.		AD patients	NA
11[C]-Verapamil AUC/rCBF					
1.06	not reported	100		Age Matched	29.7 (MMSE)
1.35	not reported	127.4		Mild AD	24.3 (MMSE)
1.06	not reported	100		Age Matched	29.7 (MMSE)
1.26	not reported	118.9		Mild AD	24.3 (MMSE)
1.05	not reported	100		Age Matched	29.7 (MMSE)
1.24	not reported	118.1		Mild AD	24.3 (MMSE)
1.12	not reported	100		Age Matched	29.7 (MMSE)
1.25	not reported	N.S.		Mild AD	24.3 (MMSE)
Brain microvasculature volume					
NA	not reported	100		healthy elderly	NA
NA	not reported	N.S.		mild-moderate AD	14-26 (MMSE)
NA	NA	100		healthy elderly	NA
NA	NA	N.S.		mild AD	22 (MMSE)
NA	NA	100		healthy elderly	27.55 (MMSE) | 0 (CDR)
NA	NA	N.S.		moderate AD	19.08 (MMSE) | 1 (CDR)
0.89	NA	100		healthy elderly	29.8 (MMSE)
0.92	NA	N.S.		moderate AD	17.8 (MMSE)
78	ml	100		healthy elderly	30 (MMSE)
79	ml	N.S.		moderate AD	18 (MMSE)
0	ml/6 mo	NA		AD	NA
BBB paracellular transport (by Ktrans)					
NA	NA	NS		probable AD	(NINCDS-ADRDA)

	Age	Age range	Number pts	Technique	Notes	Ref.
	NA	64-91	5	IHC	Global brain	[85]
	NA	66-89	5	IHC	Global brain	[85]
	78.75	53-90 (14.3)	12	LC-MS/MS	NA	[86]
	78.75	53-90 (14.3)	5	LC-MS/MS	NA	[86]
	73.2	(1.9)	9	PET	Left temporal	[87]
	72.9	(2)	9	PET	Left temporal	[87]
	73.2	(1.9)	9	PET	Left parietal	[87]
	72.9	(2)	9	PET	Left parietal	[87]
	73.2	(1.9)	9	PET	Right temporal	[87]
	72.9	(2)	9	PET	Right temporal	[87]
	73.2	(1.9)	9	PET	Right parietal	[87]
	72.9	(2)	9	PET	Right parietal	[87]
	67.5	(3.5)	15	perfusion CT	NA	[88]
	69.7	(5.5)	20	perfusion CT	Front temp occ cortex & lentiform nucleus; A non-sginificant decrease of CBV	[88]
	67.4	(8.9)	23	DSC-MRI	cerebellum, hippocampus, temp. tempoparietal frontal sensimotoric cortex, lentiform nuc., cingulate gyrus	[89]
	71.8	(8.8)	34	DSC-MRI	A non-sginificant decrease of CBV	[89]
	71.65	(7.04)	20	MRI	whole brain cortex	[90]
	77.42	(6.97)	12	MRI	whole brain cortex	[90]
	68.1	(7.1)	20	PWI-DCS MRI	hippocampus	[91]
	71.2	(8)	30	PWI-DCS MRI	hippocampus	[91]
	65	(8)	12	ultrasound	not corrected by total brain volume	[92]
	66	(13)	20	ultrasound	not corrected by total brain volume	[92]
	64.47	(6.94)	32	MRI	No significant change of VMV after 6 month of longitudinal study, PVE considered	[93]
	73.7	NA	15	Dynamic MRI. Gd-DTPA	Uses spouses of AD patients as control group	[94]

Supplementary table 5. Continued

Value	unit	%	Database	cohort	Severity score (method)
NA	NA	100		Control	(NINCDS-ADRDA)
1.61	*10^-3 per min	123.8		MCI patient	0.5 (CDR)
1.3	*10^-3 per min	100		NCI elderly	0 (CDR)
0.9	*10^-4 per min	529.4		Pre-AD - Mild	26.3 (MMSE)
0.17	*10^-4 per min	100		Control	29.5 (MMSE)
0.84	*10^-4 per min	1050		Pre-AD - Mild	26.3 (MMSE)
0.08	*10^-4 per min	100		Control	29.5 (MMSE)
0.66	*10^-4 per min	N.S.		Pre-AD - Mild	26.3 (MMSE)
0.7	*10^-4 per min	100		Control	29.5 (MMSE)
0.65	*10^-4 per min	N.S.		Pre-AD - Mild	26.3 (MMSE)
0.7	*10^-4 per min	100		Control	29.5 (MMSE)
1.25	*10^-4 per min	N.S.		Pre-AD - Mild	26.3 (MMSE)
0.84	*10^-4 per min	100		Control	29.5 (MMSE)
1.06	*10^-4 per min	N.S.		Pre-AD - Mild	26.3 (MMSE)
0.61	*10^-4 per min	100		Control	29.5 (MMSE)
2.75	*10^-4 per min	N.S.		Pre-AD - Mild	NA
1.8	*10^-4 per min	100		Control	NA
3.84	ul/gm/min	100		healthy elderly	(CAST)
4.15	ul/gm/min	N.S.		mild AD	(CAST)
BCSFB paracellular transport					
				NA	
0.79	NA	100		healthy volunteers	NA

Age	Age range	Number pts	Technique	Notes	Ref.
72.7	NA	15	Dynamic MRI. Gd-DTPA	Uses spouses of AD patients as control group	[94]
	55-85	21	Dynamic MRI	Hippocampus	[56]
	55-91	18	Dynamic MRI	Hippocampus	[56]
73.6	59-85 (7.9)	16	Dynamic MRI. Gadobutrol	Grey Matter	[95]
75.8	65-85 (6.2)	17	Dynamic MRI. Gadobutrol	Grey Matter	[95]
73.6	59-85 (7.9)	16	Dynamic MRI. Gadobutrol	Cortex	[95]
75.8	65-85 (6.2)	17	Dynamic MRI. Gadobutrol	Cortex	[95]
73.6	59-85 (7.9)	16	Dynamic MRI. Gadobutrol	White Matter	[95]
75.8	65-85 (6.2)	17	Dynamic MRI. Gadobutrol	White Matter	[95]
73.6	59-85 (7.9)	16	Dynamic MRI. Gadobutrol	Normal appearing white matter	[95]
75.8	65-85 (6.2)	17	Dynamic MRI. Gadobutrol	Normal appearing white matter	[95]
73.6	59-85 (7.9)	16	Dynamic MRI. Gadobutrol	Deep Grey Matter	[95]
75.8	65-85 (6.2)	17	Dynamic MRI. Gadobutrol	Deep Grey Matter	[95]
73.6	59-85 (7.9)	16	Dynamic MRI. Gadobutrol	White Matter Hyperintensities	[95]
75.8	65-85 (6.2)	17	Dynamic MRI. Gadobutrol	White Matter Hyperintensities	[95]
75.3	65-85	16	Dynamic MRI. Gadobutrol	Grey matter; Not significant but trend of patients higher ktrans (p=0.055)	[96]
76.4	65-85	18	Dynamic MRI. Gadobutrol	Grey matter; Not significant but trend of patients higher ktrans (p=0.055)	[96]
83.4	(3.1)	9	CT-meglumine iothalamate	Average values of frontal, temporal, accipital, hippocampus, basal ganglia	[97]
87.3	(3.8)	14	CT-meglumine iothalamate	Average values of frontal, temporal, accipital, hippocampus, basal ganglia	[97]
				BCSFB permeability might increase as indicated by increased CSF:plasma albumin ratio, while no indication of the impact of small drug molecules	[98]
46	28-77 (11)	21	Biochemical (CSF:serum urea)	volunteers and AD are not age matched	[99]

Supplementary table 5. Continued

Value	unit	%	Database	cohort	Severity score (method)
0.85	NA	107.6		mild AD	22 (MMSE)
1.5	NA	100		healthy volunteers	NA
1.15	NA	123.3		mild AD	22 (MMSE)
Brain phospholipids					
100	NA	100		Elderly	NA
89.9	NA	89.9		AD	NA
NA	NA	NA		NA	NA
NA	NA	100		Elderly	NA
NA	NA	50		AD	NA
0.35	umol/mg protein	100		Elderly	NA (CERAD)
0.28	umol/mg protein	80		AD	NA (CERAD)
0.4	umol/mg protein	100		Elderly	NA (CERAD)
0.37	umol/mg protein	92.5		AD	NA (CERAD)
52.43	umol/g brain wet wt	100		Elderly	4-5 (global deterioration scale)
50.55	umol/g brain wet wt	N.S.		moderate-severe AD	4-5 (global deterioration scale)
84.8	umol/g brain wet wt	100		Elderly	4-5 (global deterioration scale)
102.7	umol/g brain wet wt	N.S.		moderate-severe AD	4-5 (global deterioration scale)
98.89	NA	100		Elderly	NA
99.85	NA	100.9		AD	NA

Age	Age range	Number pts	Technique	Notes	Ref.
67	49-83 (10)	11	Biochemical (CSF:serum urea)	volunteers and AD are not age matched	[99]
46	28-77 (11)	21	Biochemical (CSF:serum creatinine)	volunteers and AD are not age matched	[99]
67	49-83 (10)	11	Biochemical (CSF:serum creatinine)	volunteers and AD are not age matched	[99]
74.4	38-89 (4.6)	10	homogn and extraction	Change mean of ptdCho, PtdEtn, PtdSer, Shingmyl, PtdIns/PA weighted by amount at frontal cortex of Controls	[100]
75.7	51-95 (3.6)	10	homogn and extraction	postmortum, pairwised on age, postmortum & storage times	[100]
NA	NA	NA	NA	phospholipds decrease in AD compared to aging	[101]
NA	76-92	3	HPLC	mean different phospholip from parietal, frontal	[102]
NA	76-92	5	HPLC	mean different phospholip from parietal, frontal	[102]
72	(13)	13	homogn and extraction	frontal cortex/total phospholipids	[103]
80	(8)	15	homogn and extraction	frontal cortex/total phospholipids	[103]
72	(13)	13	homogn and extraction	hippocampus/total phospholipids	[103]
80	(8)	15	homogn and extraction	hippocampus/total phospholipids	[103]
70.1	(8.1)	9	homogn and extraction	prefrontal cortex/ total phospholipids	[104]
70.6	(7.6)	10	homogn and extraction	prefrontal cortex/ total phospholipids	[104]
78.4	(6.9)	6	homogn and extraction	Anterior Temporal Cortex/ total phospholipids	[105]
80.3	(8)	6	homogn and extraction	Anterior Temporal Cortex/ total phospholipids	[105]
69.9	(3)	11	31P NMR	Postmortum, cerebellum, inf. Parietal, occip, sup. med front,sup. Temp	[106]
72.9	(0.8)	45	31P NMR	Post mortum, cerebellum, inf. Parietal, occip, sup. med front,sup. Temp	[106]

Supplementary table 5. Continued

Value	unit	%	Database	cohort	Severity score (method)
NA	NA	100		Elderly	NA
NA	NA	N.S.		AD/SDAT	NA
NA	NA	100		Elderly	NA
NA	NA	80.96		early onset AD patients	NA
NA	NA	100		Elderly	NA
NA	NA	N.S.		late onset AD patients	NA
BBB surface area: Arteriolar density					
14.5	mm/mm^3	100.0		Healthy elderly	(SDAT)
14.4	mm/mm^3	NS		Unknown severity	(SDAT)
5.58	mm/mm^3	100.0		Healthy elderly	(pathologically confirmed)
6.64	mm/mm^3	119.0		Unknown severity	(pathologically confirmed)
BBB surface area: Capillary density					
212	mm/mm^3	100.0		Healthy elderly	(pathologically confirmed)
206	mm/mm^3	NS		Unknown severity	(pathologically confirmed)
102	mm/mm^3	100.0		Healthy elderly	(pathologically confirmed)
101	mm/mm^3	NS		Unknown severity	(pathologically confirmed)
291	mm/mm^3	100.0	Neurological Foundation Human Brain Bank, New Zealand	Healthy elderly	(pathologically confirmed)
361	mm/mm^3	124.1	Neurological Foundation Human Brain Bank, New Zealand	Mild-severe AD	2-3 (CERAD)

	Age	Age range	Number pts	Technique	Notes	Ref.
	78.1	67-91 (8.8)	9	homogn and extraction	fron,temp,occi,precentral cortex, fron WM, hippo, pons, cerebellum, Med. obl, Nuc. caud	[107]
	77.4	70-91 (6.3)	9	homogn and extraction	no change in phopholipids in different regions except frontal WM (81,9) & caudate nucleus(86,51)	[107]
	71.9	(7.6)	16	homogn and extraction	GM: front, temporal lobes, caudate nucl, hippocampus, mean value of multiple regions weighted by amounts of control	[108]
	71.9	(6.5)	11	homogn and extraction	GM: front, temporal lobes, caudate nucl, hippocampus	[108]
	80.8	(5.7)	12	homogn and extraction	GM: front, temporal lobes, caudate nucl, hippocampus	[108]
	81	(7)	21	homogn and extraction	GM: front, temporal lobes, caudate nucl, hippocampus	[108]
	78.8	67-95 (9.1)	8	Histological staining	Occipital cortex (visual)	[109]
	79.3	63-92 (9)	10	Histological staining	Occipital cortex (visual)	[109]
	74.0	60-88	5	Histological staining	Hippocampal cortex	[58]
	78.0	66-94	5	Histological staining	Hippocampal cortex	[58]
	78.8	67-95 (9.1)	8	Histological staining	Occipital cortex (visual)	[109]
	79.3	63-92 (9)	10	Histological staining	Occipital cortex (visual)	[109]
	74.0	60-88	5	Histological staining	Hippocampal cortex	[58]
	78.0	66-94	5	Histological staining	Hippocampal cortex	[58]
	75.2	63-83 (4.78)	16	Immunohistochemical staining & stereological analysis	Frontal cortex	[110]
	76.3	65-83 (4.98)	16	Immunohistochemical staining & stereological analysis	Frontal cortex	[110]

Supplementary table 5. Continued

Value	unit	%	Database	cohort	Severity score (method)
6.29	% covered by capillaries of area	NS	Banner Sun Health Research Institute Brain and Body Donation Program	Moderate-severe AD	14 (MMSE)
6.25	% covered by capillaries of area	100.0	Banner Sun Health Research Institute Brain and Body Donation Program	Questionable	27.7 (MMSE)
6.05	% covered by capillaries of area	100.0	Banner Sun Health Research Institute Brain and Body Donation Program	Healthy elderly	29.6 (MMSE)
5.12	% covered by capillaries of area	100.0	Banner Sun Health Research Institute Brain and Body Donation Program	Questionable	28 (MMSE)
13.97	% covered by capillaries of area	NS	Banner Sun Health Research Institute Brain and Body Donation Program	Moderate-severe AD	14 (MMSE)
13.37	% covered by capillaries of area	100.0	Banner Sun Health Research Institute Brain and Body Donation Program	Questionable	27.7 (MMSE)
13.41	% covered by capillaries of area	100.0	Banner Sun Health Research Institute Brain and Body Donation Program	Healthy elderly	29.6 (MMSE)
12.97	% covered by capillaries of area	100.0	Banner Sun Health Research Institute Brain and Body Donation Program	Questionable	28 (MMSE)
18.95	% of total cortical field area	NA		Healthy elderly	NA
16.5	% of total cortical field area	87.1		Possible AD	24 (NINCDS-ADRDA)
BBB surface area: MV density					
108	mm/mm^3	100.0		Healthy elderly	(pathologically confirmed)
107	mm/mm^3	NS		Unknown severity	(pathologically confirmed)
7.25	% area occupied by laminin	100.0	Kinsmen Laboratory brain bank, University of British Columbia	Healthy elderly	(NINCDS-ADRDA)

	Age	Age range	Number pts	Technique	Notes	Ref.
	94.2	90-96 (2.6)	6	Immunohistochemical staining	White matter (frontal, temporal, parietal and occipital lobe)	[111]
	92.8	90-100 (3.3)	8	Immunohistochemical staining	White matter (frontal, temporal, parietal and occipital lobe)	[111]
	92.5	91-99 (3.2)	6	Immunohistochemical staining	White matter (frontal, temporal, parietal and occipital lobe)	[111]
	70.8	65-75 (4.4)	5	Immunohistochemical staining	White matter (frontal, temporal, parietal and occipital lobe)	[111]
	94.2	90-96 (2.6)	6	Immunohistochemical staining	Gray matter (frontal, temporal, parietal, hippocampal and entorhinal regions)	[111]
	92.8	90-100 (3.3)	8	Immunohistochemical staining	Gray matter (frontal, temporal, parietal, hippocampal and entorhinal regions)	[111]
	92.5	91-99 (3.2)	6	Immunohistochemical staining	Gray matter (frontal, temporal, parietal, hippocampal and entorhinal regions)	[111]
	70.8	65-75 (4.4)	5	Immunohistochemical staining	Gray matter (frontal, temporal, parietal, hippocampal and entorhinal regions)	[111]
	79.0	(1)	3	Histological staining & photomicroscopy	Frontal, temporal and occipital cortex	[112]
	80.0	(5.6)	7	Histological staining & photomicroscopy	Frontal, temporal and occipital cortex	[112]
	74.0	60-88	5	Histological staining	Hippocampal cortex	[58]
	78.0	66-94	5	Histological staining	Hippocampal cortex	[58]
	83.0	75-99 (2.5)	4	Immunohistochemical staining	Medial cortex, emphasized on 'hotspots': areas with high laminin staining	[113]

Supplementary table 5. Continued

Value	unit	%	Database	cohort	Severity score (method)
12.25	% area occupied by laminin	168.8	Kinsmen Laboratory brain bank, University of British Columbia	Mild-severe AD	(NINCDS-ADRDA)
6.59	% area occupied by laminin	100.0	Kinsmen Laboratory brain bank, University of British Columbia	Healthy elderly	(NINCDS-ADRDA)
10.75	% area occupied by laminin	163.1	Kinsmen Laboratory brain bank, University of British Columbia	Mild-severe AD	(NINCDS-ADRDA)
1.32	% area per standard field	100.0	UWNP Core, tissue repository	Healthy elderly	0-II (Braak)
1.29	% area per standard field	NS	UWNP Core, tissue repository	Mild AD	III-IV (Braak)
1.34	% area per standard field	NS	UWNP Core, tissue repository	Severe AD	V-VI (Braak)
2.15	% area per standard field	100.0	UWNP Core, tissue repository	Healthy elderly	0-II (Braak)
2.24	% area per standard field	NS	UWNP Core, tissue repository	mild AD	III-IV (Braak)
2.05	% area per standard field	NS	UWNP Core, tissue repository	Severe AD	V-VI (Braak)
1.52	% area per standard field	100.0	UWNP Core, tissue repository	Healthy elderly	0-II (Braak)
2.13	% area per standard field	NS	UWNP Core, tissue repository	mild AD	III-IV (Braak)
1.84	% area per standard field	NS	UWNP Core, tissue repository	Severe AD	V-VI (Braak)
89.8	Number of arterioles or capillares/mm^2	100.0		Healthy elderly	NA
62.9	Number of arterioles or capillares/mm^3	70.0	St. Louis University AD Research Center Brain Bank	Unknown severity	23.3 (dementia scale)
7.08	%	100.0	Kinsmen Laboratory brain bank, University of British Columbia	Healthy elderly	NA
8.38	%	NS	Kinsmen Laboratory brain bank, University of British Columbia	mild AD	(NINCDS-ADRDA)

	Age	Age range	Number pts	Technique	Notes	Ref.
	75.6	58-99	4	Immunohistochemical staining	Medial cortex, emphasized on 'hotspots': areas with high laminin staining	[113]
	83.0	75-99 (2.5)	4	Immunohistochemical staining	Hippocampus, emphasized on 'hotspots': areas with high laminin staining	[113]
	75.6	58-99	4	Immunohistochemical staining	Hippocampus, emphasized on 'hotspots': areas with high laminin staining	[113]
	83.5	71-95	19	IF after IHC	Parietal cortex	[114]
	87.8	72-100	15	IF after IHC	Parietal cortex	[114]
	85.9	70-99	23	IF after IHC	Parietal cortex	[114]
	83.5	71-95	19	IHC	Parietal cortex	[114]
	87.8	72-100	15	IHC	Parietal cortex	[114]
	85.9	70-99	39	IHC	Parietal cortex	[114]
	83.5	71-95	10	IHC	Parietal cortex	[114]
	87.8	72-100	9	IHC	Parietal cortex	[114]
	85.9	70-99	17	IHC	Parietal cortex	[114]
	59.2	23-90 (26.8)	6	Fixation in formalin	Pre-frontal area, basal forebrain, motor/sensory area, hippocampus	[115]
	84.6	76-91 (4.9)	16	Fixation in formalin	Pre-frontal area, basal forebrain, motor/sensory area, hippocampus	[115]
	83.0	75-99 (2.5)	9	Immunohistochemical staining	Medial temporal cortex	[116]
	77.7	58-99 (5.9)	6	Immunohistochemical staining	Medial temporal cortex	[116]

Supplementary table 5. Continued

Value	unit	%	Database	cohort	Severity score (method)
9.99	%	119.3	Kinsmen Laboratory brain bank, University of British Columbia	Severe AD	(NINCDS-ADRDA)
23.84	NA	100.0	CFAS	Healthy elderly	0-II (Braak)
24.32	NA	102.0	CFAS	mild AD	III-IV (Braak)
26.42	NA	110.8	CFAS	Severe AD	V-VI (Braak)
BBB surface area: Capillary length					
110.07	m	100	Department of Geriatrics and Psychiatry, University of Geneva School of Medicine	Healthy elderly	0 (CDR)
110.01	m	NS		Questionable	0.5 (CDR)
78.92	m	NS		mild AD	1 (CDR)
90.42	m	NS		moderate AD	2 (CDR)
42.83	m	100		Healthy elderly	0 (CDR)
83.14	m	NS		Questionable	0.5 (CDR)
45.5	m	NS		mild AD	1 (CDR)
47.17	m	NS		moderate AD	2 (CDR)
BBB surface area: MV diameter					
8.61	µm	100.0	UWNP Core, tissue repository	Healthy elderly	0-II (Braak)
7.97	µm	NS	UWNP Core, tissue repository	mild AD	III-IV (Braak)
8.11	µm	NS	UWNP Core, tissue repository	Severe AD	V-VI (Braak)
6.07	µm	100.0		Healthy elderly	(pathologically confirmed)
6.07	µm	NS		Unknown severity	(pathologically confirmed)
BBB surface area: Capillary diameter					
7.9	µm	100.0	Department of Geriatrics and Psychiatry, University of Geneva School of Medicine	Healthy elderly	0 (CDR)

	Age	Age range	Number pts	Technique	Notes	Ref.
	74.2	65-87 (2.6)	9	Immunohistochemical staining	Medial temporal cortex	[116]
	85.6	70-103 (7.5)	28	Immunohistochemical staining	Temporal cortex (lateral temporal neocortex)	[117]
	85.6	70-103 (7.5)	47	Immunohistochemical staining	Temporal cortex (lateral temporal neocortex)	[117]
	85.6	70-103 (7.5)	17	Immunohistochemical staining	Temporal cortex (lateral temporal neocortex)	[117]
	95.0	91-97 (2.7)	4	Gallyas silver staining	Hippocampus, CA1	[118]
	88.5	82-96 (7.1)	4	Gallyas silver staining	Hippocampus, CA1	[118]
	90.7	88-92 (2.3)	3	Gallyas silver staining	Hippocampus, CA1	[118]
	94.4	83-101 (5.5)	8	Gallyas silver staining	Hippocampus, CA1	[118]
	95.0	91-97 (2.7)	4	Gallyas silver staining	Entorhinal cortex	[118]
	88.5	82-96 (7.1)	4	Gallyas silver staining	Entorhinal cortex	[118]
	90.7	88-92 (2.3)	3	Gallyas silver staining	Entorhinal cortex	[118]
	94.4	83-101 (5.5)	8	Gallyas silver staining	Entorhinal cortex	[118]
	83.5	71-95	19	IF after IHC	Parietal cortex	[114]
	87.8	72-100	15	IF after IHC	Parietal cortex	[114]
	85.9	70-99	23	IF after IHC	Parietal cortex	[114]
	74.0	60-88	5	Histological staining	Hippocampal cortex	[58]
	78.0	66-94	5	Histological staining	Hippocampal cortex	[58]
	95.0	91-97 (2.7)	4	Gallyas silver staining	Hippocampus, CA1	[118]

Supplementary table 5. Continued

Value	unit	%	Database	cohort	Severity score (method)
6.83	µm	NS	Department of Geriatrics and Psychiatry, University of Geneva School of Medicine	Questionable	0.5 (CDR)
6.53	µm	NS	Department of Geriatrics and Psychiatry, University of Geneva School of Medicine	mild AD	1 (CDR)
6.26	µm	79.2	Department of Geriatrics and Psychiatry, University of Geneva School of Medicine	moderate AD	2 (CDR)
7.39	µm	100.0	Department of Geriatrics and Psychiatry, University of Geneva School of Medicine	Healthy elderly	0 (CDR)
6.88	µm	NS	Department of Geriatrics and Psychiatry, University of Geneva School of Medicine	Questionable	0.5 (CDR)
6.51	µm	NS	Department of Geriatrics and Psychiatry, University of Geneva School of Medicine	mild AD	1 (CDR)
5.59	µm	75.6	Department of Geriatrics and Psychiatry, University of Geneva School of Medicine	moderate AD	2 (CDR)
12.62	µm	100.0	Department of Geriatrics and Psychiatry, University of Geneva School of Medicine	Healthy elderly	0 (CDR)

	Age	Age range	Number pts	Technique	Notes	Ref.
	88.5	82-96 (7.1)	4	Gallyas silver staining	Hippocampus, CA1	[118]
	90.7	88-92 (2.3)	3	Gallyas silver staining	Hippocampus, CA1	[118]
	94.4	83-101 (5.5)	8	Gallyas silver staining	Hippocampus, CA1	[118]
	95.0	91-97 (2.7)	4	Gallyas silver staining	Entorhinal cortex	[118]
	88.5	82-96 (7.1)	4	Gallyas silver staining	Entorhinal cortex	[118]
	90.7	88-92 (2.3)	3	Gallyas silver staining	Entorhinal cortex	[118]
	94.4	83-101 (5.5)	8	Gallyas silver staining	Entorhinal cortex	[118]
	94.7	91-97 (3.2)	3	Gallyas silver staining	Frontal cortex, Brodmann area 9	[118]

Supplementary table 5. Continued

Value	unit	%	Database	cohort	Severity score (method)
11.57	µm	NS	Department of Geriatrics and Psychiatry, University of Geneva School of Medicine	Questionable	0.5 (CDR)
11.26	µm	100.0	Department of Geriatrics and Psychiatry, University of Geneva School of Medicine	Moderate	2 (CDR)
8.42	µm	66.7	Department of Geriatrics and Psychiatry, University of Geneva School of Medicine	Severe AD	3 (CDR)
5.01	µm	100.0		Healthy elderly	(SDAT)
5.22	µm	104.2		Unknown severity	(SDAT)
5.55	µm	100		Healthy elderly	(pathologically confirmed)
5.41	µm	NS		Unknown severity	(pathologically confirmed)
BBB surface area: Arteriolar diameter					
14.15	µm	100.0		Healthy elderly	(SDAT)
14.31	µm	101.1		Unknown severity	(SDAT)
BCSFB surface area: CP cells height					
13.7	um	100		NA	NA
10.5	um	76.6		NA	NA
$Brain_{ECF/ICF}$ pH					
6.91	unitless	0	healthy elderly	healthy elderly	29.07 (MMSE)
6.84	unitless	-0.07	AD	mild AD	21.69 (MMSE)
6.87	unitless	0	healthy elderly	healthy elderly	29.07 (MMSE)
6.88	unitless	N.S.	AD	mild AD	21.69 (MMSE)
6.87	unitless	0	healthy elderly	healthy elderly	29.07 (MMSE)
6.88	unitless	N.S.	AD	mild AD	21.69 (MMSE)
$Brain_{ICF}$ pH					
7.028	unitless	0	healthy elderly	healthy elderly	28.1 (MMSE)

	Age	Age range	Number pts	Technique	Notes	Ref.
	96.0	NA	1	Gallyas silver staining	Frontal cortex, Brodmann area 9	[118]
	96.4	91-101 (4.8)	5	Gallyas silver staining	Frontal cortex, Brodmann area 9	[118]
	93.5	93-94 (0.7)	2	Gallyas silver staining	Frontal cortex, Brodmann area 9	[118]
	78.8	67-95 (9.1)	8	Histological staining	Cerebral cortex (visual)	[109]
	79.3	63-92 (9)	10	Histological staining	Cerebral cortex (visual)	[109]
	74.0	60-88	5	Histological staining	Hippocampal cortex	[58]
	78.0	66-94	5	Histological staining	Hippocampal cortex	[58]
	78.8	67-95 (9.1)	8	Histological staining	Cerebral cortex (visual)	[109]
	79.3	63-92 (9)	10	Histological staining	Cerebral cortex (visual)	[109]
	89.1	82-96 (5.4)	8	microscopy	NA	[60]
	84.2	73-93 (6.3)	10	microscopy	NA	[60]
	65.2	(8.3)	30	MR spect (1H)	WM	[119]
	68.6	(9.9)	26	MR spect (1H)	WM	[119]
	65.2	(8.3)	24	MR spect (1H)	Hipp	[119]
	68.6	(9.9)	17	MR spect (1H)	Hipp	[119]
	65.2	(8.3)	24	MR spect (1H)	cerebellum	[119]
	68.6	(9.9)	17	MR spect (1H)	cerebellum	[119]
	73.5	(6.3)	31	MR spect (31P)	retrosplenial & anterior cingulate cortex; hippocampus	[120]

Supplementary table 5. Continued

Value	unit	%	Database	cohort	Severity score (method)
7.037	unitless	0.009	AD	mild AD	23.2 (MMSE)
$Brain_{ECF}$ pH					
6.261	unitless	0	UK brain bank aging	healthy elderly	1.4 (Braak)
6.136	unitless	-0.125	UK brain bank aging	mild AD	3.7 (Braak)
6.608	unitless	0	GSE 44770	healthy elderly	NA
6.369	unitless	-0.239	GSE 44770	Unknown severity	NA
6.5	unitless	0	GSE 84422	healthy elderly	1.3 (Braak)
6.369	unitless	-0.131	GSE 84422	moderate AD	4.8 (Braak)
6.56	unitless	0	Brain bank King's college london	healthy elderly	NA
6.39	unitless	-0.17	Brain bank King's college london	Unknown severity	NA
CSF pH					
7.311	unitless	0	NA	healthy group (not elderly)	NA
7.329	unitless	0.018		moderate-severe	NA
6.58	unitless	0	The Netherlands Brain Bank	healthy elderly	1.36 (Braak)
6.48	unitless	-0.1	The Netherlands Brain Bank	moderate-severe	5.21 (Braak)
6.71	unitless	0	The Netherlands Brain Bank	healthy elderly	NA
6.59	unitless	-0.12	The Netherlands Brain Bank	AD (severity NA)	NA

	Age	Age range	Number pts	Technique	Notes	Ref.
	73.4	(6.8)	31	MR spect (31P)	retrosplenial & anterior cingulate cortex; hippocampus	[120]
	71.6	(7.3)	146	pH electrode	postmortum	[121]
	71.3	(5)	609	pH electrode	postmortum	[121]
	68.5	(5.1)	49	pH electrode	postmortum	[121]
	68.7	(5.4)	38	pH electrode	postmortum	[121]
	82.2	(6.5)	33	pH electrode	postmortum	[121]
	82.4	(6.3)	48	pH electrode	postmortum	[121]
	71.1	41-102	81	pH electrode	homogenized postmortum tissue, death due to various cond	[122]
	78.4	49-97	90	pH electrode	homogenized postmortum tissue, death due to various cond	[122]
	NA	NA	35	pH meter	lumbar CSF	[123]
	66	57-73 (5.05)	15	pH meter	lumbar CSF	[124]
	78.1	NA (12.2)	281	pH meter	Ventricular; postmortem	[121]
	79.4	NA (10.9)	613	pH meter	Ventricular; postmortem	[121]
	74.7	NA (1.2)	82	N/A	Ventricular; postmortem	[125]
	76.3	NA (1.4)	85	N/A	Ventricular; postmortem	[125]

Supplementary table 6. CNS pathophysiological changes in aging animal models

Species	Parameter	Value	unit	%	Age in months
Brain ECF bulk flow					
Mouse	14C-inulin clearance	-33,3	%		NA
Mouse	14C-inulin clearance	30	%		NA
Mouse	14C-inulin clearance	23	%		NA
Mouse	14C-inulin clearance	20	%		18
Paracellular transport at the BCSFB					
Sheep	PPA-BCSFB	9	%	100	NA
Sheep	PPA-BCSFB	17	%	188,9	NA
Sheep	PPA-BCSFB	5	%	100	NA
Sheep	PPA-BCSFB	15	%	300	NA
Paracellular transport at the BBB					
Rats	basement membrane thickness	24,3	nm	100	NA
Rats	basement membrane thickness	93,9	nm	386,4	NA
Rats	astrocytes endfeet area	0,47	um2	100	NA
Rats	astrocytes endfeet area	3,54	um2	753,2	NA
Rats	TJ length	0,44	um	NS	NA
Rats	TJ length	0,41	um	NS	NA
Rats	passive permeability	NA	NA	NA	NA
Rats	permeability surface area product	NA	NA	NS	NA
Mice	albumin transport	NA	NA	NS	NA
Mice	IgG extravasation	0,43	%	100	3
Mice	IgG extravasation	0,51	%	118,6	22
ECF volume ratio					
rat	ECF volume ratio	0,215	unitless	100	NA

	Age range (sd) in months	N	Technique	Notes	Ref.
	NA	NA	inluin clearance	18 vs 2-3 month old mice	[126]
	2-3	6-11	inluin clearance	NA	[126]
	8-10	6-11	inluin clearance	NA	[126]
	NA	6-11	inluin clearance	NA	[126]
	12-24	36	radio-label + imaging	mannitol (MW=180) used as probe molecule	[127]
	84-120	24	radio-label + imaging	mannitol (MW=180) used as probe molecule	[127]
	12-24	36	radio-label + imaging	PEG (MW=4000) used as probe molecule	[127]
	84-120	24	radio-label + imaging	PEG (MW=4000) used as probe molecule	[127]
	2-3	NA	Electron microscopy	NA	[128]
	14-16	NA	Electron microscopy	NA	[128]
	2-3	NA	Electron microscopy	NA	[128]
	14-16	NA	Electron microscopy	NA	[128]
	2-3	NA	Electron microscopy	NA	[128]
	14-16	NA	Electron microscopy	non-significant decrease of TJ length and number	[128]
	NA	NA	SPECT imaging	slightly higher qinidine transport (+PSC) in 14-16 mo than in 2-3 month	[128]
	3-31	NA	quantitative radiography	radio-labelled sucrose	[129]
	NA	NA	brain-serum albumin ratio	SAMP8 mice (Accelerated aging)	[130]
	NA	6	brain-plasma %	receptor mediated transcytosis & shift to ligand non-specific transcytosis	[131]
	NA	6	brain-plasma %	receptor mediated transcytosis & shift to ligand non-specific transcytosis	[131]
	2-3	205	real-time iontophoresis (TMA+)	in cortex, corpus collosum, hippocampus	[132]

Supplementary table 6. Continued

Species	Parameter	Value	unit	%	Age in months
rat	ECF volume ratio	0,18	unitless	83,7	NA
mice	ECF volume ratio	0,199	unitless	100	NA
mice	ECF volume ratio	0,132	unitless	66,33	NA
mice	ECF volume ratio	0,203	unitless	100	NA
mice	ECF volume ratio	0,161	unitless	79,31	NA
mice	ECF volume ratio	0,2	unitless	100	NA
mice	ECF volume ratio	0,147	unitless	73,5	NA
Surface area of the BCSFB					
rats	CP cells height	12,39	um	100	3
rats	CP cells height	11,62	um	N.S.	18
rats	CP cells height	10,56	um	85	30
rats	microvilli height	2,66	um	100	3
rats	microvilli height	2,65	um	N.S.	18
rats	microvilli height	2,46	um	N.S.	30
rat	MV density	6,8	% of total vol	100	NA
rat	MV density	5,4	% of total vol	79,4	NA
rat	MV capillary diameter	6,2	um	100	NA
rat	MV capillary diameter	6,6	um	N.S.	NA
NA	NA	NA	NA	NA	NA

Age range (sd) in months	N	Technique	Notes	Ref.
26-32	82	real-time iontophoresis (TMA+)	in cortex, corpus collosum, hippocampus	[132]
6-8	4	real-time iontophoresis (TMA+)	females	[133]
17-25	7	real-time iontophoresis (TMA+)	females	[133]
6-8	3	real-time iontophoresis (TMA+)	males	[133]
17-25	7	real-time iontophoresis (TMA+)	males	[133]
6-8	7	real-time iontophoresis (TMA+)	average of males and females	[133]
17-25	14	real-time iontophoresis (TMA+)	average of males and females	[133]
NA	3	microscopy		[134]
NA	3	microscopy		[134]
NA	3	microscopy	compared to 3 month	[134]
NA	3	microscopy		[134]
NA	3	microscopy		[134]
NA	3	microscopy		[134]
11-15	12	microscopy		[135]
23-25	12	microscopy		[135]
11-15	12	microscopy		[135]
23-25	12	microscopy		[135]
NA	NA	NA	Increased capillary diameters and decreased capillary density. Some capillary density measurements in humans contradict these observations, as no changes observed.	[136]

Supplementary table 7. CNS pathophysiological changes in AD animal models

Species	Parameter	Value	unit	%	Age in months
ECF volume ratio					
Mice	Brain ECF volume frac-tion	0,145	unitless	100	NA
APP23 mice	Brain ECF volume frac-tion	0,207	unitless	142,7586 207	NA
Surface area of the BCSFB					
mice	BCSFB-SA	NA	NA	NA	NA

	Age range (sd) in months	N	Technique	Notes	Ref.
	17-25	13	RT Iontophoretic TMA	Cortex	Cortex
	17-25	15	RT Iontophoretic TMA	Cortex	Cortex
	NA	8-10	NA	Intracerebroventricular injection of AB42 resulted in loss of cuboidal shape and decrease of volume of choroid plexus epithelial cells	[137]

Supplementary references

1. Saleh MAA, Loo CF, Elassaiss-Schaap J, De Lange ECM (2021) Lumbar cerebrospinal fluid-to-brain extracellular fluid surrogacy is context-specific: insights from LeiCNS-PK3.0 simulations. J Pharmacokinet Pharmacodyn 48:725–741. https://doi.org/10.1007/s10928-021-09768-7
2. Flurkey K, Currer JM, Harrison DE (2007) Mouse Models in Aging Research. Mouse Biomed Res 3:637–672. https://doi.org/10.1016/B978-012369454-6/50074-1
3. Quinn R (2005) Comparing rat's to human's age: How old is my rat in people years? Nutrition 21:775–777. https://doi.org/10.1016/j.nut.2005.04.002
4. Andreollo NA, Freitas E, Araújo MR, Lopes LR (2012) Review Article Rat' s Age Versus Human' S Age : What Is The Relationship? Arq Bras Cir Dig 25:49–51. https://doi.org/10.1590/s0102-67202012000100011
5. Sigurdsson S, Aspelund T, Forsberg L, et al (2012) Brain tissue volumes in the general population of the elderly. The AGES-Reykjavik Study. Neuroimage 59:3862–3870. https://doi.org/10.1016/j.neuroimage.2011.11.024
6. Fjell AM, Walhovd KB, Fennema-Notestine C, et al (2009) One-year brain atrophy evident in healthy aging. J Neurosci 29:15223–15231. https://doi.org/10.1523/JNEUROSCI.3252-09.2009
7. Kim RE, Yun CH, Thomas RJ, et al (2018) Lifestyle-dependent brain change: a longitudinal cohort MRI study. Neurobiol Aging 69:48–57. https://doi.org/10.1016/j.neurobiolaging.2018.04.017
8. Driscoll I, Davatzikos C, An Y, et al (2009) Longitudinal pattern of regional brain volume change differentiates normal aging from MCI. Neurology 72:1906–1913
9. Takao H, Hayashi N, Ohtomo K (2012) A longitudinal study of brain volume changes in normal aging. Eur J Radiol 81:2801–2804. https://doi.org/10.1016/j.ejrad.2011.10.011
10. Scahill RI, Frost C, Jenkins R, et al (2003) A Longitudinal Study of Brain Volume Changes in Normal Aging Using Serial Registered Magnetic Resonance Imaging. Arch Neurol 60:989–994. https://doi.org/10.1016/j.ejrad.2011.10.011
11. Jack CR, Shiung MM, Weigand SD, et al (2005) Brain atrophy rates predict subsequent clinical conversion in normal elderly and amnestic MCI. Neurology 65:1227–1231. https://doi.org/10.1212/01.wnl.0000180958.22678.91
12. Jack CR, Shiung MM, Gunter JL, et al (2004) Comparison of different MRI brain athrophy rate measures with clinical disease progression in AD. Neurology 62:591–600. https://doi.org/10.1212/01.WNL.0000110315.26026.EF
13. Fjell AM, McEvoy L, Holland D, et al (2013) Brain changes in older adults at very low risk for Alzheimer's disease. J Neurosci 33:8237–8242. https://doi.org/10.1523/JNEUROSCI.5506-12.2013
14. Unay D (2012) Local and global volume changes of subcortical brain structures from longitudinally varying neuroimaging data for dementia identification. Comput Med Imaging Graph 36:464–473. https://doi.org/10.1016/j.compmedimag.2012.03.006
15. Resnick SM, Goldszal AF, Davatzikos C, et al (2000) One-year Age Changes in MRI Brain Volumes in Older Adults. Cereb Cortex 10:464–472. https://doi.org/10.1093/cercor/10.5.464

16. Liu RSN, Lemieux L, Bell GS, et al (2003) A longitudinal study of brain morphometrics using quantitative magnetic resonance imaging and difference image analysis. Neuroimage 20:22–33. https://doi.org/10.1016/S1053-8119(03)00219-2
17. Fotenos AF, Snyder AZ, Girton LE, et al (2005) Normative estimates of cross-sectional and longitudinal brain volume decline in aging and AD. Neurology 64:1032–1039. https://doi.org/10.1212/01.WNL.0000154530.72969.11
18. Vemuri P, Wiste HJ, Weigand SD, et al (2010) Serial MRI and CSF biomarkers in normal aging, MCI, and AD. Neurology 75:143–151. https://doi.org/10.1212/WNL.0b013e3181e7ca82
19. Vlek ALM, Visseren FLJ, Kappelle LJ, et al (2009) Blood pressure and progression of cerebral atrophy in patients with vascular disease. Am J Hypertens 22:1183–1189. https://doi.org/10.1038/ajh.2009.166
20. Carlson NE, Moore MM, Dame A, et al (2008) Trajectories of brain loss in aging and the development of cognitive impairment. Neurology 11:828–833. https://doi.org/10.1212/01.wnl.0000280577.43413.d9
21. Schott JM, Price SL, Frost C, et al (2005) Measuring atrophy in Alzheimer disease: A serial MRI study over 6 and 12 months. Neurology 65:119–124. https://doi.org/10.1212/01.wnl.0000167542.89697.0f
22. Wang D, Chalk JB, Rose SE, et al (2002) MR image-based measurement of rates of change in volumes of brain structures. Part II: Application to a study of Alzheimer's disease and normal aging. Magn Reson Imaging 20:41–48. https://doi.org/10.1016/S0730-725X(02)00472-1
23. Kaye JA, Moore MM, Dame A, et al (2005) Asynchronous regional brain volume losses in presymptomatic to moderate AD. J Alzheimer's Dis 8:51–56. https://doi.org/10.3233/JAD-2005-8106
24. Lemaître H, Crivello F, Grassiot B, et al (2005) Age- and sex-related effects on the neuroanatomy of healthy elderly. Neuroimage 26:900–911. https://doi.org/10.1016/j.neuroimage.2005.02.042
25. Matsumae M, Kikinis R, Mórocz IA, et al (1996) Age-related changes in intracranial compartment volumes in normal adults assessed by magnetic resonance imaging. J Neurosurg 84:982–991. https://doi.org/10.3171/jns.1996.84.6.0982
26. Sass LR, Khani M, Natividad GC, et al (2017) A 3D subject-specific model of the spinal subarachnoid space with anatomically realistic ventral and dorsal spinal cord nerve rootlets. Fluids Barriers CNS 14:1–16. https://doi.org/10.1186/s12987-017-0085-y
27. Svennerholm L, Boström K, Jungbjer B (1997) Changes in weight and compositions of major membrane components of human brain during the span of adult human life of Swedes. Acta Neuropathol 94:345–352. https://doi.org/10.1007/s004010050717
28. Söderberg M, Edlund C, Kristensson K, Dallner G (1990) Lipid Compositions of Different Regions of the Human Brain During Aging. J Neurochem 54:415–423. https://doi.org/10.1111/j.1471-4159.1990.tb01889.x
29. Mota B, Dos Santos SE, Ventura-Antunes L, et al (2019) White matter volume and white/gray matter ratio in mammalian species as a consequence of the universal scaling of cortical folding. Proc Natl Acad Sci U S A 116:15253–15261. https://doi.org/10.1073/pnas.1716956116

30. Oner Z, Kahraman AS, Kose E, et al (2017) Quantitative Evaluation of Normal Aqueductal Cerebrospinal Fluid Flow Using Phase-Contrast Cine MRI According to Age and Sex. Anat Rec 300:549–555. https://doi.org/10.1002/ar.23514
31. Stoquart-ElSankari S, Balédent O, Gondry-Jouet C, et al (2007) Aging effects on cerebral blood and cerebrospinal fluid flows. J Cereb Blood Flow Metab 27:1563–1572. https://doi.org/10.1038/sj.jcbfm.9600462
32. Barkhof F, Kouwenhoven M, Scheltens P, et al (1994) Phase-contrast cine MR imaging of normal aqueductal CSF flow: Effect of aging and relation to CSF void on modulus MR. Acta radiol 35:123–130. https://doi.org/10.1080/02841859409172348
33. Jakimovski D, Zivadinov R, Weinstock-Guttman B, et al (2020) Longitudinal analysis of cerebral aqueduct flow measures: Multiple sclerosis flow changes driven by brain atrophy. Fluids Barriers CNS 17:1–9. https://doi.org/10.1186/s12987-020-0172-3
34. Lokossou A, Metanbou S, Gondry-Jouet C, Balédent O (2020) Extracranial versus intracranial hydro-hemodynamics during aging: A PC-MRI pilot cross-sectional study. Fluids Barriers CNS 17:1–11. https://doi.org/10.1186/s12987-019-0163-4
35. Sartoretti T, Wyss M, Sartoretti E, et al (2019) Sex and age dependencies of aqueductal cerebrospinal fluid dynamics parameters in healthy subjects. Front Aging Neurosci 10:1–13. https://doi.org/10.3389/fnagi.2019.00199
36. Daners MS, Knobloch V, Soellinger M, et al (2012) Age-Specific Characteristics and Coupling of Cerebral Arterial Inflow and Cerebrospinal Fluid Dynamics. PLoS One 7:e37502. https://doi.org/10.1371/journal.pone.0037502
37. Unal O, Kartum A, Avcu S, et al (2009) Cine phase-contrast MRI evaluation of normal aqueductal cerebrospinal fluid flow according to sex and age. Diagn Interv Radiol 15:227–231. https://doi.org/10.4261/1305-3825.DIR.2321-08.1
38. Gideon P, Thomsen C, Ståhlberg F, Henriksen O (1994) Cerebrospinal fluid production and dynamics in normal aging: a MRI phase-mapping study. Acta Neurol Scand 89:362–366. https://doi.org/10.1111/j.1600-0404.1994.tb02647.x
39. Stadlbauer A, Salomonowitz E, van der Riet W, et al (2010) Insight into the patterns of cerebrospinal fluid flow in the human ventricular system using MR velocity mapping. Neuroimage 51:42–52. https://doi.org/10.1016/j.neuroimage.2010.01.110
40. Albeck MJ, Skak C, Nielsen PR, et al (1998) Age dependency of resistance to cerebrospinal fluid outflow. J Neurosurg 89:275–278. https://doi.org/10.3171/jns.1998.89.2.0275
41. Schoning M, Walter J, Scheel P (1994) Estimation of cerebral blood flow through color duplex sonography of the carotid and vertebral arteries in healthy adults. Stroke 25:17–22. https://doi.org/10.1161/01.STR.25.1.17
42. van Es ACGM, van der Grond J, ten Dam VH, et al (2010) Associations between total cerebral blood flow and age related changes of the brain. PLoS One 5:1–6. https://doi.org/10.1371/journal.pone.0009825
43. De Vis JB, Peng SL, Chen X, et al (2018) Arterial-spin-labeling (ASL) perfusion MRI predicts cognitive function in elderly individuals: A 4-year longitudinal study. J Magn Reson Imaging 48:449–458. https://doi.org/10.1002/jmri.25938
44. Parkes LM, Rashid W, Chard DT, Tofts PS (2004) Normal Cerebral Perfusion Measurements Using Arterial Spin Labeling: Reproducibility, Stability, and Age and Gender Effects. Magn Reson Med 51:736–743. https://doi.org/10.1002/mrm.20023
45. Leoni RF, Oliveira IAF, Pontes-Neto OM, et al (2017) Cerebral blood flow and vasoreactivity in aging: An arterial spin labeling study. Brazilian J Med Biol Res 50:1–9. https://doi.org/10.1590/1414-431X20175670

46. Tempel LW, Perlmutter JS (1992) Vibration-induced regional cerebral blood flow responses in normal aging. J Cereb Blood Flow Metab 12:554–561. https://doi.org/10.1038/jcbfm.1992.79
47. Meltzer CC, Cantwell MN, Greer PJ, et al (2000) Does cerebral blood flow decline in healthy aging? A PET study with partial-volume correction. J Nucl Med 41:1842–1848
48. Itoh M, Hatazawa J, Miyazawa H, et al (1990) Stability of cerebral blood flow and oxygen metabolism during normal aging. Gerontology 36:43–48. https://doi.org/10.1159/000213174
49. Buijs PC, Krabbe-Hartkamp MJ, Bakker CJG, et al (1998) Effect of Age on Cerebral Blood Flow : Measurement with Ungated Two-Dimensional Phase-Contrast MR Angiography in 250 Adults. Radiology 209:667–674
50. Chiu C, Miller MC, Monahan R, et al (2015) P-glycoprotein expression and amyloid accumulation in human aging and Alzheimer's disease: Preliminary observations. Neurobiol Aging 36:2475–2482. https://doi.org/10.1016/j.neurobiolaging.2015.05.020
51. Toornvliet R, van Berckel BNM, Luurtsema G, et al (2006) Effect of age on functional P-glycoprotein in the blood-brain barrier measured by use of (R)-[11C]verapamil and positron emission tomography. Clin Pharmacol Ther 79:540–548. https://doi.org/10.1016/j.clpt.2006.02.004
52. Bartels AL, Kortekaas R, Bart J, et al (2009) Blood-brain barrier P-glycoprotein function decreases in specific brain regions with aging: A possible role in progressive neurodegeneration. Neurobiol Aging 30:1818–1824. https://doi.org/10.1016/j.neurobiolaging.2008.02.002
53. Bauer M, Wulkersdorfer B, Karch R, et al (2017) Effect of P-glycoprotein inhibition at the blood–brain barrier on brain distribution of (R)-[11C]verapamil in elderly vs. young subjects. Br J Clin Pharmacol 83:1991–1999. https://doi.org/10.1111/bcp.13301
54. Van Assema DME, Lubberink M, Boellaard R, et al (2012) P-glycoprotein function at the blood-brain barrier: Effects of age and gender. Mol Imaging Biol 14:771–776. https://doi.org/10.1007/s11307-012-0556-0
55. Bauer M, Karch R, Neumann F, et al (2009) Age dependency of cerebral P-gp function measured with (R)-[11C]verapamil and PET. Eur J Clin Pharmacol 65:941–946. https://doi.org/10.1007/s00228-009-0709-5
56. Montagne A, Barnes SR, Sweeney MD, et al (2015) Blood-Brain barrier breakdown in the aging human hippocampus. Neuron 85:296–302. https://doi.org/10.1016/j.neuron.2014.12.032
57. Verheggen ICM, de Jong JJA, van Boxtel MPJ, et al (2020) Increase in blood–brain barrier leakage in healthy, older adults. GeroScience 42:1183–1193. https://doi.org/10.1007/s11357-020-00211-2
58. Bell MA, Ball MJ (1981) Morphometric comparison of hippocampal microvasculature in ageing and demented people: Diameters and densities. Acta Neuropathol 53:299–318. https://doi.org/10.1007/BF00690372
59. Mann DMA, Eaves NR, Marcyniuk B, Yates PO (1986) Quantitative changes in cerebral cortical microvasculature in ageing and dementia. Neurobiol Aging 7:321–330. https://doi.org/10.1016/0197-4580(86)90158-2
60. Serot JM, Béné MC, Foliguet B, Faure GC (2000) Morphological alterations of the choroid plexus in late-onset Alzheimer's disease. Acta Neuropathol 99:105–108. https://doi.org/10.1007/PL00007412
61. Henneman WJP, Sluimer JD, Barnes J, et al (2009) Hippocampal atrophy rates in Alzheimer disease: Added value over whole brain volume measures. Neurology 72:999–1007. https://doi.org/10.1212/01.wnl.0000344568.09360.31

62. Ott BR, Cohen RA, Gongvatana A, et al (2010) Brain ventricular volume and cerebrospinal fluid biomarkers of Alzheimer's disease. J Alzheimer's Dis 20:647–657. https://doi.org/10.3233/JAD-2010-1406

63. Evans MC, Barnes J, Nielsen C, et al (2010) Volume changes in Alzheimer's disease and mild cognitive impairment: Cognitive associations. Eur Radiol 20:674–682. https://doi.org/10.1007/s00330-009-1581-5

64. Yamada S, Ishikawa M, Yamamoto K (2016) Comparison of CSF distribution between idiopathic normal pressure hydrocephalus and Alzheimer disease. Am J Neuroradiol 37:1249–1255. https://doi.org/10.3174/ajnr.A4695

65. El Sankari S, Gondry-Jouet C, Fichten A, et al (2011) Cerebrospinal fluid and blood flow in mild cognitive impairment and Alzheimer's disease: A differential diagnosis from idiopathic normal pressure hydrocephalus. Fluids Barriers CNS 8:12. https://doi.org/10.1186/2045-8118-8-12

66. Luetmer PH, Huston J, Friedman JA, et al (2002) Measurement of cerebrospinal fluid flow at the cerebral aqueduct by use of phase-contrast magnetic resonance imaging: technique validation and utility in diagnosing idiopathic normal pressure hydrocephalus. Neurosurgery 50:534–544

67. Adak S, Illouz K, Gorman W, et al (2004) Predicting the rate of cognitive decline in aging and early Alzheimer disease. Neurology 63:108–114. https://doi.org/10.1212/01.WNL.0000132520.69612.AB

68. Condon B, Wyper D, Grant R, et al (1986) Use of Magnetic Resonance Imaging To Measure Intracranial Cerebrospinal Fluid Volume. Lancet 327:1355–1357. https://doi.org/10.1016/S0140-6736(86)91666-1

69. Coutu JP, Goldblatt A, Rosas HD, Salat DH (2015) White matter changes are associated with ventricular expansion in aging, mild cognitive impairment, and Alzheimer's disease. J Alzheimer's Dis 49:329–342. https://doi.org/10.3233/JAD-150306

70. Dodge HH, Zhu J, Harvey D, et al (2014) Biomarker progressions explain higher variability in stage-specific cognitive decline than baseline values in Alzheimer disease. Alzheimer's Dement 10:690–703. https://doi.org/10.1016/j.jalz.2014.04.513

71. Harris GJ, Rhew EH, Noga T, Pearlson GD (1991) User-friendly method for rapid brain and CSF volume calculation using transaxial MRI images. Psychiatry Res Neuroimaging 40:61–68. https://doi.org/10.1016/0925-4927(91)90029-P

72. Hsu Y-Y, Schuff N, Amend DL, et al (2002) Quantitative Magnetic Resonance Imaging Differences Between Alzheimer Disease With and Without Subcortical Lacunes, Alzheimer Disease and Associated Disorders. Alzheimer Dis Assoc Disord 16:58–64. https://doi.org/10.1097/01.WAD.0000013690.85676.21

73. Nestor SM, Rupsingh R, Borrie M, et al (2008) Ventricular enlargement as a possible measure of Alzheimer's disease progression validated using the Alzheimer's disease neuroimaging initiative database. Brain 131:2443–2454. https://doi.org/10.1093/brain/awn146

74. Pantel J, Schröder J, Schad LR, et al (1997) Quantitative magnetic resonance imaging and neuropsychological functions in dementia of the {Alzheimer} type. Psychol Med 27:221–229

75. Serulle Y, Rusinek H, Kirov II, et al (2014) Differentiating shunt-responsive normal pressure hydrocephalus from alzheimer disease and normal aging: Pilot study using automated mri brain tissue segmentation. J Neurol 261:1994–2002. https://doi.org/10.1007/s00415-014-7454-0

76. Shirzadi Z, Stefanovic B, Mutsaerts HJMM, et al (2019) Classifying cognitive impairment based on the spatial heterogeneity of cerebral blood flow images. J Magn Reson Imaging 50:858–867. https://doi.org/10.1002/jmri.26650

77. Matsuda H, Kanetaka H, Ohnishi T, et al (2002) Brain SPET abnormalities in Alzheimer's disease before and after atrophy correction. Eur J Nucl Med 29:1502–1505. https://doi.org/10.1007/s00259-002-0930-2

78. Chen Y, Wolk DA, Reddin JS, et al (2011) Voxel-level comparison of arterial spin-labeled perfusion MRI and FDG-PET in Alzheimer disease. Neurology 77:1977–1985. https://doi.org/10.1212/WNL.0b013e31823a0ef7

79. Yoshiura T, Hiwatashi A, Yamashita K, et al (2009) Simultaneous measurement of arterial transit time, arterial blood volume, and cerebral blood flow using arterial spin-labeling in patients with Alzheimer disease. Am J Neuroradiol 30:1388–1393. https://doi.org/10.3174/ajnr.A1562

80. Benedictus MR, Binnewijzend MAA, Kuijer JPA, et al (2014) Brain volume and white matter hyperintensities as determinants of cerebral blood flow in Alzheimer's disease. Neurobiol Aging 35:2665–2670. https://doi.org/10.1016/j.neurobiolaging.2014.06.001

81. Leeuwis AE, Benedictus MR, Kuijer JPA, et al (2017) Lower cerebral blood flow is associated with impairment in multiple cognitive domains in Alzheimer's disease. Alzheimer's Dement 13:531–540. https://doi.org/10.1016/j.jalz.2016.08.013

82. Binnewijzend MAA, Kuijer JPA, Van Der Flier WM, et al (2014) Distinct perfusion patterns in Alzheimer's disease, frontotemporal dementia and dementia with Lewy bodies. Eur Radiol 24:2326–2333. https://doi.org/10.1007/s00330-014-3172-3

83. Storelli F, Billington S, Kumar AR, Unadkat JD (2021) Abundance of P-Glycoprotein and Other Drug Transporters at the Human Blood-Brain Barrier in Alzheimer's Disease: A Quantitative Targeted Proteomic Study. Clin Pharmacol Ther 109:667–675. https://doi.org/10.1002/cpt.2035

84. Wijesuriya HC, Bullock JY, Faull RLM, et al (2010) ABC efflux transporters in brain vasculature of Alzheimer's subjects. Brain Res 1358:228–238. https://doi.org/10.1016/j.brainres.2010.08.034

85. Kannan P, Schain M, Kretzschmar WW, et al (2017) An automated method measures variability in P-glycoprotein and ABCG2 densities across brain regions and brain matter. J Cereb Blood Flow Metab 37:2062–2075. https://doi.org/10.1177/0271678X16660984

86. Al-Majdoub ZM, Al Feteisi H, Achour B, et al (2019) Proteomic Quantification of Human Blood–Brain Barrier SLC and ABC Transporters in Healthy Individuals and Dementia Patients. Mol Pharm 16:1220–1233. https://doi.org/10.1021/acs.molpharmaceut.8b01189

87. Deo AK, Borson S, Link JM, et al (2014) Activity of P-glycoprotein, a β-amyloid transporter at the blood-brain barrier, is compromised in patients with mild Alzheimer disease. J Nucl Med 55:1106–1111. https://doi.org/10.2967/jnumed.113.130161

88. Yildirim T, Karakurum Göksel B, Demır Ş, et al (2016) Evaluation of brain perfusion in Alzheimer disease with perfusion computed tomography and comparison to elderly patient without dementia. Turkish J Med Sci 46:834–839. https://doi.org/10.3906/sag-1411-77

89. Hauser T, Schönknecht P, Thomann PA, et al (2013) Regional Cerebral Perfusion Alterations in Patients with Mild Cognitive Impairment and Alzheimer Disease Using Dynamic Susceptibility Contrast MRI. Acad Radiol 20:705–711. https://doi.org/10.1016/j.acra.2013.01.020

90. Lacalle-Aurioles M, Mateos-Pérez JM, Guzmán-De-Villoria JA, et al (2014) Cerebral blood flow is an earlier indicator of perfusion abnormalities than cerebral blood volume in Alzheimer's disease. J Cereb Blood Flow Metab 34:654–659. https://doi.org/10.1038/jcbfm.2013.241

91. Zimny A, Bladowska J, Neska M, et al (2013) Quantitative MR evaluation of atrophy, as well as perfusion and diffusion alterations within hippocampi in patients with Alzheimer's disease and mild cognitive impairment. Med Sci Monit 19:86–94. https://doi.org/10.12659/MSM.883757

92. Schreiber SJ, Doepp F, Spruth E, et al (2005) Ultrasonographic measurement of cerebral blood flow, cerebral circulation time and cerebral blood volume in vascular and Alzheimer's dementia. J Neurol 252:1171–1177. https://doi.org/10.1007/s00415-005-0826-8

93. Nielsen RB, Egefjord L, Angleys H, et al (2017) Capillary dysfunction is associated with symptom severity and neurodegeneration in Alzheimer's disease. Alzheimer's Dement 13:1143–1153. https://doi.org/10.1016/j.jalz.2017.02.007

94. Starr JM, Farrall AJ, Armitage P, et al (2009) Blood-brain barrier permeability in Alzheimer's disease: a case-control MRI study. Psychiatry Res - Neuroimaging 171:232–241. https://doi.org/10.1016/j.pscychresns.2008.04.003

95. Van De Haar HJ, Burgmans S, Jansen JFA, et al (2016) Blood-brain barrier leakage in patients with early Alzheimer disease. Radiology 281:527–535. https://doi.org/10.1148/radiol.2016152244

96. van de Haar HJ, Jansen JFA, van Osch MJP, et al (2016) Neurovascular unit impairment in early Alzheimer's disease measured with magnetic resonance imaging. Neurobiol Aging 45:190–196. https://doi.org/10.1016/j.neurobiolaging.2016.06.006

97. Caserta MT, Caccioppo D, Lapin GD, et al (1998) Blood-brain barrier integrity in Alzheimer's disease patients and elderly control subjects. J Neuropsychiatr 10:78–84. https://doi.org/10.1176/jnp.10.1.78

98. Farrall AJ, Wardlaw JM (2009) Blood-brain barrier: Ageing and microvascular disease - systematic review and meta-analysis. Neurobiol Aging 30:337–352. https://doi.org/10.1016/j.neurobiolaging.2007.07.015

99. Ott BR, Jones RN, Daiello LA, et al (2018) Blood-cerebrospinal fluid barrier gradients in mild cognitive impairment and Alzheimer's disease: Relationship to inflammatory cytokines and chemokines. Front Aging Neurosci 10:1–12. https://doi.org/10.3389/fnagi.2018.00245

100. Nitsch RM, Blusztajn JK, Pittas AG, et al (1992) Evidence for a membrane defect in Alzheimer disease brain. Proc Natl Acad Sci U S A 89:1671–1675. https://doi.org/10.1073/pnas.89.5.1671

101. Kosicek M, Hecimovic S (2013) Phospholipids and Alzheimer's disease: Alterations, mechanisms and potential biomarkers. Int J Mol Sci 14:1310–1322. https://doi.org/10.3390/ijms14011310

102. Wells K, Farooqui AA, Liss L, Horrocks LA (1995) Neural membrane phospholipids in alzheimer disease. Neurochem Res 20:1329–1333. https://doi.org/10.1007/BF00992508

103. Guan Z, Wang Y, Cairns NJ, et al (1999) Decrease and structural modifications of phosphatidylethanolamine plasmalogen in the brain with Alzheimer disease. Neurol J Neuropathol Exp 58:740–747. https://doi.org/10.1097/00005072-199907000-00008

104. Igarashi M, Ma K, Gao F, et al (2011) Disturbed choline plasmalogen and phospholipid fatty acid concentrations in Alzheimer's disease prefrontal cortex. J Alzheimer's Dis 24:507–517. https://doi.org/10.3233/JAD-2011-101608

105. Stokes CE, Hawthorne JN (1987) Reduced Phosphoinositide Concentrations in Anterior Temporal Cortex of Alzheimer-Diseased Brains. J Neurochem 48:1018–1021. https://doi.org/10.1111/j.1471-4159.1987.tb05619.x

106. Pettegrew JW, Panchalingam K, Hamilton RL, Mcclure RJ (2001) Brain membrane phospholipid alterations in Alzheimer's disease. Neurochem Res 26:771–782. https://doi.org/10.1023/A:1011603916962

107. Söderberg M, Edlund C, Alafuzoff I, et al (1992) Lipid Composition in Different Regions of the Brain in Alzheimer's Disease/Senile Dementia of Alzheimer's Type. J Neurochem 59:1646–1653. https://doi.org/10.1111/j.1471-4159.1992.tb10994.x

108. Svennerholm L, Gottfries C yG (1994) Membrane Lipids, Selectively Diminished in Alzheimer Brains, Suggest Synapse Loss as a Primary Event in EarlyyOnset Form (Type I) and Demyelination in LateyOnset Form (Type II). J Neurochem 62:1039–1047. https://doi.org/10.1046/j.1471-4159.1994.62031039.x

109. Bell MA, Ball MJ (1990) Neuritic plaques and vessels of visual cortex in aging and Alzheimer's dementia. Neurobiol Aging 11:359–370. https://doi.org/10.1016/0197-4580(90)90001-G

110. Fernandez-Klett F, Brandt L, Fernández-Zapata C, et al (2020) Denser brain capillary network with preserved pericytes in Alzheimer's disease. Brain Pathol 30:1071–1086. https://doi.org/10.1111/bpa.12897

111. Hunter JM, Kwan J, Malek-Ahmadi M, et al (2012) Morphological and pathological evolution of the brain microcirculation in aging and Alzheimer's disease. PLoS One 7:1–12. https://doi.org/10.1371/journal.pone.0036893

112. Buée L, Hof PR, Bouras C, et al (1994) Pathological Alterations of the Cerebral Microvasculature in Alzheimer's Disease and Related Dementing Disorders. Acta Neuropathol 87:469–480. https://doi.org/10.1007/BF00294173

113. Biron KE, Dickstein DL, Gopaul R, Jefferies WA (2011) Amyloid triggers extensive cerebral angiogenesis causing blood brain barrier permeability and hypervascularity in alzheimer's disease. PLoS One 6:. https://doi.org/10.1371/journal.pone.0023789

114. Damodarasamy M, Vernon RB, Pathan JL, et al (2020) The microvascular extracellular matrix in brains with Alzheimer's disease neuropathologic change (ADNC) and cerebral amyloid angiopathy (CAA). Fluids Barriers CNS 17:1–11. https://doi.org/10.1186/s12987-020-00219-y

115. Fischer VW, Siddiqi A, Yusufaly Y (1990) Altered angioarchitecture in selected areas of brains with Alzheimer's disease. Acta Neuropathol 79:672–679. https://doi.org/10.1007/BF00294246

116. Jantaratnotai N, Schwab C, K. Ryu J, et al (2010) Converging Perturbed Microvasculature and Microglial Clusters Characterize Alzheimer Disease Brain. Curr Alzheimer Res 7:625–636. https://doi.org/10.2174/156720510793499039

117. Viggars AP, Wharton SB, Simpson JE, et al (2011) Alterations in the blood brain barrier in ageing cerebral cortex in relationship to Alzheimer-type pathology: A study in the MRC-CFAS population neuropathology cohort. Neurosci Lett 505:25–30. https://doi.org/10.1016/j.neulet.2011.09.049

118. Bouras C, Kövari E, Herrmann FR, et al (2006) Stereologic analysis of microvascular morphology in the elderly: Alzheimer disease pathology and cognitive status. J Neuropathol Exp Neurol 65:235–244. https://doi.org/10.1097/01.jnen.0000203077.53080.2c

119. Lyros E, Ragoschke-Schumm A, Kostopoulos P, et al (2020) Normal brain aging and Alzheimer's disease are associated with lower cerebral pH: an in vivo histidine 1H-MR spectroscopy study. Neurobiol Aging 87:60–69. https://doi.org/10.1016/j.neurobiolaging.2019.11.012

120. Rijpma A, van der Graaf M, Meulenbroek O, et al (2018) Altered brain high-energy phosphate metabolism in mild Alzheimer's disease: A 3-dimensional 31P MR spectroscopic imaging study. NeuroImage Clin 18:254–261. https://doi.org/10.1016/j.nicl.2018.01.031

121. Decker Y, Németh E, Schomburg R, et al (2021) Decreased pH in the aging brain and Alzheimer's disease. Neurobiol Aging 101:40–49. https://doi.org/10.1016/j.neurobiolaging.2020.12.007

122. Preece P, Cairns NJ (2003) Quantifying mRNA in postmortem human brain: Influence of gender, age at death, postmortem interval, brain pH, agonal state and inter-lobe mRNA variance. Mol Brain Res 118:60–71. https://doi.org/10.1016/S0169-328X(03)00337-1

123. Posner JB, Swanson AG, Plum F (1965) Acid-Base Balance in Cerebrospinal Fluid. Arch Neurol 12:479–496. https://doi.org/10.1001/archneur.1965.00460290035006

124. Gottfries CG, Kjallquist A, Ponten U, et al (1974) Cerebrospinal fluid pH and monoamine and glucolytic metabolites in Alzheimer's disease. Br J Psychiatry 124:280–287. https://doi.org/10.1192/bjp.124.3.280

125. Liu RY, Zhou JN, Van Heerikhuize J, et al (1999) Decreased melatonin levels in postmortem cerebrospinal fluid in relation to aging, Alzheimer's disease, and apolipoprotein E-ε4/4 genotype. J Clin Endocrinol Metab 84:323–327. https://doi.org/10.1210/jc.84.1.323

126. Kress BT, Iliff JJ, Xia M, et al (2014) Impairment of paravascular clearance pathways in the aging brain. Ann Neurol 76:845–861. https://doi.org/10.1002/ana.24271

127. Chen RL, Kassem NA, Redzic ZB, et al (2009) Age-related changes in choroid plexus and blood-cerebrospinal fluid barrier function in the sheep. Exp Gerontol 44:289–296. https://doi.org/10.1016/j.exger.2008.12.004

128. Bors L, Tóth K, Tóth EZ, et al (2018) Age-dependent changes at the blood-brain barrier. A Comparative structural and functional study in young adult and middle aged rats. Brain Res Bull 139:269–277. https://doi.org/10.1016/j.brainresbull.2018.03.001

129. Wadhwani KC, Koistinaho J, BALBO A, Rapoport SI (1991) Blood-nerve and blood-brain barrier permeabilities and nerve vascular space in Fischer-344 rats of different ages. Mech Ageing Dev 58:177–190. https://doi.org/doi.org/10.1016/0047-6374(91)90091-D

130. Banks WA, Farr SA, Morley JE (2000) Permeability of the blood-brain barrier to albumin and insulin in the young and aged SAMP8 mouse. Journals Gerontol - Ser A Biol Sci Med Sci 55:B601–B606. https://doi.org/10.1093/gerona/55.12.B601

131. Yang AC, Stevens MY, Chen MB, et al (2020) Physiological blood–brain transport is impaired with age by a shift in transcytosis. Nature 583:425–430. https://doi.org/10.1038/s41586-020-2453-z

132. Syková E, Mazel T, Simonová Z (1998) Diffusion constraints and neuron-glia interaction during aging. Exp Gerontol 33:837–851. https://doi.org/10.1016/s0531-5565(98)00038-2

133. Syková E, Vorříšek I, Antonova T, et al (2005) Changes in extracellular space size and geometry in APP23 transgenic mice: A model of Alzheimer's disease. Proc Natl Acad Sci U S A 102:479–484. https://doi.org/10.1073/pnas.0408235102

134. Serot JM, Foliguet B, Béné MC, Faure GC (2001) Choroid plexus and ageing in rats: A morphometric and ultrastructural study. Eur J Neurosci 14:794–798. https://doi.org/10.1046/j.0953-816X.2001.01693.x

135. Desjardins M, Berti R, Lefebvre J, et al (2014) Aging-related differences in cerebral capillary blood flow in anesthetized rats. Neurobiol Aging 35:1947–1955. https://doi.org/10.1016/j.neurobiolaging.2014.01.136

136. Costea L, Mészáros, Bauer H, et al (2019) The blood–brain barrier and its intercellular junctions in age-related brain disorders. Int J Mol Sci 20:1–28. https://doi.org/10.3390/ijms20215472

137. Brkic M, Balusu S, Van Wonterghem E, et al (2015) Amyloid β oligomers disrupt blood–CSF barrier integrity by activating matrix metalloproteinases. J Neurosci 35:12766–12778. https://doi.org/10.1523/JNEUROSCI.0006-15.2015